A CONSERVED ANTIVIRAL ROLE FOR A VIRUS-INDUCED CYTOPLASMIC EXOSOME COMPLEX

Jerome M Molleston

A DISSERTATION

in

Cell and Molecular Biology

Presented to the Faculties of the University of Pennsylvania

in

Partial Fulfillment of the Requirements for the

Degree of Doctor of Philosophy

2016

Supervisor of Dissertation

_____

Sara Cherry

Associate Professor of Microbiology

Graduate Group Chairperson

_____

Daniel S Kessler

Associate Professor of Cell and Developmental Biology

Dissertation Committee:
Susan R Ross, Professor of Microbiology (Chair)
Paul Bates, Professor of Microbiology
Kristen W Lynch, Professor of Biochemistry and Biophysics
Beatrice H Hahn, Professor of Medicine

DEDICATION

I would like to dedicate this thesis to my mother, Jean P Molleston, who is an unmatched role model as a scientist, as a doctor, and as a person.

ACKNOWLEDGEMENTS

I would like to thank the following individuals for their contributions to this work:

Sara Cherry, who has taught me how to think about, present about, and write about science. Her mentorship has been unparalleled, and she has served as a much-needed balancing force during my highest highs and lowest lows.

My thesis committee members **Susan Ross** (chair), **Kristen Lynch**, **Paul Bates**, and **Beatrice Hahn** for their guidance at every stage of my graduate studies.

Rui Zhou, who contributed the 177 gene set for screening.

Torben Jensen, for TRAMP component tagged constructs.

Leah Sabin, who initially performed the 177-gene screen which led to the exosome, and without whose phenomenal memory and record keeping this project would not have been a success.

Ryan Moy and **Kaycie Hopkins**, both of whom contributed data to the exosome project and taught me the methods both experimental and social of the Cherry Lab. They have been excellent graduate student role models and good friends.

Sanjay Menghani, who helped perform 3' RACE cloning and analysis, and who allowed me to have a taste of mentoring another budding scientist.

Keiko Rausch, who helped perform several of the RVFV experiments in DL1 cells and kept the Cherry Lab running.

Beth Gold and the rest of the Cherry Lab fly team, who performed *Drosophila* injection experiments, harvested flies, and maintained the fly stocks.

Jeremy Wilusz, for creating the RVFV 3' UTR reporter constructs, and for his advice and feedback during the preparation of the manuscript.

Brent Hackett for friendship, scientific advice, and distraction when I needed it.

All current and former members of the **Cherry Lab**, who have contributed ideas, reagents, cells, and support, and who have tolerated every one of my mood swings during the past four years.

The **Medical Scientist Training Program**, particularly **Maggie Krall** and **Skip Brass**, who have created an amazing training environment and have been universally supportive.

My **friends**, both at Penn and elsewhere, who have shared in the triumphs and tribulations.

My **family**, who have listened to more about viruses than they've ever cared to know, and who have felt close even half a country away.

Eva Klinman, whose love and encouragement always drive me to be my best.

This work was funded by NIH training grant T32AI07324-21A1

ABSTRACT

A CONSERVED ANTIVIRAL ROLE FOR A VIRUS-INDUCED

CYTOPLASMIC EXOSOME COMPLEX

Jerome M Molleston

Sara Cherry

RNA degradation is a tightly regulated and highly conserved process which selectively targets aberrant RNAs using both 5' and 3' exonucleases. The RNAs degraded by this process include viral RNA, but the mechanisms by which viral RNA is identified and recruited to the degradation machinery are incompletely understood. To identify new antiviral genes, we performed RNAi screening of genes with known roles in RNA metabolism in *Drosophila* cells. We identified the RNA exosome, which targets RNA for 3' end decay, and two components of the exosome cofactor TRAMP complex, dMtr4 and dZcchc7, as antiviral against a panel of RNA viruses. As these genes are highly conserved, I extended these studies to human cells and found that the exosome as well as TRAMP components hMTR4 and hZCCHC7 are antiviral. While hMTR4 and hZCCHC7 are normally nuclear, I found that infection by cytoplasmic RNA viruses induces their export to cytoplasmic granules, where they form a complex that specifically recognizes and induces degradation of viral mRNAs. Furthermore, I found that the 3' UTR of bunyaviral mRNA is sufficient to confer virus-induced exosomal degradation, demonstrating cis-regulation.

Several types of ribonucleoprotein (RNP) granules interact with both 5' and 3' decay machinery to facilitate degradation of sequestered RNAs. In order to determine whether TRAMP component-containing granules contain components of other defined RNP granules, I performed immunofluorescence for hZCCHC7 as well as components of P-bodies, stress granules, and exosome granules and found that hZCCHC7 can colocalize with proteins resident in exosome

granules and stress granules during viral infection, suggesting that hZCCHC7 may bind translationally-stalled viral RNAs and bring them to exosome granules for degradation.

To further characterize the regulation of TRAMP component nuclear export during infection, I investigated the viral signals necessary for this transport. I found that transfection with dsRNA is sufficient to induce relocalization, while infection with UV-inactivated viruses is not. Moreover, I tested the role of canonical innate immune adaptors in this process and found that the dsRNA sensor PKR promoted relocalization during Sindbis virus infection. Altogether, my results reveal that the presence of replicating viral RNA causes TRAMP components to be repurposed to a cytoplasmic surveillance role in several classes of RNP granules including stress granules and exosome granules. There, they selectively engage viral RNAs for degradation to restrict a broad range of viruses.

TABLE OF CONTENTS

LIST OF TABLES AND ILLUSTRATIONS

I. INTRODUCTION

RNA decay

While much of RNA biology focuses on regulation of RNA transcription, RNA decay is also tightly regulated. Controlled RNA degradation is essential for maturation of complex RNAs, degradation of misprocessed RNAs, and rapid downregulation of cohorts of RNAs in response to particular stimuli. Partial degradation of RNAs is an important part of processing; a plethora of RNAs, including rRNAs, snRNAs, and snoRNAs, must be trimmed to their mature forms (Allmang et al. 1999a). Additionally, RNA degradation acts as a quality control measure to prevent aberrant species of RNA from building up and occupying or disabling either the translational machinery or other RNA-binding proteins. Moreover, RNAs which fail to be properly matured, such as hypoadenylated mRNAs and hypomodified tRNAs, are degraded before they can leave the nucleus (Kadaba 2004; Milligan et al. 2005). Additional checkpoints such as nonsense-mediated decay or no-go decay detect stalled ribosomes or premature stop codons and degrade the aberrant mRNA messages that caused these problems in order to release the translational machinery (Isken and Maquat 2007). More recent studies have shown that RNA decay also serves a key role in post-transcriptional regulation of groups of RNAs, known as regulons, which are rapidly co-regulated through specific recognition of sequences in their 5' and 3' UTRs such as AU-rich elements (AREs) (Keene 2007).

5' decapping and decay

RNA decay is largely dependent on exonucleases and can proceed from either the 5' or 3' end of an RNA transcript. Messenger RNAs targeted for decay are first deadenylated by the CCR4-NOT complex, often assisted by other deadenylating enzymes, before they can be degraded (Lejeune et al. 2003; Parker and Sheth 2007). Though deadenylation is the first and rate-limiting step in mRNA degradation, it is sometimes reversible, and can act to "pause" translation of mRNAs rather than degrading them (Huarte et al. 1992). Removal of the 5' cap of RNA by decappers such as Dcp2 is irreversible, and permits degradation by the 5' to 3' exonuclease Xrn1 (Hsu and Stevens 1993; Muhlrad et al. 1994). This process is largely conserved from yeast to mammals,

though mammals have developed multiple partially redundant decapping enzymes for different degradation methods; Dcp2 is preferentially utilized in nonsense-mediated decay, while Nudt16 is preferentially involved in degradation of mRNAs containing AREs or 5' terminal oligopyrimidines (Li et al. 2011; Hopkins et al. 2015).

P-bodies

Deadenylation, decapping, and 5' degradation activities are especially concentrated at ribonucleoprotein (RNP) structures called processing bodies (P-bodies). These structures consist primarily of deadenylated mRNAs targeted for decay as well as components of the decapping and 5' degradation machinery, including Dcp2, its activators, and Xrn1 (Sheth and Parker 2003; Parker and Sheth 2007). RNAs sent to P-bodies are removed from translation, and can either be degraded or subsequently returned to the active pool of mRNAs (Brengues et al. 2005). Though P-bodies are present in normal cells at baseline, their number and size increase in response to a variety of stressors such as cold-shock or arsenic treatment (Kedersha et al. 2005; Ayache et al. 2015). They can interact and exchange RNAs with other RNP granules such as stress granules, which are composed of translationally-stalled RNAs and chaperone proteins (Kedersha et al. 2005; Wilczynska et al. 2005). There is evidence that P-bodies are a consequence of high concentrations of mRNAs undergoing decay rather than being necessary for decay; P-body integrity is RNA-dependent, and P-body structure can be disrupted without preventing RNA degradation (Teixeira et al. 2005; Eulalio et al. 2007). Furthermore, upregulation of 5' decapping and decay can prevent formation of the P-body RNP structure by depleting RNA targets (Hopkins et al. 2015).

The 3' to 5' RNA exosome

Many RNA decay roles also employ 3' to 5' degradation, mediated by the RNA exosome complex. The exosome is a barrel-like complex consisting of a hexameric structure (6 proteins with RNase PH homology) and a cap structure (3 proteins with S1 RNA-binding domains)

(Raijmakers et al. 2002; Liu et al. 2006; Schneider and Tollervey 2013). These structural components of the exosome form an internal channel wide enough to permit entry of single-stranded but not double-stranded RNA (Makino et al. 2013). Exosome proteins share structural and sequence homology to RNases; however, the structural components of the exosome are not believed to contribute directly to RNA degradation *in vivo.* Rather, in yeast where it has been highly characterized, the 3' to 5' exonuclease activity is performed by two exosome-associated RNA exonucleases: Rrp6, which is exclusive to the nucleus, and Dis3, which is present in both the nucleus and the cytoplasm (Mitchell et al. 1997; Allmang et al. 1999b; Dziembowski et al. 2007).

The exosome is both structurally and functionally conserved from yeast to humans (Houseley and Tollervey 2009). As such, mutations in the yeast exosomal genes Rrp4, Csl4, or Dis3 can be complemented with the human orthologs to rescue function (Allmang et al. 1999b). Despite this conservation, the localization of the exosome exonucleases has diverged over evolutionary history. Rrp6 is present in both the nuclear and cytoplasmic fractions of human cells, and Dis3 has two additional paralogs in humans, Dis3L1 and Dis3L2, which function exclusively in the cytoplasm (Tomecki et al. 2010). Dis3L2, which lacks the exosome-associating PIN domain, operates independently of the larger exosome complex in a separate 3' to 5' degradation system which favors terminally uridylated RNAs (Chang et al. 2013; Ustianenko et al. 2013; Thomas et al. 2015).

Exosome cofactor complexes

Though the exosome degrades RNAs indiscriminately *in vitro*, it degrades RNAs *in vivo* in a regulated fashion using RNA-binding cofactor complexes (Houseley et al. 2006). All known exosome cofactor complexes are anchored by helicases. The definitive role of these helicases is unknown, but it is hypothesized that they unwind higher-order structures to permit single-stranded RNA to be inserted into the exosome (de la Cruz et al. 1998). The exosome targets different

RNAs for processing and degradation in the nucleus, nucleolus, and cytoplasm, and thus relies on different cofactors in each subcellular compartment to target RNAs for degradation (Figure 1). Two major complexes, the cytoplasmic Ski and nuclear TRAMP complexes, have been extensively characterized in yeast.

The Ski complex

The Superkiller (Ski) complex is the major cytoplasmic exosome cofactor complex in yeast, named for the “superkilling” phenotype of dsRNA viruses, which are lethal to yeast deficient in these genes (Toh-E et al. 1978). The Ski genes were identified before the discovery of the exosome, and though mutants in Ski genes lead to increased viral RNA, this has not yet been definitively linked to exosomal RNA degradation (Masison et al. 1995). The Ski complex consists of a DExH/D-box helicase, Ski2, a tetratricopeptide repeat-containing protein, Ski3, and a WD repeat-containing protein, Ski8 (Brown et al. 2000). It also uses the adaptor G-protein Ski7 to interact with the exosome (Araki et al. 2001). In addition to affecting the half-life of normal mRNAs, the Ski complex is involved in recruiting the exosome to RNAs targeted for nonsense-mediated decay as well as nonstop decay (Jacobs Anderson and Parker 1998; van Hoof et al. 2002; Horikawa et al. 2016). Orthologs for all three Ski genes are present in higher organisms including *Drosophila* and humans and have RNA decay roles, though their specific targets remain unclear (Orban and Izaurralde 2005; Zhu et al. 2005).

The TRAMP complex

The yeast TRAMP (Trf4/5-Air1/2-Mtr4-Polyadenylation) complex, located in the nucleus, has known roles in degrading hypomodified tRNAs, hypoadenylated mRNAs, and in the processing of normal rRNA, snRNA, and snoRNA during maturation (Kadaba 2004; LaCava et al. 2005; Milligan et al. 2005; Wyers et al. 2005; Houseley et al. 2006). The complex is anchored by a DExD/H box helicase, Mtr4, which binds the other TRAMP components through its arch domain (de la Cruz et al. 1998; Jackson et al. 2010). The Zn-knuckle RNA-binding proteins Air1 and Air2

are believed to convey RNA-binding specificity to the complex, identifying specific targets for degradation (Schmidt et al. 2012). These two proteins are partially functionally redundant; mutants in each protein accumulate different but overlapping populations of snRNAs, snoRNAs, and mRNAs, and double-mutant strains fail to grow. Trf4 and Trf5 are non-canonical poly(A) polymerases which add 5-6 adenines to RNAs bound to the TRAMP complex (LaCava et al. 2005). The addition of short poly(A) tails creates an unstructured 3' end which is thought to facilitate insertion of the RNA into the exosome barrel (Paolo et al. 2009). Furthermore, this adenylation parallels the role of polyadenylation in *E. coli*, which, unlike eukaryotic polyadenylation, targets RNAs for decay (Li et al. 2002; Deutscher 2006). In addition to the canonical TRAMP complex, Mtr4 can form other modular cofactor complexes by associating with the adaptors Nop53 or Utp18, which assist in some rRNA maturation steps (Thoms et al. 2015).

The TRAMP complex is conserved in humans, but nuclear RNA degradation has additional complexity. As in yeast, human TRAMP is composed of a helicase, hMTR4, a zinc-finger Air-like protein, hZCCHC7, and a poly(A) polymerase, hTRF4-1 or hTRF4-2 (Fasken et al. 2011; Lubas et al. 2011). However, unlike yeast TRAMP, the human TRAMP complex is restricted to the nucleolus, and is only known to process rRNA (Shcherbik et al. 2010; Lubas et al. 2011). Most of the yeast TRAMP targets, such as mRNAs, snRNAs, snoRNAs, and promoter upstream transcripts (PROMTs) appear to be regulated in human cells by the nucleoplasmic NEXT (Nuclear EXosome Targeting) complex, which shares hMTR4 with the TRAMP complex but also contains the zinc-finger protein hZCCHC8 and the RNA-binding motif protein RBM7 (Lubas et al. 2011; Andersen et al. 2013; Lubas et al. 2015). Other targets are likely to exist for mammalian TRAMP-like complexes; murine cells depleted of Mtr4 accumulate adenylated 5' miRNA fragments, suggesting that adenylation and Mtr4-mediated degradation may be important for these RNAs (Dorweiler et al. 2014). The full spectrum of Mtr4-anchored complexes in mammals and the regulation of other classical yeast TRAMP targets (such as misprocessed tRNAs) remain unclear.

Exosome cofactor localization

The localization of exosome core and cofactor components in yeast is generally used as a basis for understanding exosomal regulation in different cellular compartments across species. However, the localization of exosome cofactors is poorly conserved between species. For example, while Rrp6 is exclusively nuclear in yeast, it localizes to both the nucleus and cytoplasm in human cells (Allmang et al. 1999b; Tomecki et al. 2010). Furthermore, though the yeast Ski complex is restricted to the cytoplasm, the human Ski complex components Ski2 and Ski8 both localize to the nucleus as well as the cytoplasm and associate with transcriptionally active genes (Brown et al. 2000; Zhu et al. 2005). Even within fungi, yeast Mtr4 is exclusively nuclear, while in the mold *Neurospora,* Mtr4 also localizes to the cytoplasm, where it functions in regulating circadian rhythms as well as maturation of microRNA-like RNAs (Guo et al. 2009; Xue et al. 2012). Thus, it is likely that there is more complexity in the regulation of the exosome and its cofactors outside of their canonical roles.

Viral RNAs as degradation targets

Cellular RNAs targeted for degradation have sequences or structures that make them susceptible to recognition by the RNA degradation machinery, such as missing 5' caps or poly(A) tails, or regulatory sequences in the 5' or 3' UTRs. Similarly, the RNAs produced by RNA viruses can differ substantially from normal cellular RNAs, leading to recognition by host RNA-binding proteins. RNA viruses encode an RNA-dependent RNA polymerase (RdRp) which replicates RNA through the generation of antigenome intermediates. This creates transient dsRNA structures and 5' triphosphate ends not usually present in cellular mRNAs (Moon and Wilusz 2013). Furthermore, cytoplasmic RNA viruses are isolated from the normal cellular capping machinery, and thus the RdRp or associated viral proteins must generate a cap or cap mimic, or acquire one from cellular mRNA through a process known as cap-snatching (Decroly et al. 2012). Additionally, viral RNAs must protect their 3' ends, either through RdRp-mediated polyadenylation or through 3' structures which impede exonucleases (Moon et al. 2012b). Protective 3' structures act either

by recruiting protective proteins like poly(A) binding protein, or by directly inhibiting exonuclease progression (Ford and Wilusz 1999; Iwakawa et al. 2012). All of this must be done with limited protein machinery, as RNA virus genomes are generally small.

Innate immune recognition of viral RNA

RIG-I like receptors

The RNAs produced during viral replication serve as an important sign of infection in mammalian cells. Cytosolic viral RNAs are primarily recognized by the RIG-I-like receptors (RLRs), RIG-I and MDA-5, which are both DExD/H-box RNA helicases (Barbalat et al. 2011). Each recognizes different foreign RNA structures. RIG-I recognizes short dsRNAs and RNAs with 5' triphosphates, and has roles in restricting viruses such as paramyxoviruses, orthomyxoviruses, and flaviviruses (Hornung et al. 2006; Kato et al. 2006). Meanwhile, MDA-5 recognizes longer dsRNAs and higher-order RNA structures, and is integral for recognition of picornaviruses (Gitlin et al. 2006; Pichlmair et al. 2009). Both are able to respond to the synthetic dsRNA polyinosinic-polycytidylic acid (poly(I:C)) dependent on length; long poly(I:C) is a traditional ligand of MDA-5, while shortened poly(I:C) can activate RIG-I (Kato et al. 2008). The RLRs primarily act by signaling the interferon system through their adaptor, MAVS; interferon in turn signals a variety of antiviral programs (Kawai et al. 2005; Meylan et al. 2005; Seth et al. 2005; Xu et al. 2005). Diverse RNA viruses are able to evade the interferon system and thus avoid the consequences of RLR detection; for example, both Rift Valley fever virus (RVFV) and Sindbis virus (SINV) make accessory proteins (NSs and nsP2) which inhibit the transcription of interferon genes (Bouloy et al. 2001; Frolova et al. 2002; Billecocq et al. 2004; Gorchakov et al. 2004; Garmashova et al. 2006).

Toll-like receptors

Endosomal RNAs are sensed by TLR3 and TLR7, which detect dsRNA and ssRNA respectively, and signal interferon through the adaptors TRIF and MyD88 (Barbalat et al. 2011). Many cell

culture systems such as the U2OS osteosarcoma cells used in this dissertation lack cell surface TLR's such as TLR3 and can only effectively sense cytosolic RNA (Laredj and Beard 2011).

PKR

Mammalian cells possess several other sensors of viral RNA. Within the cytoplasm, the dsRNA-activated protein kinase PKR is upregulated by interferon signaling (Clemens et al. 1993; Gale and Katze 1998). Activation of PKR by dsRNAs from viruses or poly(I:C) induces autophosphorylation of PKR and subsequent phosphorylation of eIF2α, shutting down protein translation in order to block synthesis of viral proteins (Meurs et al. 1990; Hinnebusch 1994; Balachandran et al. 2000; Chacko and Adamo 2011). Several viral methods to avoid PKR-mediated translational shutdown exist in different virus species; RVFV infection causes PKR degradation, and the SINV genome, despite activating PKR, has internal sequences which allow viral proteins to be translated efficiently despite widespread host translational shutdown (Gorchakov et al. 2004; Ikegami et al. 2009; Kainulainen et al. 2016). PKR may also have additional phosphorylation targets which are yet to be discovered. Several studies of viruses such as vaccinia and rotavirus have found that some MAVS-mediated signaling requires PKR and vice-versa, suggesting that the two cytosolic viral RNA sensor pathways have some crosstalk (Zhang et al. 2009; Sen et al. 2011).

OAS and RNASEL

Part of the interferon-induced antiviral response targets viral RNA for degradation. Another cytoplasmic sensor of viral dsRNA, oligoadenylate synthetase (OAS), is upregulated by treatment with interferon (Hovanessian et al. 1987; Jensen and Thomsen 2012). Upon sensing viral RNA, OAS synthesizes 2,5-adenylate, which in turn serves as an activator of RNASEL, a cytoplasmic RNase. RNASEL indiscriminately cleaves viral RNA and cellular RNA, creating an antiviral and pre-apoptotic pathway (Castelli et al. 1997). Recent studies have begun to characterize RNAs as more or less susceptible to RNASEL and to further postulate functions for RNASEL-mediated

regulation of RNAs. Regardless, RNASEL broadly cleaves cellular RNAs and thus serves as a precursor to cell death rather than as a targeted antiviral response (Brennan-Laun et al. 2014).

Antiviral roles for the RNA silencing machinery

Just as mammalian cells utilize RNA helicases (the RLRs) to recognize cytosolic viral RNA, the closest *Drosophila* homolog, Dicer-2, recognizes the dsRNA intermediates generated during viral infection (Lee et al. 2004; Galiana-Arnoux et al. 2006; Takeuchi and Akira 2008). Dicer-2 functions as both sensor and effector; in addition to its helicase domain, it has an RNase III domain which cleaves dsRNAs into siRNAs, which in turn are loaded into the Argonaute 2-containing RISC (RNA-induced silencing complex), preventing RNA transcription and cleaving viral RNAs (Wang et al. 2006). The antiviral RNA silencing pathway in *Drosophila* is essential to immunity; flies with mutations in this pathway succumb to viral infection much more rapidly. In turn, natural *Drosophila* pathogens such as *Drosophila* C virus encode suppressors of RNAi to evade this type of degradation (Galiana-Arnoux et al. 2006; van Rij et al. 2006). Dicer-2 likely has silencing-independent antiviral functions as well which may more closely parallel the signaling functions of the RLRs; recent evidence shows that Dicer-2 induces transcription of the antiviral factor Vago in addition to its role in silencing, suggesting that it is a regulator of antiviral transcription during viral infection in fly cells (Deddouche et al. 2008).

RNA silencing has not yet been clearly demonstrated as a biologically relevant antiviral pathway in mammalian cells; mammalian Dicer is functionally orthologous to *Drosophila* Dicer-1 rather than Dicer-2, and thus primarily processes pre-miRNAs rather than viral dsRNAs (Lee et al. 2004). However, recent work has suggested that under some conditions mammalian cells can use components of the silencing machinery to degrade viral RNA. Murine embryonic stem cells have been shown to make Dicer-dependent siRNAs in response to several RNA viruses (Maillard et al. 2013). Infection of murine fibroblasts with SINV containing a pri-miRNA sequence results in the formation of mature miRNAs which restrict replication of the virus (Shapiro et al. 2010).

Finally, Drosha, a nuclear RNase III enzyme which has a canonical role in processing pri-miRNAs to pre-miRNAs before they are exported to the cytoplasm for Dicer processing, has recently been identified as an antiviral factor (Shapiro et al. 2014). Drosha is exported to the cytoplasm in response to infection with a variety of RNA viruses, and is capable of cleaving viral RNA in the cytoplasm to restrict replication.

Antiviral roles for 5' to 3' RNA decay

Several RNA decay pathways are emerging as antiviral and can target viruses that antagonize classical innate immune RNA recognition pathways. The 5' to 3' RNA decay machinery can inhibit viral replication in a number of different ways (Figure 2). Studies have shown that the cytoplasmic 5' RNA exonuclease, Xrn1, can target flavivirus RNAs and in response these viruses antagonize Xrn1 by encoding structured RNAs that result in Xrn1 stalling (Jones et al. 2010; Silva et al. 2010; Moon et al. 2012a). Furthermore, poliovirus induces the degradation of host 5' decay factors such as Xrn1 and Dcp2 through a combination of viral and host proteases, suggesting evolutionary pressure to evade host 5' RNA decay machinery (Dougherty et al. 2011). In addition to directly targeting viral RNAs, the 5' decay machinery can also impact viral replication indirectly. Recent studies showed that decappers limit the pool of host mRNAs available for RVFV to cap snatch from, attenuating replication in both insects and mammals (Hopkins et al. 2013; Hopkins et al. 2015). Furthermore, in mammals, RVFV infection induces NUDT16-mediated decapping and decay of 5' TOP-containing mRNAs encoding the translational machinery, limiting both global and virus-specific translation (Hopkins et al. 2015).

In addition, P-body structure is disturbed during infection with a number of viruses. This can be due to an increase in RNA decay; the upregulation of 5' decay in RVFV infection prevents the formation of P-bodies due to depletion of the RNA targets around which they nucleate (Hopkins et al. 2015). In contrast, poliovirus induces the degradation of 5' decay proteins such as Xrn1 and Dcp1a, preventing P-body formation (Dougherty et al. 2011). Amazingly, P-body components can

be repurposed by viruses to facilitate infection; flaviviruses relocalize P-body components to viral replication centers, where they bind viral 3' UTRs and are necessary for efficient viral replication (Emara and Brinton 2007; Ward et al. 2011; Chahar et al. 2013).

Antiviral roles for the RNA exosome

Studies have implicated the 3'-5' exosome in antiviral defense in several contexts. A number of antiviral RNA-binding proteins co-immunoprecipitate with the exosome, suggesting that their mechanism of action may involve exosomal degradation (Figure 2). DDX17 restricts RVFV by binding a miRNA-like stem loop structure encoded in the viral RNA (Moy et al. 2014a). Though its mechanism of restriction is unknown, DDX17 binds to exosomal proteins, suggesting the possibility that it directly recruits the exosome to degrade viral RNA (Chen et al. 2008; Lubas et al. 2011). DDX60, which is antiviral against vesicular stomatitis virus (VSV), also binds the exosome (Miyashita et al. 2011). However, DDX60 does not depend on the exosome for its antiviral function, but rather bridges viral RNA and the RLRs to potentiate signaling. The cytidine deaminase AID, which binds the exosome and hepatitis B virus (HBV) RNA in a complex, is antiviral when overexpressed only if the exosome is present, suggesting the possibility that it recruits the exosome to degrade HBV RNA (Liang et al. 2015). The zinc-finger antiviral protein (ZAP) binds SINV and retrovirus RNA as well as components of the exosome (Guo et al. 2004). In overexpression systems, ZAP restricts MLV viral replication in an exosome-dependent fashion, as well as affecting the expression and stability of viral luciferase reporters for both MLV and HIV (Guo et al. 2007; Zhu et al. 2011). It remains unclear if the exosome is required for the activity of endogenous ZAP or degrades ZAP-bound viral RNAs. The cell biology of these factors is largely unexplored but overexpressed DDX60 and ZAP localize to the cytoplasm, while overexpressed AID binds the exosome in both the nucleus and cytoplasm (Liu et al. 2004; Miyashita et al. 2011; Liang et al. 2015). DDX17 moves from the nucleus to the cytoplasm in response to viral infection (Moy et al. 2014a).

One final role was demonstrated for the exosome cofactor Ski complex in immunity, though this role was in preventing autoimmunity rather than restricting viral replication. The human Ski helicase SKI2L was found to degrade extraneous RIG-I targets in uninfected cells, protecting cells from autoimmune activation (Eckard et al. 2014). Furthermore, patients with mutations in this gene were identified and had anomalously high interferon signatures. Though no core exosome components or exonucleases were shown in this role, it does suggest that the Ski complex, potentially with the exosome, may serve to protect the intracellular milieu from overactive RIG-I signaling, paralleling the role of the DNA exonuclease TREX, which degrades cytoplasmic DNA to prevent overactivation of the DNA sensor cGAS (Stetson et al. 2008; Crow and Rehwinkel 2009; Cai et al. 2014).

The arthropod-borne viruses

Arthropod-borne viruses (arboviruses) are transmitted from arthropod hosts such as mosquitos to vertebrates such as humans (Weaver and Barrett 2004). All arboviruses that infect humans are RNA viruses, and belong to the *Alphaviridae*, *Flaviviridae*, or *Bunyaviridae* families, though members of other virus families such as *Rhabdoviridae* can be transmitted to other animals from arthropods (Weaver and Reisen 2010). Both alphaviruses and flaviviruses are positive-sense RNA viruses, and thus have a genome which functions as an mRNA. In contrast, bunyaviruses and rhabdoviruses are negative-sense RNA viruses which must bring the RdRp within the viral particle in order to synthesize positive-sense mRNA from the genome (Tao and Ye 2010). Three viruses were used in this dissertation: vesicular stomatitis virus, Sindbis virus, and Rift Valley fever virus.

Vesicular stomatitis virus

Vesicular stomatitis virus (VSV) is a negative-sense rhabdovirus transmitted to cattle from biting flies (Letchworth et al. 1999). It is an important model virus, serving as the prototype for more deadly rhabdoviruses such as rabies virus. It has a single 5’ triphosphorylated genomic RNA

which is tightly encapsidated by the nucleocapsid protein. The mRNAs, N, M, G, P, and L, are synthesized by the RdRp through a start-stop mechanism which results in a capped and polyadenylated mRNA for each gene (Schnell et al. 1996). The RdRp synthesizes a 5' cap at the beginning of each mRNA, and polyadenylates by "slipping" during transcription of a U-rich track at the end of each mRNA (Schubert et al. 1980; Koonin and Moss 2010).

Sindbis virus

Sindbis virus (SINV) is a positive-sense alphavirus transmitted to humans by mosquitos, causing a mild febrile illness (Strauss and Strauss 1994). It serves as the prototype for emerging alphaviruses including chikungunya virus. SINV has a single genomic RNA which is capped and polyadenylated and serves as an mRNA for the nonstructural polyprotein, which is cleaved into several functional proteins. During replication it synthesizes a negative-sense antigenome as well as a positive-sense subgenomic mRNA expressing only the structural proteins. The SINV replicase complex synthesizes a 5' cap for both the genomic and subgenomic RNAs. Though SINV RNAs are covered by a nucleocapsid in the virion, they are not protected from RNAses *in vitro,* making them accessible by RNA decay machinery *in vivo* (Coombs et al. 1984). This is consistent with the fact that the genomic and subgenomic RNAs serve as messenger RNAs and thus require access to the host translational machinery. To counter this vulnerability, SINV mRNA has evolved sequences in its 3' UTR which protect it from host deadenylation (Garneau et al. 2008).

Rift Valley fever virus

Rift Valley fever virus (RVFV) is a bunyavirus, a negative-sense trisegmented RNA virus which is transmitted to humans by mosquitos (Bird et al. 2009). It causes Rift Valley fever, which results in flu-like symptoms in humans with occasional severe complications such as hepatitis or retinitis. It is of particular concern agriculturally, as RVFV causes abortion and juvenile death in livestock populations. RVFV has three RNA segments of different sizes. The large segment contains the

polymerase gene (L), the medium segment encodes a polyprotein which is processed into two glycoproteins (Gn and Gc) and a nonstructural protein (NSm), and the small segment encodes nucleocapsid (N) as well as a nonstructural protein (NSs). The small segment is unique in that the NSs gene is transcribed from the antigenome rather than the genome, making this RNA segment ambisense (Bouloy and Weber 2010). N and NSs mRNAs are non-overlapping, and each is significantly shorter than the genomic and antigenomic small segment RNA. Though the genomic and antigenomic RNAs are not capped or adenylated, they are tightly encapsidated by nucleocapsid protein which protects them from RNases *in vitro (Kolakofsky and Hacker 1991)*. Synthesis of RVFV mRNAs involves cytoplasmic cap-snatching of host mRNAs targeted for degradation, and thus mRNAs possess a natural 5' cap and 12-18 nt of host mRNA sequence (Patterson et al. 1984; Reguera et al. 2010; Hopkins et al. 2013; Hopkins et al. 2015). However, these mRNAs are not polyadenylated; each mRNA has a different 3' UTR, which are hypothesized to be protected by stem-loop structures (Ikegami et al. 2007). How these mRNAs are translated without polyadenylation is not yet well understood.

Aims of present studies

The work of this dissertation arises from the identification of several exosome genes as antiviral from *Drosophila* RNAi screens in VSV, SINV, and RVFV. In chapter 2, I demonstrate a broadly antiviral role for the exosome and two components of the TRAMP cofactor complex, Mtr4 and Zcchc7. I found that this antiviral role is conserved from flies to human cells, and involves the export of basally nucleolar TRAMP components to the cytoplasm upon cellular sensing of viral infection. These components accumulate in cytoplasmic granules in infected cells, and immunoprecipitate with each other, the RNA exosome, and viral mRNA. I found that the exosome regulates RVFV mRNA stability specifically through recognition of sequences in the 3' UTR. In chapter 3, I explore the cellular sensing that leads to TRAMP component relocalization during SINV infection. I show that sensing of viral RNA rather than viral protein triggers TRAMP export, and that this export is dependent on PKR. Previous work has shown that SINV viral replication

can induce the formation of RNP granules such as stress granules (Onomoto et al. 2012). I demonstrate here that the cytoplasmic TRAMP punctae can colocalize with stress granule and exosome granule markers. I suggest that TRAMP identifies translationally-stalled viral RNA targets in stress granules and brings them to exosome granules for decay, linking these two types of RNP granule. Together, my dissertation work characterizes a new antiviral role for the exosome and two TRAMP cofactors, as well as a new mechanism that regulates viral RNA decay.

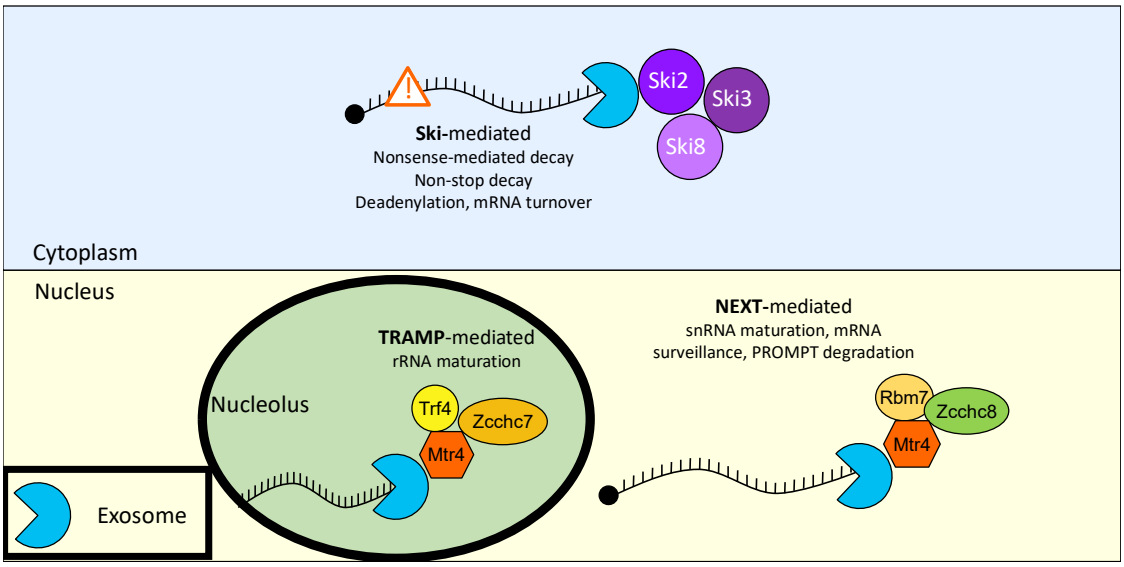

Figure 1: The cofactor complexes of the human RNA exosome. 3'-5' RNA exosome degrades diverse RNA species in different subcellular compartments and thus relies on different cofactor complexes to identify RNA targets in the cytoplasm, nucleus, and nucleolus. Each complex is anchored by a helicase (Ski2 in the cytoplasm, Mtr4 in the nucleus and nucleolus) and uses other RNA-binding proteins to identify specific RNA targets for degradation. These are the complexes in humans and other higher animals; in yeast, TRAMP is the sole nuclear cofactor complex and performs the roles of human TRAMP and NEXT.

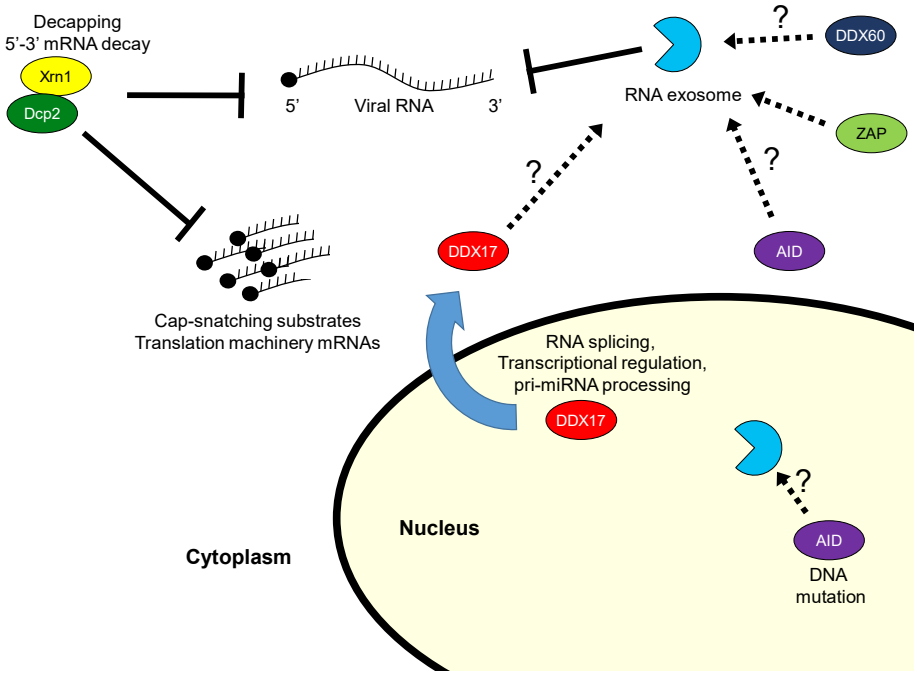

Figure 2: Both 5' and 3' decay machinery restrict virus infection. The 5' to 3' decay machinery can inhibit viral infection directly through degradation of viral RNA (flaviviruses) or indirectly through decapping and degradation of RNAs needed for viral transcription and translation (bunyaviruses). The 3' to 5' decay machinery, the RNA exosome, interacts with a variety of RNA-binding proteins, some of which are exported to the cytoplasm in response to viral infection. Recruitment of the exosome can result in degradation of viral RNA.

II. A CONSERVED VIRUS-INDUCED CYTOPLASMIC TRAMP-LIKE COMPLEX RECRUITS THE EXOSOME TO TARGET VIRAL RNA FOR DEGRADATION [1]

Background

RNA decay is tightly regulated to ensure cellular homeostasis. This requires specific recognition and targeting by RNA exonucleases (Garneau et al. 2007). The 5' RNA degradation machinery utilizes decapping enzymes to remove the 5' cap, allowing 5' to 3' exonucleases to degrade target RNA (Hsu and Stevens 1993; Muhlrad et al. 1994). Degradation from the 3' end is largely mediated by the RNA exosome, a highly conserved multisubunit complex generally consisting of 9 core factors that form a barrel structure (Schneider and Tollervey 2013). RNAs are inserted into this barrel and subsequently degraded by the two associated 3' to 5' exonucleases, Rrp6 and Dis3. Exosomal degradation has roles in normal RNA biogenesis and turnover as well as surveillance of aberrant RNAs including misfolded or mismodified tRNAs and mRNAs with defective polyadenylation (Allmang et al. 1999a; Kadaba 2004; Milligan et al. 2005). The exosome has also been implicated in regulation of RNA regulons, functionally related sets of mRNAs which are tightly co-regulated through common sequences in their 3' UTRs (Chen et al. 2001; Mukherjee et al. 2002; Keene 2007; Singer et al. 2012; Blackinton and Keene 2014).

Specificity for exosomal degradation is provided by RNA-binding cofactor complexes anchored by DExD/H-box helicases that directly associate with the target RNA and the exosome, inserting these RNAs for decay (Houseley and Tollervey 2009). The best-characterized cofactors are the yeast TRAMP (Trf4/5-Air1/2-Mtr4-Polyadenylation) and Ski (Superkiller) complexes, which have known roles in the nucleus and cytoplasm, respectively (Brown et al. 2000; LaCava et al. 2005;

---

[1] This chapter is reprinted from Molleston JM, Sabin LR, Moy RH, Menghani SV, Rausch K, Gordesky-Gold B, Hopkins KC, Zhou R, Jensen TH, Wilusz JE, and Cherry S. 2016. A conserved virus-induced cytoplasmic TRAMP-like complex recruits the exosome to target viral RNA for degradation. *Genes & Development* **30**: 1658-1670. With permission from Cold Spring Harbor Laboratory Press.

Vanácová et al. 2005; Wyers et al. 2005). In yeast, the TRAMP complex facilitates nuclear surveillance of improperly processed mRNAs, rRNAs, snRNAs, snoRNAs, and tRNAs, while the Ski complex is involved in mRNA turnover, nonsense-mediated decay, and nonstop decay (Anderson and Parker 1998; Kadaba 2004; Milligan et al. 2005; Wyers et al. 2005; Houseley et al. 2006). In human cells, the nuclear surveillance roles are only beginning to be elucidated, but appear to be further subdivided into two Mtr4-anchored complexes: human TRAMP is restricted to the nucleolus and engages rRNA precursors, while the NEXT (Nuclear Exosome Targeting) complex, which is restricted to the nucleoplasm, binds mRNAs, snRNAs, snoRNAs, and promoter upstream transcripts (PROMPTs) (Lubas et al. 2011; Andersen et al. 2013; Lubas et al. 2015). The full spectrum of RNA targets of these cofactor complexes and the exosome remains unknown.

Viral RNAs, much like aberrant cellular transcripts, differ from normal RNAs. These differences can include the presence of double stranded RNA structures, 5' triphosphates, and short or absent poly-A tails (Barbalat et al. 2011; Moon and Wilusz 2013). From mammals to arthropods, RNA-binding proteins can recognize these foreign RNA motifs and trigger a range of antiviral responses. Diverse helicases recognize viral RNAs; mammalian RIG-I and MDA5 recognize 5' triphosphates and long dsRNAs, respectively, to induce antiviral transcriptional responses (Hornung et al. 2006; Kato et al. 2006; Pichlmair et al. 2006), and DDX17 recognizes bunyaviral RNA stem-loops to restrict infection in both *Drosophila* and human cells (Moy et al. 2014a). Other RNA-binding proteins have been implicated in recognition or restriction of viral RNAs suggesting that there are additional players to be discovered (Guo et al. 2004; Miyashita et al. 2011; Dong et al. 2016).

Emerging evidence suggests that viral RNAs are targeted for decay. RNASEL, which is induced by interferon signaling, non-specifically degrades both viral and cellular RNA as a step toward cell death (Hassel et al. 1993; Castelli et al. 1997; Brennan-Laun et al. 2014). In contrast, recent

studies have shown that 5’ exonucleases and decapping machinery selectively target flaviviruses and bunyaviruses respectively (Hopkins et al. 2013; Moon and Wilusz 2013; Hopkins et al. 2015). The 3’ to 5’ RNA exosome and its associated co-factor complexes have been implicated in some immune functions, but are less understood. Early work showed that the yeast Ski complex restricts dsRNA viruses, though the mechanism is not clearly understood (Masison et al. 1995; Anderson and Parker 1998; Benard et al. 1998). More recently, the human Ski component hSKIV2L has been shown to regulate endogenous RIG-I RNA targets to prevent autoimmunity; however, it likely does so independent of the canonical Ski complex and the exosome (Eckard et al. 2014). Additionally, other mammalian antiviral RNA-binding proteins (ZAP, DDX60, and AID) have been shown to bind the exosome and in some cases depend on the exosome for their antiviral function; however, none of these factors has been shown to induce exosome-mediated degradation of viral RNAs (Guo et al. 2007; Miyashita et al. 2011; Liang et al. 2015). Furthermore, no studies have explored potential roles of the nuclear exosome cofactors in viral infection.

We performed a series of RNAi screens to identify previously unknown RNA processing factors that restrict RNA viruses. First, we screened a library of 177 genes implicated in RNA biology in *Drosophila* cells (Zhou et al. 2008) against two disparate arthropod-borne RNA viruses (arboviruses): vesicular stomatitis virus (VSV) and Sindbis virus (SINV). VSV is a negative-sense rhabdovirus which causes oral and skin lesions in livestock and an influenza-like fever in humans (Letchworth et al. 1999). SINV, a positive-sense alphavirus, causes chronic polyarthritic disease (Kurkela et al. 2005). Second, we mined our previously-published genome-wide RNAi screen against Rift Valley Fever virus (RVFV), a tri-segmented negative-sense bunyavirus which causes a febrile illness with 1-3% mortality in humans as well as abortions and juvenile mortality in livestock (Bird et al. 2009; Hopkins et al. 2013). The screens converged on the identification of the two exosome-associated exonucleases, Rrp6 and Dis3, as antiviral against all three viruses in insect cells. Since the exonucleases may have functions outside of the RNA exosome (Schneider et al. 2007; Callahan and Butler 2008; Kiss and Andrulis 2011), we tested the role of two core

exosome structural components, Rrp4 and Rrp41, and found that these also restrict infection. Since the exosome does not target RNAs directly but uses cofactor complexes, we screened orthologs of three major cofactor complexes, Ski, NEXT, and TRAMP, for their roles in viral infection. These studies revealed that only the TRAMP-associated helicase dMtr4 (l(2)35Df) and TRAMP-associated zinc-finger RNA-binding protein dZcchc7 (CG9715) are antiviral in flies. We extended our studies to human cells where we found that the broadly antiviral role for the RNA exosome and TRAMP orthologs hMTR4 and hZCCHC7 is conserved. Mechanistically, we found that infection with these cytoplasmic viruses induces the export of hMTR4 and hZCCHC7, which are nuclear in uninfected cells, to the cytoplasm, where they form a complex with the exosome as well as viral RNAs. Furthermore, we found that viral RNAs are shortened at the 3' end and are stabilized by disruption of the exosome or the RNA binding protein hZCCHC7. Additionally, we found that the RVFV mRNA 3' UTR confers exosomal regulation. These findings show that a virus-induced cytoplasmic TRAMP-like complex specifically targets viral RNAs for exosome-mediated degradation to attenuate infection.

Results

RNAi screen identifies the RNA exosome as antiviral in Drosophila cells

We previously identified an antiviral role in *Drosophila* for dArs2 and the nuclear cap-binding complex through RNA silencing (Sabin et al. 2009). We hypothesized that additional genes involved in RNA metabolism and degradation have antiviral roles against RNA viruses, so we conducted a targeted RNAi screen against a panel of 177 genes with previously characterized roles in RNA metabolism in *Drosophila* cells, including dArs2 (Zhou et al. 2008). In order to identify broadly antiviral genes, this gene set was screened against two disparate arthropod-borne viruses: VSV and SINV. *Drosophila* DL1 cells were treated with previously validated double-stranded RNAs (dsRNAs) targeting each gene in the panel and knockdown was allowed to proceed for three days, after which cells were infected with GFP-expressing VSV or SINV and percent infection was quantified by automated fluorescence microscopy. Each screen was

performed in duplicate, and genes with robust Z-scores ≥ 2 for percent infection in both replicates ($p<0.001$) were considered antiviral hits. Using these metrics, the positive control dArs2 as well as 25 other genes were antiviral against both viruses (Table 1). One of these hits, dRrp6, is a catalytic 3'-5' exonuclease associated with the RNA exosome, and the only member of the RNA exosome in the 177-gene screening set (Figure 3A,B). We compared these data to our published genome-wide RVFV screen and found that another exosome-associated exonuclease, dDis3, was a validated antiviral hit (Hopkins et al. 2013). The identification of exosome components in multiple screens suggested a broadly antiviral role, and thus we focused on the exosome for further study.

Since these exonucleases can potentially function outside of the canonical exosome (Schneider et al. 2007; Callahan and Butler 2008; Kiss and Andrulis 2011), we tested two core components of the exosome, dRrp4 and dRrp41. In addition, we validated our screening results using independent dsRNAs against dRrp6 and dDis3. Knockdown of dRrp4 and dRrp6 was verified by immunoblot of ectopically expressed tagged proteins (Hessle et al. 2009), as antibodies against the endogenous proteins are not commercially available (Figure 4A). Depletion of each of these genes had little impact on cell viability as measured by cell number (Figure 4B) but led to significantly increased infection of VSV, SINV, and RVFV as measured both by immunofluorescence microscopy (Figure 3C,D) and RT-qPCR (Figure 3E). The effect of the exonucleases dRrp6 and dDis3 on viral RNA was stronger than that of the structural genes dRrp4 and dRrp41, suggesting the possibility that the exonucleolytic activity of the exosome is limiting. Taken together, these studies suggest that the RNA exosome complex restricts a broad range of RNA viruses in *Drosophila* cells.

Orthologs of TRAMP complex components are antiviral in Drosophila

The exosome is dependent on RNA-binding cofactor complexes to bring RNA targets to the exosome for degradation. The best-characterized of these are the Ski, TRAMP, and NEXT

complexes (Lubas et al. 2011; Schneider and Tollervey 2013). The Ski complex is cytoplasmic and consists of a DExH/D-box helicase, Ski2, a tetratricopeptide repeat-containing protein, Ski3, and a WD repeat-containing protein, Ski8, all of which have characterized *Drosophila* orthologs (Brown et al. 2000; Orban and Izaurralde 2005). Depletion of the three Ski components (dSki2/tst, dSki3/CG8777, and dSki8/CG3909) had no significant effect on viral infection (Figure 5B,6A)

The TRAMP complex, which is nuclear in yeast and nucleolar in humans, consists of a DExH/D-box helicase, Mtr4, a poly-A polymerase, Trf4/5 (Trf4-1 is the active TRAMP polymerase in *Drosophila*), and a zinc-finger RNA-binding protein, Air1/2 (LaCava et al. 2005; Houseley and Tollervey 2008; Nakamura et al. 2008; Fasken et al. 2011; Lubas et al. 2011). The *Drosophila* ortholog of Air1/2 is not well characterized: previous BLAST searches with *S. cerevisiae* Air1p and the human Air ortholog hZCCHC7 found that CG9715 is the closest *Drosophila* ortholog, which we will refer to as dZcchc7 (Fasken et al. 2011; Lubas et al. 2011). Mining of our recent RVFV genome-wide RNAi screen revealed that dZcchc7 was also a validated antiviral gene (Hopkins et al. 2013).

In humans, Mtr4 forms an additional nuclear complex called the NEXT (Nuclear Exosome Targeting) complex which is excluded from nucleoli (Lubas et al. 2011). This complex is composed of hMTR4, hZCCHC8 (a zinc-finger RNA-binding protein similar to hZCCHC7), and hRBM7, an RNA-binding motif-containing protein (Guo et al. 2003; Gustafson et al. 2005).

We tested each of the *Drosophila* TRAMP orthologs (dMtr4/l(2)35Df, dTrf4-1, and dZcchc7/CG9715) as well as the NEXT orthologs (dZcchc8/CG4622 and dRbm7/CG11454) for their roles in antiviral defense. While depletion of the TRAMP component dTrf4-1 or the NEXT components dZcchc8 and dRbm7 did not increase infection, depletion of dMtr4 or dZcchc7 significantly increased infection of VSV, SINV, and RVFV both by microscopy (Figure 5A,B) and RT-qPCR (Figure 5C). Knockdown of dMtr4 was confirmed by immunoblot of tagged overexpressed dMtr4 (Figure 6B), and RT-qPCR of endogenous transcripts for the other genes

(Figure 6C). Altogether, this demonstrates that the helicase (dMtr4) and RNA-binding zinc-finger (dZcchc7) TRAMP orthologs have a role in control of viral infection in *Drosophila* cells.

The exosome and TRAMP orthologs restrict RVFV infection of adult flies

By taking advantage of genome-wide *in vivo* RNAi transgenic libraries, we tested the roles of exosome and TRAMP genes during infection of adult animals. Because these genes are essential, *in vivo* RNAi was performed in a non-essential organ, the fat body, which is the primary target of RVFV infection in adult flies (Moy et al. 2014b). We expressed inverted repeats targeting dRrp4, dRrp6, dMtr4, or dZcchc7 in the female fat body (Vidal et al. 2001) and challenged these flies with RVFV for 6 days, after which infection was assessed by northern blot. We found that depletion of all four genes resulted in a significant increase in RVFV replication compared to control (Figure 5D,E). Flies with exosome components depleted in the fat body had similar survival to control flies, suggesting that increased viral replication is not due to generalized frailty (Figure 6D). These data suggest that the RNA exosome and TRAMP orthologs dMtr4 and dZcchc7 are antiviral both in cell culture and at the organismal level.

The antiviral role of the exosome, Mtr4, and Zcchc7 is conserved from flies to humans

The RNA exosome and TRAMP have conserved roles from yeast to flies to humans (Houseley and Tollervey 2009; Schneider and Tollervey 2013). While some studies have explored the human RNA exosome, the human TRAMP components were only recently identified and few RNA targets have been characterized (Fasken et al. 2011; Lubas et al. 2011). We tested whether the exosome and TRAMP genes hMTR4 and hZCCHC7 also restrict viral infection in human cells. We depleted the human exosome exonucleases hRRP6 and hDIS3, the core exosome subunits hRRP4 and hRRP41, and the TRAMP components hMTR4 and hZCCHC7 using siRNAs in human osteosarcoma cells (U2OS), which are permissive to infection by a large number of viruses including VSV, SINV, and RVFV (Moy et al. 2014a). Knockdown was confirmed by immunoblot for genes with a commercial antibody we could validate, or RT-qPCR

for the remaining genes (Figure 7A,B). Quantification of cell number revealed only modest effects on cell number under these conditions (Figure 7C). Cells depleted of exosome, hMTR4, or hZCCHC7 and infected with VSV, SINV, or RVFV showed increased viral RNA levels as measured by RT-qPCR (Figure 8A) and increased viral protein by immunoblot (Figure 8B-D). Together, these data suggest that the RNA exosome and TRAMP components are antiviral in human cells against diverse RNA viruses.

MTR4 and ZCCHC7 form a cytoplasmic complex with the exosome upon viral infection

While the RNA exosome is present in the nucleus and cytoplasm, the human TRAMP complex is thought to be exclusively nucleolar (Fasken et al. 2011; Lubas et al. 2011). However, VSV, SINV, and RVFV are all cytoplasmic RNA viruses that are not thought to transport their RNAs into the nucleus (Strauss and Strauss 1994; Letchworth et al. 1999; Moon and Wilusz 2013). Therefore, we hypothesized that if the TRAMP components were directly targeting viral RNA, they would have to relocalize to the cytoplasm during infection. We validated an antibody against hZCCHC7 both by immunoblot and immunofluorescence (Figure 7B,10A). While we validated an hMTR4 antibody by immunoblot (Figure 7B), it did not recognize hMTR4 by immunofluorescence (not shown). Next, U2OS cells were either mock infected or infected with RVFV or SINV, and hZCCHC7 localization was monitored. While hZCCHC7 was exclusively nucleolar in uninfected cells, in RVFV- or SINV-infected cells hZCCHC7 accumulated in cytoplasmic punctae (Figure 9A-D; monochrome images in Figure 10B,C). Furthermore, the average number of cytoplasmic punctae per infected cell was similar between RVFV and SINV infection (Figure 10D).

Next we set out to explore the localization of these factors using biochemical fractionation. Nuclear and cytoplasmic lysates were isolated and the purity of fractionation was established by monitoring the nuclear protein lamin and the cytoplasmic protein tubulin. As expected, hMTR4 and hZCCHC7 were detected in the nuclear but not cytoplasmic fraction of uninfected cells (Figure 9E). However, upon infection with VSV or SINV, both hMTR4 and hZCCHC7

accumulated in the cytoplasm. We also examined localization of the NEXT component hZCCHC8 since it is similar in structure to hZCCHC7 and also associates with hMTR4 in the nucleus (Lubas et al. 2011). In contrast to hMTR4 and hZCCHC7, hZCCHC8 was exclusively nuclear in both uninfected and infected cells (Figure 9F, 10E), suggesting that there is specificity in the proteins relocalized to the cytoplasm.

To determine whether the accumulation of these TRAMP components in the cytoplasm was due to their export from the nucleus or from increased synthesis, we first examined whether viral infection altered overall levels of these proteins and observed no increase upon infection with VSV, SINV, or RVFV (Figure 9G). Next, we assessed whether cytoplasmic accumulation was dependent on nuclear export by testing whether the major nuclear export protein CRM1, which we have previously found to be broadly antiviral (Yasunaga et al. 2014), was required for virus-induced cytoplasmic accumulation. We validated that siRNA treatment efficiently depleted CRM1 (Figure 10F). Next, CRM1-depleted or control cells were infected with RVFV, and the nuclear and cytoplasmic fractions were isolated. As with VSV and SINV, RVFV infection led to the accumulation of hMTR4 and hZCCHC7 in the cytoplasm (Figure 9H). Furthermore, this virus-induced increase was lost upon CRM1 depletion. These data suggest that signals from viral infection induce the export of these antiviral proteins from the nucleus to the cytoplasm.

The TRAMP components hMTR4 and hZCCHC7 function in the nucleolus as a complex with the exosome (Lubas et al. 2011). We reasoned that in order to target viral RNAs for exosomal degradation, these proteins must both relocalize and form a complex in the cytoplasm. To test this hypothesis we first expressed FLAG-tagged hMTR4 (Lubas et al. 2011) or a vector control and confirmed expression by immunoblot (Figure 12A). Next, transfected cells were infected with RVFV or mock infected and anti-FLAG immunoprecipitations were performed. As expected, hMTR4-FLAG immunoprecipitated hZCCHC7 and the exosomal protein hRRP6 in both infected and uninfected cells in whole cell lysates (Figure 11A). In contrast, cytoplasmic hMTR4-FLAG

precipitated hZCCHC7 and hRRP6 only in RVFV-infected cells (Figure 11B). While the specificity of hZCCHC7 co-immunoprecipitation during infection can be explained by its export to the cytoplasm, hRRP6 was co-immunoprecipitated only during infection despite having a cytoplasmic localization in uninfected cells as well. Co-immunoprecipation of these factors was unchanged upon RNase A treatment (data not shown), suggesting that these interactions are not RNA-dependent. Taken together, our data indicate that hZCCHC7 and hMTR4 are exported and form a complex with the exosome in the cytoplasm upon viral infection.

ZCCHC7 specifically binds RVFV mRNA and SINV RNA

In yeast, the zinc-finger-containing Air proteins are thought to confer RNA binding specificity to TRAMP, which in turn delivers its RNA cargo to the exosome for degradation (Schmidt et al. 2012). This led us to hypothesize that hZCCHC7, as the human Air ortholog, may be the specificity factor that binds viral RNAs to target them to the exosome. To examine this possibility, we performed RNA immunoprecipitation (RNA-IP) with hZCCHC7. We transfected FLAG-tagged hZCCHC7 (Lubas et al. 2011) or control vector and verified expression and cytoplasmic localization of hZCCHC7-FLAG during infection by immunoblot (Figure 12A). Next, transfected cells were infected with RVFV or SINV, and cytoplasmic fractions were collected (input) and a fraction was subjected to FLAG-immunoprecipitation followed by RT-qPCR. RNA quantification was normalized to vector control for both input and FLAG immunoprecipitation to demonstrate that ectopic expression of hZCCHC7 did not increase the input levels and to remove any signal from nonspecific RNA binding to beads or FLAG antibody. We found that RVFV nucleocapsid (N) and nonstructural (NSs) mRNAs, but not the S segment genome or antigenome from which they were transcribed, were selectively and significantly bound by hZCCHC7 (Figure 13A; schematic of RNAs in Figure 12B). This selective binding is not explained by RNA abundance, as northern blot analysis revealed that N mRNA levels are lower than those of S segment genome/antigenome in both *Drosophila* and humans ((Figure 5D) and (Moy et al. 2014b)). An endogenous mRNA, hDCP2 (the levels of which are unaffected by RVFV infection (Hopkins et al.

2015)), was not significantly bound. Similar results were found for SINV infection, in which SINV genomic and subgenomic RNAs, which function as mRNAs, were significantly bound by hZCCHC7 (Figure 13B). These data suggest that hZCCHC7 selectively binds viral mRNAs in the cytoplasm during infection.

RVFV mRNA, but not genomic or antigenomic RNA, is shortened at the 3' end

The exosome processively degrades RNA 3' to 5'; however, RNAs partially degraded by the exosome can leave 3' truncated degradation intermediates (Eckwahl et al. 2015). Since we found that hZCCHC7 selectively bound RVFV mRNA, but not RVFV genomic or antigenomic RNA, we hypothesized that the mRNA would be truncated at the 3' end. To test this, 3' rapid amplification of cDNA ends (3' RACE) was performed and individual RNAs were sequenced. Briefly, RNA was harvested from RVFV-infected cells and a linker was ligated to the 3' end of the RNA. RT-PCR was then performed using a linker-specific reverse primer and a virus-specific forward primer targeting S segment genomic RNA, antigenomic RNA, or nucleocapsid (N) mRNA. PCR products were cloned and individual clones were sequenced to identify the proportion of full length clones. We classified reads as full length or shortened based on the full length sequences of the genomic segment as well as the transcription termination site that defines the 3' end of the N mRNA, N coding sequence (ORF), and 3'UTR (Ikegami et al. 2007). 3' RACE revealed that while most sequence reads from genomic and antigenomic S segment RNA clones were full-length, the majority of N mRNA reads were shortened at the 3' end (Figure 14A). A variety of truncated N mRNA sequences were found with both intact and disrupted N coding sequence (Figure 14B). This suggests that the viral mRNA, but not genomic or antigenomic RNA, is subject to 3' degradation.

RVFV mRNA stability is dependent on the exosome and ZCCHC7

Bunyaviruses such as RVFV are unique in that mRNA transcription but not the replication of the genome requires concomitant protein translation (Barr 2007). Cycloheximide, which inhibits

translational elongation, can therefore be used to block new mRNA synthesis, allowing us to assess the rate of decay of previously transcribed RVFV mRNA (Hopkins et al. 2013). To determine whether the stability of RVFV mRNA is exosome- and hZCCHC7-dependent, we depleted the two exosome exonucleases, hRRP6 and hDIS3, or hZCCHC7, by siRNA in U2OS cells. Cells were infected with RVFV (MOI = 1, 12h) and treated with cycloheximide for 0, 1, or 2 hours and RNA was processed for RT-qPCR. As previously observed (Hopkins et al. 2013), we found that RVFV mRNA significantly decayed after addition of cycloheximide in control cells (Figure 14C), but RVFV genome/antigenome did not (Figure 12C). Furthermore, we observed that depletion of hRRP6/hDIS3 or hZCCHC7 significantly reduced this decay, suggesting that RVFV mRNA is destabilized by the RNA exosome and hZCCHC7.

The RVFV NSs 3' UTR is specifically regulated by the exosome during infection

We set out to determine if there are specific signals in the RVFV mRNA that direct exosomal degradation. Since cellular mRNAs are often targeted to the exosome through signals at the 3' end including hypoadenylation, 3' extension, and AU-rich elements in the 3' UTR (Chen et al. 2001; Milligan et al. 2005; Lubas et al. 2015), we hypothesized that the 3' UTR of a RVFV mRNA would be sufficient to render an mRNA susceptible to control by the exosome. To test this, we used a reporter system in which the RVFV NSs 3' UTR is cloned downstream of a cGFP ORF. Since the mRNAs of RVFV are not polyadenylated, we generated the exact 3' end by cloning the mascRNA sequence downstream of the 3'UTR, which is processed by endogenous RNase P, leaving the mature viral 3' end (Figure 15A-D) (Wilusz et al. 2012). U2OS cells stably expressing this reporter or a control reporter with the SV40 polyadenylation signal cloned downstream of cGFP were transfected with siRNAs targeting hRRP6 and hDIS3 or control and either mock infected or infected with RVFV (MOI = 10, 18h). Automated fluorescence microscopy was used to calculate the percent of cells expressing cGFP. We found that while the NSs 3' UTR reporter was unaffected by exosome depletion in uninfected cells, RVFV infection caused a significant reduction in reporter signal that was rescued to uninfected control levels by exosome depletion

(Figure 14D). In contrast, the SV40 poly A reporter was unaffected by either exosome depletion or viral infection. This demonstrates that upon viral infection the exosome specifically regulates the RVFV 3' UTR, but not a conventional polyadenylated mRNA.

Discussion

Increasing evidence suggests that the RNA recognition and decay machinery plays an important role in the control of viral infection. Through RNAi screening, we found that the RNA exosome and two components of the exosomal cofactor TRAMP complex were antiviral against diverse RNA viruses from insects to humans.

Since the TRAMP complex normally binds specific RNAs for exosome-dependent processing, we hypothesized that the antiviral TRAMP components would recognize viral RNAs and recruit the exosome to degrade them. However, human TRAMP is thought to exclusively reside in the nucleolus (Fasken et al. 2011; Lubas et al. 2011); therefore, we tested whether these antiviral TRAMP components translocate upon infection to the cytoplasm, where the viral RNAs are located. Indeed, we found that hMTR4 and hZCCHC7 are dependent on the nuclear export protein CRM1 for their cytoplasmic accumulation and associate with each other and the exosome in the cytoplasm during infection. In contrast, the related NEXT complex component hZCCHC8 remained exclusively nuclear during infection, suggesting that the export of antiviral TRAMP components to the cytoplasm is specific. Furthermore, immunofluorescence analysis revealed infection-induced hZCCHC7 cytoplasmic punctae. The RNA exosome and some cofactors have previously been found in cytoplasmic granules distinct from P bodies or stress granules (Sheth and Parker 2003; Graham et al. 2006; Lin et al. 2007). These data suggest that hZCCHC7 and hMTR4 accumulate in exosome granules during viral infection to facilitate the specific degradation of viral RNA.

The virus-induced translocation of antiviral factors from the nucleus to the cytoplasm is an emerging theme; we previously found that two additional RNA-binding proteins, DDX17 and

Drosha, are exported during infection for their roles in antiviral defense (Moy et al. 2014a; Shapiro et al. 2014). Furthermore, we have found CRM1 to be broadly antiviral in both *Drosophila* and human cells (Yasunaga et al. 2014), suggesting that this is at least in part related to the requirement for the export of antiviral RNA-binding proteins. The sensors necessary for export of these effectors of antiviral defense are not yet well understood; we hypothesize that detection of virus-specific signals such as dsRNA by sensors like RIG-I, MDA5, or PKR may trigger export of hMTR4 and hZCCHC7. Indeed, PKR sensing of viral RNA has been shown to induce the formation of antiviral stress granules in the cytoplasm, opening the possibility that a similar process may induce hZCCHC7 granules (Onomoto et al. 2012).

Next, we investigated whether this exported complex binds viral RNA. We found that RVFV and SINV mRNA are bound by hZCCHC7, but RVFV genome, RVFV antigenome, and an endogenous mRNA are not. This specificity may be explained at least in part by accessibility; bunyaviral genome and antigenome RNAs are coated by nucleocapsid and as such may not be accessible to cellular degradation machinery, while mRNA must be accessible in order to be translated and thus is vulnerable to RNases (Kolakofsky and Hacker 1991; Strauss and Strauss 1994). Furthermore, 3' RACE revealed that while RVFV S segment genome and antigenome were largely full-length, the majority of RVFV N mRNA was shortened at the 3' end. Though RVFV N mRNA has been studied using 3' RACE, previous studies only sequenced pooled and size-selected RACE products, which would mask shortened ends (Albarino et al. 2007; Lara et al. 2011). This led us to test whether the exosome impacts the stability of viral mRNAs. Using cycloheximide to disrupt protein translation and thus RVFV mRNA transcription (Barr 2007), we found that RVFV mRNA decay is exosome- and hZCCHC7-dependent and that the genomic RNA is not subject to this targeting.

This specificity suggests that there may be signals or sequences in the viral mRNAs that direct their decay. Indeed, the exosome degrades several classes of mRNAs based on signals in their

3’ UTR’s. Therefore, we tested whether the 3’ UTR of RVFV mRNA confers this specificity and found that the RVFV NSs 3’ UTR directs exosome-dependent decay only during RVFV infection. This regulated decay of viral mRNAs is reminiscent of other cohorts of mRNAs, known as RNA regulons, which are co-regulated through signals in their 3’ UTRs such as AU-rich elements or C-rich motifs; regulation of these RNAs is also exosome-dependent (Chen et al. 2001; Mukherjee et al. 2002; Keene 2007; Singer et al. 2012; Blackinton and Keene 2014).

We characterized a new role for an RNA-binding exosome cofactor complex that is regulated by infection to specifically target viral RNAs for exosome-dependent degradation. This may be part of a larger spectrum of exosomal co-factors activated during infection. The antiviral RNA-binding proteins DDX17, DDX60, ZAP, and AID have all been found to co-immunoprecipitate with the exosome (Guo et al. 2007; Lubas et al. 2011; Miyashita et al. 2011; Moy et al. 2014a; Liang et al. 2015). Furthermore, both ZAP and AID restrict viral infection only if the exosome is intact. Further studies are needed to determine if these complexes drive exosomal degradation of viral RNAs. Nevertheless, taken together with the current study, these data suggest that viral infection may induce a panel of RNA binding cofactor complexes to target viral RNAs for selective exosome-dependent decay.

Materials and Methods

Cells, viruses, antibodies, and reagents

Drosophila DL1 cells and human U2OS cells were grown and maintained as previously described (Cherry and Perrimon 2004; Moser et al. 2012). VSV-eGFP (gift from J. Rose) was grown in BHK cells as described (Ramsburg et al. 2005). SINV-GFP (gift from R. Hardy) and SINV-mKate (gift from M. Heise) was grown in C636 cells as described (Burnham et al. 2007). An attenuated strain of RVFV (MP-12) was grown in Vero cells as described (Filone et al. 2010). Viral titers were calculated by plaque assay on BHK cells. Primary antibodies to GFP, CRM1, and Beta-actin were obtained from Santa Cruz. Antibodies to hRRP6 (EXOSC10), hMTR4 (SKIV2L2), hZCCHC8, and

lamin B1 were obtained from Abcam. Antibodies to hZCCHC7 and alpha-tubulin were obtained from Sigma. Primary antibodies to RVFV N and Gn were gifts from R. Doms. Fluorescent secondary antibodies were obtained from Invitrogen, and HRP-conjugated antibodies were from Amersham. Other chemicals were purchased from Sigma.

Drosophila RNAi

Double-stranded RNAs (dsRNAs) were generated as described (Boutros et al. 2004). Knockdowns for RNAi screening were performed in 384 well plates pre-arrayed with 0.25μg of dsRNA per well, as described (Zhou et al. 2008; Hopkins et al. 2013). Briefly, to knock down genes using RNAi, DL1 cells were passaged into serum-free media and seeded into plates containing dsRNAs targeting the indicated genes or β-galactosidase as a non-targeting control. Cells were serum starved for one hour, after which complete media was added and cells were incubated for 3 days. Knockdown was validated by co-transfection of dsRNAs with plasmids expressing dRrp4-V5, dRrp6-V5, or dMtr4-FLAG using Effectene transfection reagent (Qiagen) (Hessle et al. 2009).

Mammalian RNAi

Ambion Silencer Select siRNAs were used for all genes except hCRM1, for which a Santa Cruz siRNA was used. Transfection into U2OS cells was performed using HiPerFect (Qiagen) as per the manufacturer's protocol. Cells were incubated for 3 days. Silencer Select Negative Control #2 (Ambion) was used as a non-targeting control.

Viral infections

Three days post-RNAi, cells were infected with the indicated viruses. MOI was calculated based on viral titers on BHK cells. For DL1 cells, VSV-GFP (MOI = 0.1) was processed at 24 hpi. SINV-GFP (MOI = 2.5) and RVFV (MOI = 0.1) were spinoculated at 1200 rpm for 2 h and processed at 36 and 30 hpi, respectively. For infectivity studies in U2OS cells, VSV-GFP (MOI = 0.05), SINV-GFP (MOI = 1) and RVFV (MOI = 0.03) were added to cells in complete media for 14, 16, and 18

hours respectively for RNA, or 14, 8, and 18 hours respectively for protein. For immunofluorescence localization studies, U2OS cells were infected with RVFV or SINV-mKate (MOI = 10) for 12 and 5 hours respectively. For fractionation and immunoprecipitation, U2OS cells were infected with VSV-GFP (MOI = 10, 8h), SINV-GFP (MOI = 10, 8h), or RVFV (MOI = 10, 12h).

Immunofluorescence

Cells were processed as previously described (Shelly et al. 2009). Cells were imaged with an ImageXpress Micro automated microscope. At least four sites in each of three wells were imaged per condition per experiment, and MetaXpress cell scoring was used to calculate the number of cells and percent infection. For protein relocalization studies, U2OS cells grown on coverslips were imaged with a Leica DMI 4000 B fluorescent microscope. MetaXpress software was used to quantify cytoplasmic hZCCHC7 punctae between .8 and 2 μm in size in mock infected and infected cells (infection was verified by immunofluorescence for each cell to be quantified) with at least 25 cells quantified per condition. All experiments were performed at least three times.

RNA quantification

Total RNA was extracted and northern blotting or RT-qPCR were performed as previously described (Cherry 2005; Xu et al. 2012). Primer sequences are described below.

Adult fly infections

Transgenic flies for in vivo RNAi were obtained from the Vienna *Drosophila* RNAi Center (UAS-dRrp4 IR, UAS-dMtr4 IR, UAS-dZcchc7 IR) or Bloomington *Drosophila* Stock Center (UAS-dRrp6 IR) and crossed to Yp1-GAL4, which was also obtained from Bloomington. 4-7 day old flies were challenged with RVFV (Cherry and Perrimon 2004) and 15 flies per condition were processed for RNA 6 days post-infection as previously described (Xu et al. 2012).

Nuclear/cytoplasmic fractionation

Cells were lysed in Buffer A (30 mM Hepes pH 7.4, 2 mM MgOAc, .1% NP40) supplemented with 5 mM DTT, PMSF, and protease inhibitors (Roche complete tablets, 25x) by pipetting three times through a 26g needle. Nuclei were pelleted for 20 minutes at 500g. Cytoplasmic supernatant was removed and the nuclear pellet was rinsed twice with Buffer A, then lysed with sonication in RIPA buffer (50 mM Tris-HCl pH 7.4, 1% NP-40, 0.5% Na-deoxycholate, 0.1% SDS, 150 mM NaCl, 2 mM EDTA, 50 mM NaF) supplemented with PMSF and protease inhibitors. Lysates were analyzed by immunoblot. Each experiment was repeated at least three times and representative blots shown.

Immunoprecipitation

U2OS cells were transfected with doxycycline-inducible hMTR4-FLAG, hZCCHC7-FLAG, or empty vector control, using Xtremegene 9 (Roche) (Lubas et al. 2011). Plasmid expression was induced at 24 hours with 1 µg/mL doxycycline and cells were infected at 48 hours with RVFV (MOI = 10) for 12h. Cytoplasmic extracts or whole cell lysates were immunoprecipitated with anti-FLAG M2 magnetic beads (Sigma). For analysis of proteins, beads were treated with 100ug/mL RNase A or untreated, washed with Buffer A and analyzed by immunoblot. For analysis of bound RNA, beads were washed in Buffer A supplemented with 150 mM NaCl and .5% NP40 and analyzed by RT-qPCR for efficient expression of the construct and target RNA binding. Each experiment was repeated at least three times and representative blots shown.

3' RACE

3' RACE was performed as previously described (Wilusz et al. 2008). U2OS cells were infected with RVFV (MOI = 0.3) for 18 hours. Total RNA was harvested and treated with CIP (New England Biolabs) to remove terminal phosphates, ligated to miRNA linker #3 (IDT) and reverse transcribed using a linker-specific primer. RACE PCR was performed against S segment genome, antigenome, or N mRNA (see Supplement for primers) and products were cloned using

TOPO-TA (Invitrogen). Individual colonies were screened for insert with colony hybridization Southern blot and sequenced. Sequences were classified based on previous studies of RVFV transcriptional termination (Ikegami et al. 2007).

RNA stability assay

Three days post-RNAi, cells were infected with RVFV (MOI = 1) for 12 hours. Cells were treated with 50 µg/ml cycloheximide for 0, 1, or 2 hours, after which cells were processed for RT-qPCR. DCP2 was used as a control.

GFP 3' UTR reporters

To generate plasmids encoding cGFP-3' UTR reporters, the previously described pCRII-TOPO CMV-cGFP-SV40 Poly(A) Sense plasmid (Wilusz et al. 2012) was cleaved by the NotI restriction enzyme to remove the SV40 polyadenylation signal. The 3' UTR of RVFV NSs, RNase P cleavage site, and mascRNA sequences, flanked by NotI sites (sequence: GCGGCCGCAGGTTAAGGCTGCCCCACCCCCCACCCCCTAATCCCGACCGTAACCCCAACT CCCCTTCCCCCCAACCCCCTGG GACGCTGGTGGCTGGCACTCCTGGTTTCCAGGACGGGGTTCAAGTCCCTGCGGTGTCTTTG CTTGCGGCCGC) were then inserted downstream of the cGFP ORF. The original plasmid expressing cGFP with a downstream SV40 polyadenylation signal was used as a control. Proper processing of cGFP mRNA and mascRNA was validated by northern blot and small RNA northern blot, respectively. Expression of cGFP protein was validated by western blot. Stable cell lines were generated and used for immunofluorescence experiments.

Oligonucleotide sequences

qVSV N F	CGGAGGATTGACGACTAATGC
qVSV N R	ACCATCCGAGCCATTCGA
qSINV Nsp1/genomic F	GCTGAAACACCATCGCTCTGCTTT
qSINV Nsp1/genomic R	TGGTGTCGAAGCCAATCCAGTACA
qRVFV N F	CAAGCAGTGGACCGCAATGAGA
qRVFV N R	GGGCTTGTTGCCACGAGTTAGA

RVFV N northern F	CATCTAATATTGCCCTTAGA
RVFV N northern R	TTACAATAATGGACAACTAT
dRps6 northern F	GCCGTGTGCGTCTGCTCCTG
dRps6 northern R	TTACTTCTTGTCGCTGGAGA
qdRp49 F	AAGAAGCGCACCAAGCACTTCATC
qdRp49 R	TCTGTTGTCGATACCCTTGGGCTT
qdZcchc7 F	TGGATAGCCGGGTACAGTATAG
qdZcchc7 R	TGCTACGAAAGTCACCAATCC
qdZcchc8 F	CTGCCGAGTCCGGAAATAAT
qdZcchc8 R	CACAGGCAGTCTGTCGTAAA
qdRbm7 F	GCCATCACTACGTCCGATTT
qdRbm7 R	CCGACGCACCACTATACATTT
qdTrf4-1 F	CCTGTGGAGCACAAAGATCA
qdTrf4-1 R	GCTTCGTCCTTTCACCTCTATC
qdTrf4-2 F	AGGAGATCGAGCAGTTCTACA
qdTrf4-2 R	CAAATGGAAAGCACCACATCC
qdSki2 F	GGGAGCACCAAGAAGAGAAA
qdSki2 R	CTTTCCTCCAGCACCAGTATAG
qdSki3 F	GTCGTTCCAGGGATTTCTCTAC
qdSki3 R	CTCCAGGTTCGCACAACTTA
qdSki8 F	CAGGAGGACAACACCCTAAAG
qdSki8 R	ATGGTGGAGTCCAGAGAACTA
qhGAPDH F	ACCAAATCCGTTGACTCCGACCTT
qhGAPDH R	TCGACAGTCAGCCGCATCTTCTTT
3' RACE S genome F	GCATCAAACCCTTGATAAGCAAACTCTC
3' RACE S antigenome F	GTGACTAGGACGATGGTGCATGAGAAAG
3' RACE N F	CACGCAGCCAATGAATGCAGC
3' RACE adapter primer R	GACTAGCTGGAATTCGCGGTTAAA
qRVFV genome antigenome F	CTTTATAAGCCATGAGAAGAGGAGAG
qRVFV genome antigenome R	GGAGGAGAGCCTGATGCTGC
qhRRP4 F	CACCTGTAGTCCCAGCTATTTG
qhRRP4 R	GGAGTGTGGTACGCGATTT
qhRRP41 F	GGCCCTAGTGAACTGTCAAT
qhRRP41 R	GCCCATCTCACAGGACTTAC
qhDIS3 F	GCTAAGCAGGTTACGTGGAATA
qhDIS3 R	GCAGTGTGAGAACAGACCATAA
qhDCP2 F	TGCAGAACACACCAGGATTAC
qhDCP2 R	CACATCTTCACCTTGAGGCA
qSINV subgenomic F	AACACCACCACCATGAATAGA
qSINV subgenomic R	GTCAGTTGCTGGATTTGAGAAG
qhZCCHC7 F	CAGACATCGTGAAGTGGATGAG
qhZCCHC7 R	GAACGGTGAAAGGGCTTAGAA
cGFP northern probe	TCCATGCCGTGGGTGATGCC
beta-actin northern probe	AGCACTGTGTTGGCGTACAG
mascRNA northern probe	GCAAAGACACCGCAGGGATTTGAAC CCCGTCCTGGAAACCAGGAGTGCCA

U6 northern probe	GCTAATCTTCTCTGTATCGTTCC AATTTTAGTATATGTGCTGCCG

Table 1: Antiviral screen hits in VSV and SINV								
	Z % INFECTION				RANK ORDER			
Gene	VSV A	VSV B	SINV A	SINV B	VSV A	VSV B	SINV A	SINV B
Ago1	3.061	2.951	3.360	3.988	21	19	19	18
Ars2	3.933	3.326	3.699	4.344	12	15	12	12
Bx42	3.837	3.285	2.152	2.092	14	16	26	26
Cbp20	3.354	3.720	3.602	4.335	18	10	15	13
Cbp80	3.484	2.755	3.119	3.547	15	21	21	23
CG7185	3.274	2.987	2.945	3.407	19	18	24	24
Dsor1	2.677	2.558	3.669	4.190	23	25	13	16
eIF-4a	3.464	3.333	3.783	4.375	16	14	11	10
hrg	3.126	3.118	2.988	3.703	20	17	23	21
l(1)10Bb	4.849	3.944	3.617	4.372	4	6	14	11
l(2)01424	2.629	2.849	3.369	3.906	25	20	18	19
noi	2.859	2.603	3.438	4.235	22	24	17	15
Pep	2.648	3.387	4.468	5.954	24	13	2	1
RpL21	4.566	4.052	3.233	4.121	8	3	20	17
RpL22	4.671	4.000	3.455	4.283	7	5	16	14
RpL5	3.971	4.015	3.025	3.646	11	4	22	22
RpS13	4.790	4.098	4.337	5.093	5	2	3	2
RpS15	4.749	3.692	4.142	4.643	6	11	6	7
RpS26	4.292	3.836	4.075	4.567	10	8	9	9
RpS28b	3.895	2.698	4.226	4.826	13	23	5	4
RpS30	4.339	3.690	3.868	4.934	9	12	10	3
RpS6	5.057	4.144	4.142	4.810	1	1	7	5
RpS7	4.935	3.916	4.128	4.634	2	7	8	8
RpS9	4.858	3.767	4.281	4.792	3	9	4	6
Rrp6	3.381	2.314	2.400	3.188	17	26	25	25
Sos	2.525	2.716	4.479	3.757	26	22	1	20

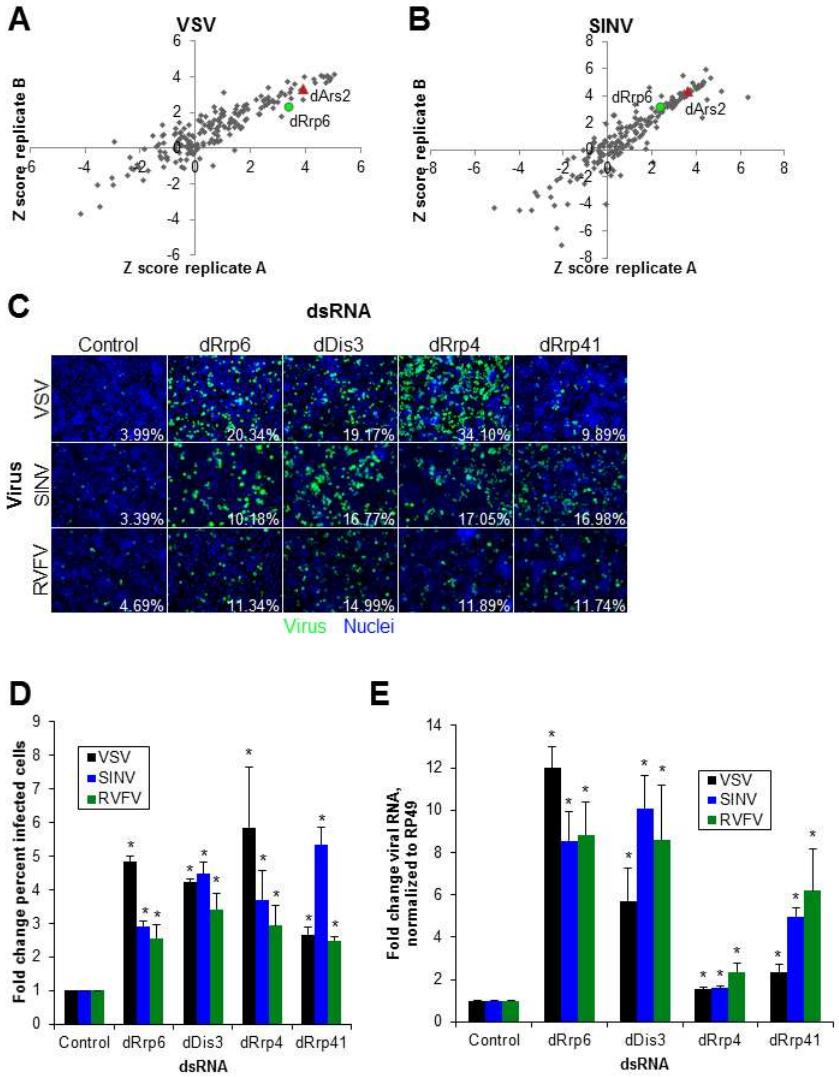

Figure 3: The RNA exosome is broadly antiviral in *Drosophila* cells. A panel of 177 genes with roles in RNA biology were depleted by RNAi in DL1 cells for three days and infected with (A) VSV-GFP (MOI 0.1, 24h), or (B) SINV-GFP (MOI 2.5, 36h) and screened by immunofluorescence measuring the percentage of infected cells. Robust Z-scores are shown for two replicates. These screens identified the positive control dArs2 (red) and the exosome component dRrp6 (green). (C) DL1 cells were treated with dsRNAs targeting the indicated genes or negative control dsRNA targeting β-galactosidase and infected with VSV-GFP (MOI 0.1, 24h), SINV-GFP (MOI 2.5, 36h), or RVFV (MOI 0.1, 30h), and subsequently processed for automated immunofluorescence microscopy for GFP or RVFV nucleocapsid. Representative images are shown with quantification of percent infected cells. (D) Mean±SEM of at least 3 experiments as shown in B normalized to control. Mean percent infection in control cells was 5.40% (VSV), 3.80% (SINV), and 5.62% (RVFV). *p<0.05 compared to control by Student's t-test. (E) Cells were infected as above and processed for RT-qPCR for VSV N, SINV Nsp1, or RVFV N compared to the housekeeping gene Rp49. Mean±SEM normalized to control shown (n≥3). *p<0.05 compared to control by Student's t-test. A-B in collaboration with Leah Sabin. C-E in collaboration with Ryan Moy.

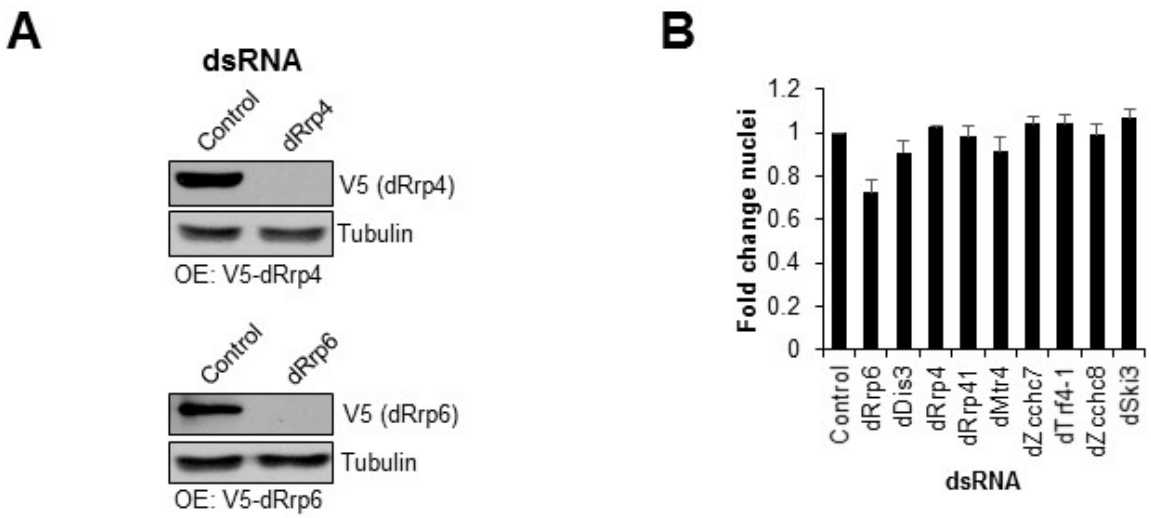

Figure 4: The RNA exosome can be depleted in *Drosophila* cells. (A) DL1 cells were co-transfected with the indicated expression vectors and the indicated dsRNAs. 48 hours later cells were processed for anti-V5 immunoblot. A representative blot is shown (n=2). (B) DL1 cells were treated with the indicated dsRNAs and infected with RVFV (MOI 0.1, 30h), and subsequently processed for automated immunofluorescence microscopy and quantification of nuclei. Mean±SEM normalized to control is shown (n≥3). B in collaboration with Ryan Moy.

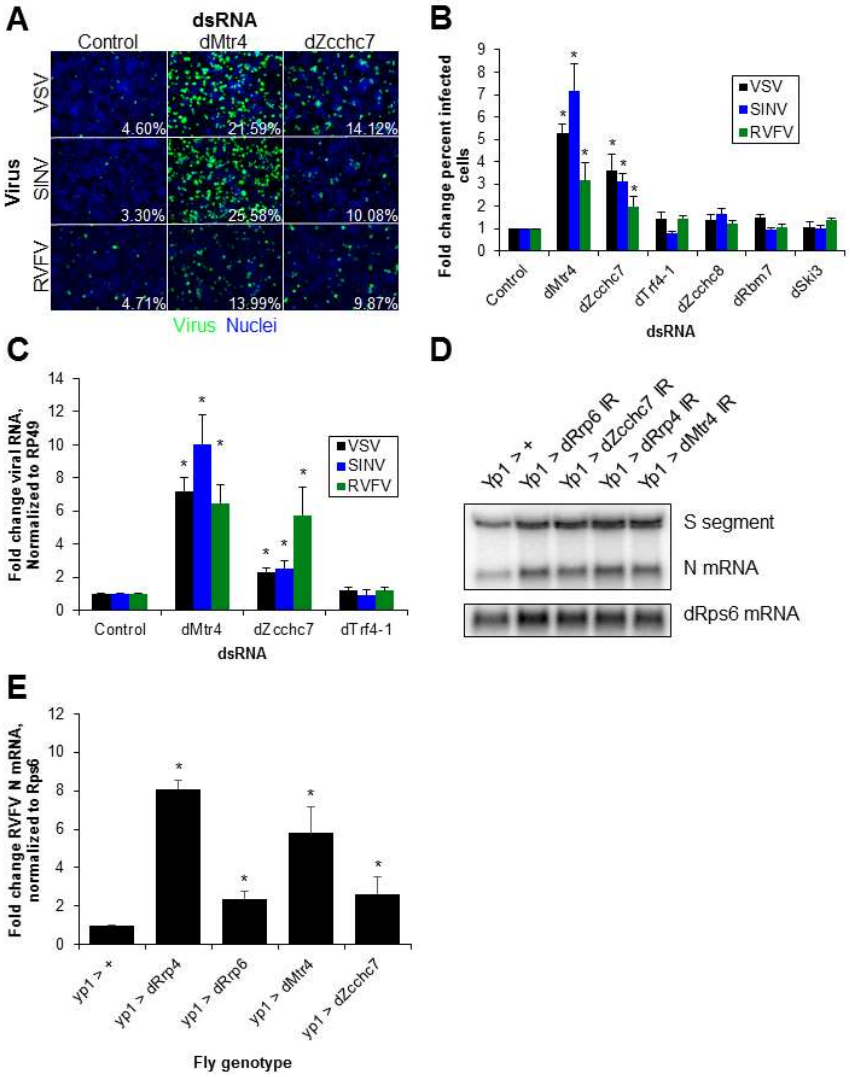

Figure 5: TRAMP orthologs dMtr4 and dZcchc7 are antiviral in *Drosophila*. (A) DL1 cells were treated with dsRNAs targeting the indicated genes or negative control dsRNA targeting β-galactosidase and infected with VSV-GFP (MOI 0.1, 24h), SINV-GFP (MOI 2.5, 36h), or RVFV (MOI 0.1, 30h), and subsequently processed for automated immunofluorescence microscopy for GFP or RVFV nucleocapsid. Representative images are shown with quantification of percent infected cells. (B) Mean±SEM of at least 3 experiments as shown in A normalized to control. *p<0.05 compared to control by Student's t-test. (C) Cells were infected as above and processed for RT-qPCR for VSV N, SINV Nsp1, or RVFV N compared to the housekeeping gene Rp49. Mean±SEM normalized to control shown (n≥3). *p<0.05 compared to control by Student's t-test. (D) Adult flies depleted of exosome or TRAMP genes in the fat body (YP1-Gal4 > IR) or controls (YP1-Gal4 > +) were challenged with RVFV for 6 days then processed for northern blot. A probe which identified the S segment genome/antigenome and the N mRNA was used. The housekeeping gene RpS6 was used as a loading control. (E) Quantification of RVFV N mRNA from ≥3 experiments as shown in D. Mean±SEM normalized to control. *p<0.05 compared to control by Student's t-test. A-C in collaboration with Ryan Moy. D-E in collaboration with Beth Gold.

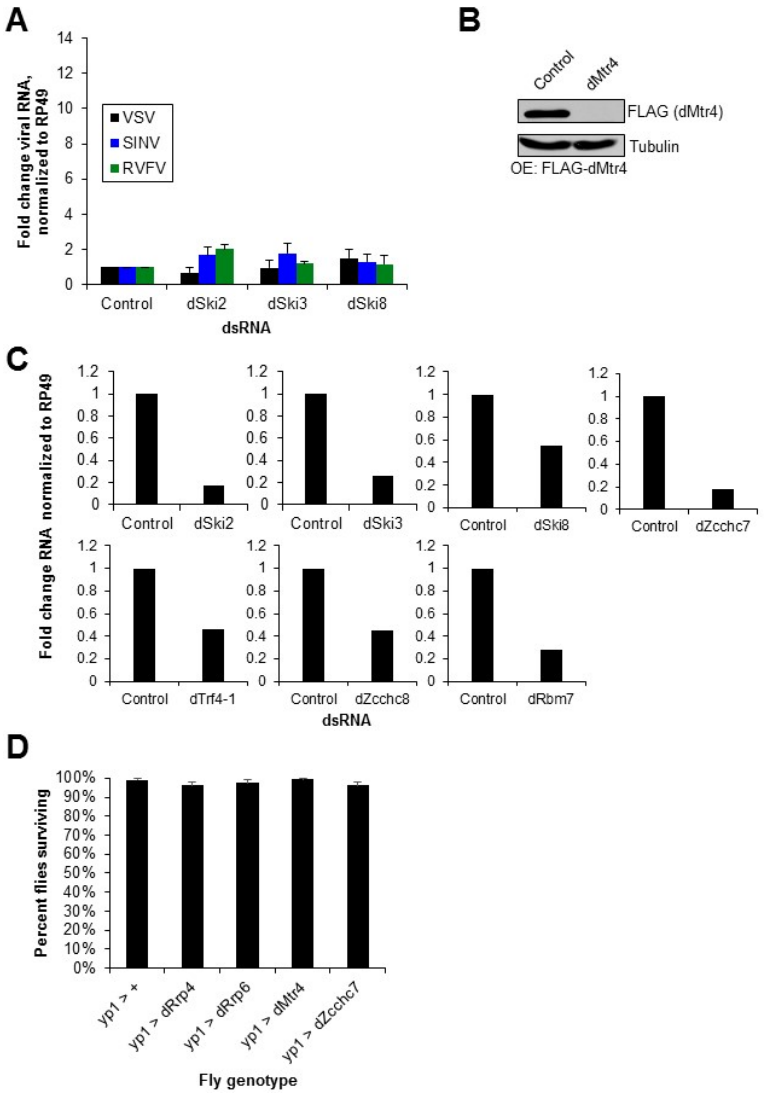

Figure 6: Exosome cofactors can be depleted in *Drosophila*. (A) DL1 cells were treated with the indicated dsRNAs and infected with VSV-GFP (MOI 0.1, 24h), SINV-GFP (MOI 2.5, 36h), or RVFV (MOI 0.1, 30h), and subsequently processed for RT-qPCR for the indicated viruses compared to the housekeeping gene Rp49. Mean±SEM normalized to control is shown (n=3). (B) DL1 cells were co-transfected with a FLAG-dMtr4 expression vector and the indicated dsRNAs. 48 hours later cells were processed for anti-FLAG immunoblot. A representative blot is shown (n=2). (C) DL1 cells were treated with the indicated dsRNAs and subsequently processed for RT-qPCR for the depleted genes relative to control. Mean normalized to control is shown (n=2). (D) Adult flies depleted of exosome or TRAMP genes in the fat body (YP1-Gal4 > IR) or controls (YP1-Gal4 > +) were challenged with RVFV for 6 days and survival was quantified. Mean±SEM is shown (n≥3). D in collaboration with Beth Gold.

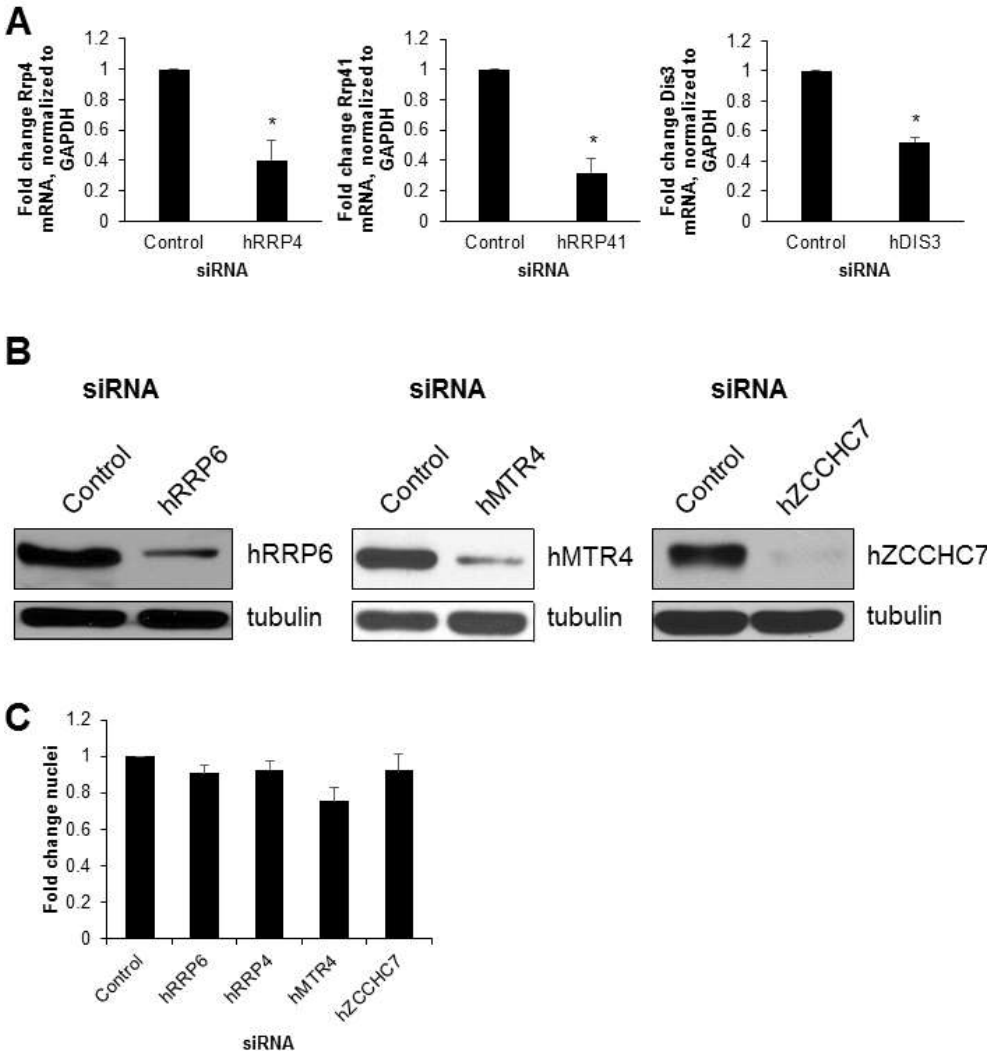

Figure 7: RNA exosome and TRAMP orthologs can be depleted in human cells. (A) U2OS cells were transfected with the indicated siRNAs for 72h, then processed for RT-qPCR for the indicated genes compared to the housekeeping gene GAPDH. Mean±SEM normalized to control is shown (n≥3). *p<0.05 compared to control by Student's t-test. (B) U2OS cells were transfected with the indicated siRNA's for 72h, and subsequently processed for immunoblot. A representative blot is shown (n≥3). (C) U2OS cells were transfected with the indicated siRNAs and infected with RVFV (MOI .03, 18h), and subsequently processed for automated immunofluorescence microscopy. Mean±SEM of the number of nuclei in at least 3 experiments is shown normalized to control.

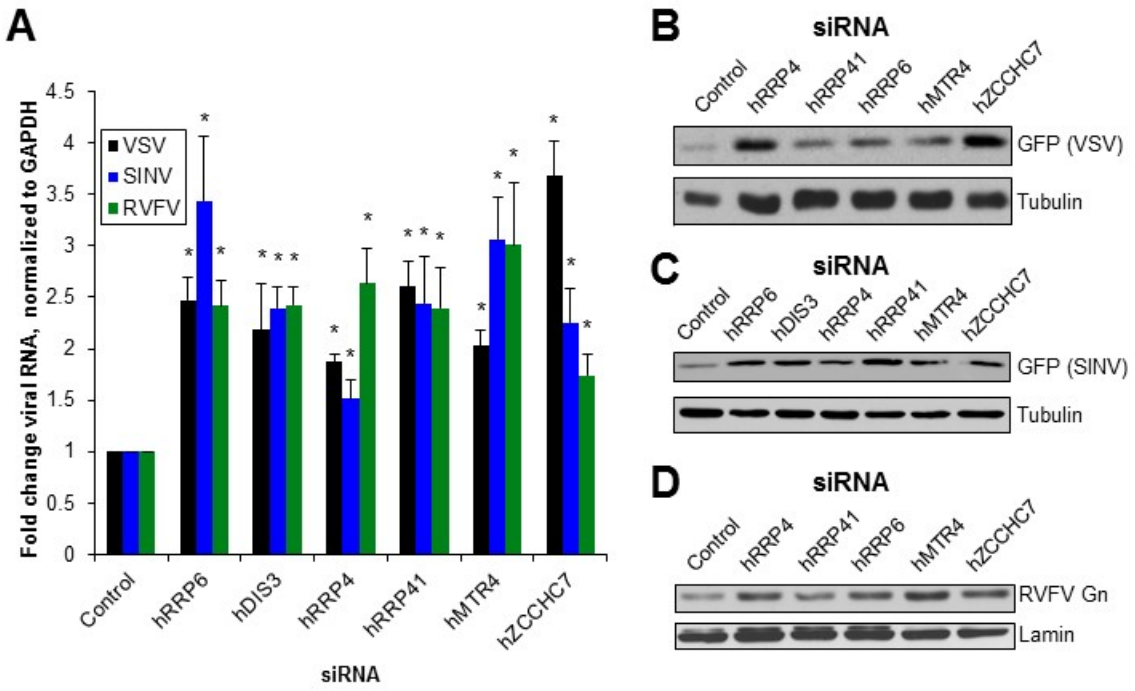

Figure 8: The RNA exosome and TRAMP orthologs are antiviral in human cells. (A) U2OS cells were transfected with the indicated siRNAs and infected with VSV-GFP (MOI 0.05, 14h), SINV-GFP (MOI 1, 16h), or RVFV (MOI 0.03, 18h), and subsequently processed for RT-qPCR for VSV N, SINV Nsp1, or RVFV N compared to the housekeeping gene GAPDH. Mean±SEM shown normalized to control (n≥3). *p<0.05 compared to control by Student's t-test. (B) Cells were transfected with the indicated siRNAs and infected with VSV-GFP (MOI 0.05, 14h), then processed for GFP immunoblot. A representative blot is shown (n≥3). (C) Cells were transfected with the indicated siRNAs and infected with SINV-GFP (MOI 1, 8h), then processed for GFP immunoblot. A representative blot is shown (n≥3). (D) Cells were transfected with the indicated siRNAs and infected with RVFV (MOI 0.3, 18h), then processed for RVFV Gn glycoprotein immunoblot. A representative blot is shown (n≥3).

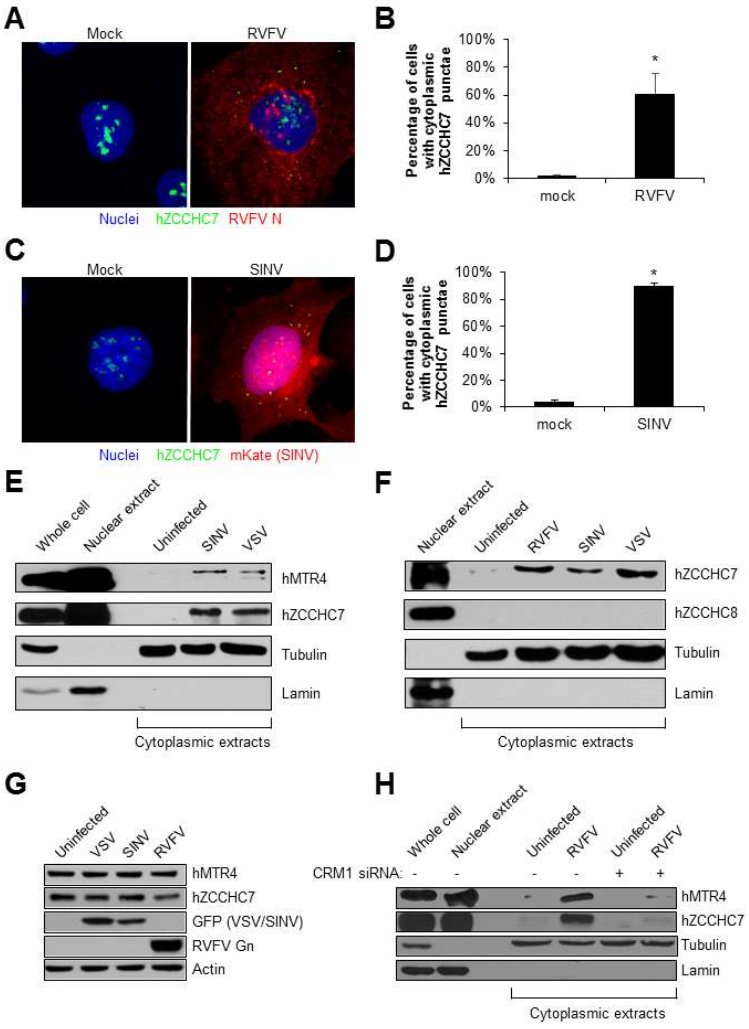

Figure 9: Human MTR4 and ZCCHC7 are exported to the cytoplasm upon viral infection. (A) U2OS cells were infected with RVFV (MOI 10, 12h) or mock infected and processed for immunofluorescence microscopy for hZCCHC7 (green), RVFV N (red), and nuclei (blue). (B) Quantification of the percentage of cells with cytoplasmic hZCCHC7 punctae in mock- or RVFV-infected cells in at least 3 experiments as in A. Mean±SEM shown. *p<0.05 compared to mock by Student's t-test. (C) U2OS cells were infected with SINV-mKate (MOI 10, 5h) or mock infected and processed for immunofluorescence microscopy for hZCCHC7 (green), mKate (red), and nuclei (blue). (D) Quantification of the percentage of cells with cytoplasmic hZCCHC7 punctae in mock- or SINV-infected cells in at least 3 experiments as in C. Mean±SEM shown. *p<0.05 compared to mock by Student's t-test. (E) U2OS cells were infected with SINV-GFP or VSV-GFP (MOI 10, 8h) and subjected to nuclear/cytoplasmic fractionation and immunoblot and probed for the nuclear protein lamin and the cytoplasmic protein tubulin to verify extract purity along with hMTR4 and hZCCHC7. A representative blot is shown (n≥3). (F) U2OS cells were infected with RVFV (MOI 10, 12h), SINV-GFP (MOI 10, 8h), or VSV-GFP (MOI 10, 8h) and subjected to nuclear/cytoplasmic fractionation and immunoblot and probed for the nuclear protein lamin and the cytoplasmic protein tubulin to verify extract purity along with hZCCHC7 and hZCCHC8. A representative blot is shown (n≥3). (G) U2OS cells were infected with VSV-GFP (MOI 10, 8h), SINV-GFP (MOI 10, 8h), or RVFV (MOI 10, 12h) and whole-cell lysates were processed for immunoblot. A representative image is shown (n=2). (H) U2OS cells were transfected with siRNA specific to CRM1 or control and infected with RVFV (MOI 10, 12h), then subjected to nuclear/cytoplasmic fractionation and immunoblot and probed for the nuclear protein Lamin and the cytoplasmic protein tubulin to verify extract purity along with hMTR4 and hZCCHC7. A representative image is shown (n≥3).

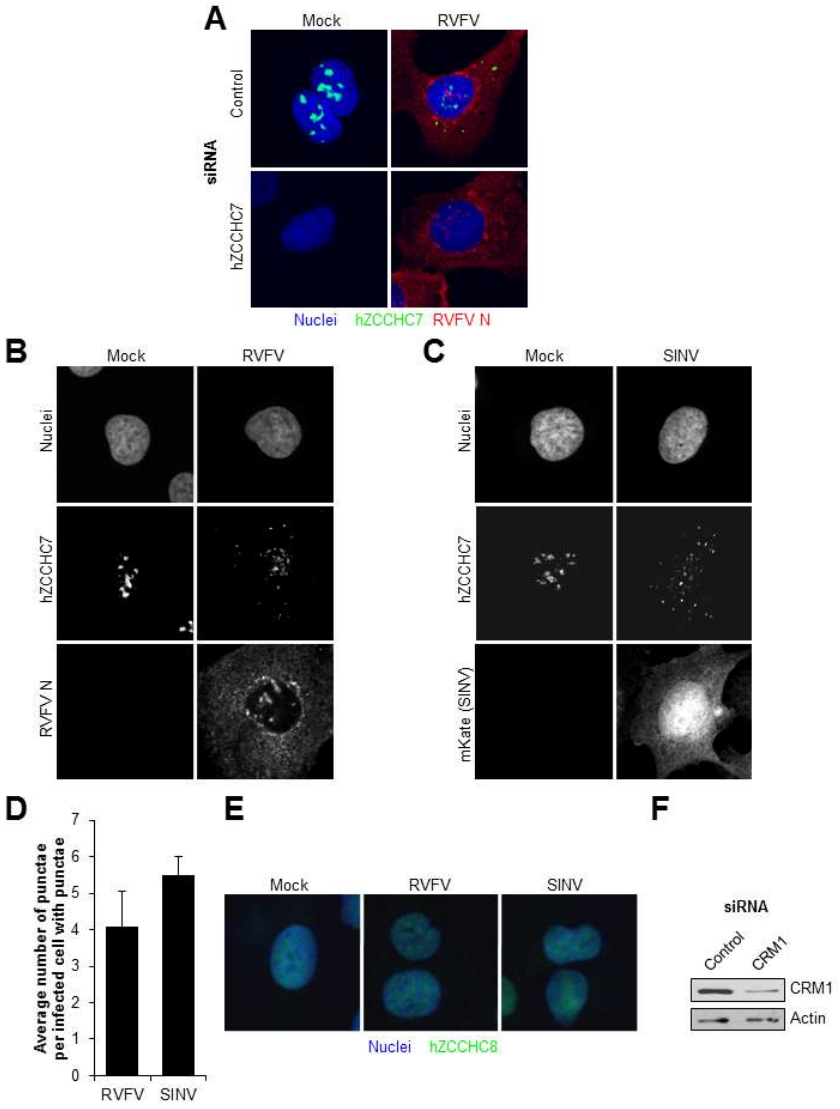

Figure 10: Human ZCCHC7 localization can be assessed by immunofluorescence. (A) U2OS cells were transfected with the indicated siRNAs, then infected with RVFV (MOI 10, 12h) or mock infected and processed for immunofluorescence microscopy for hZCCHC7 (green), RVFV N (red), and nuclei (blue). (B) U2OS cells were infected with RVFV (MOI 10, 12h) or mock infected and processed for immunofluorescence microscopy for the indicated proteins. Monochrome images of cells in Fig 4A. (C) U2OS cells were infected with SINV-mKate (MOI 10, 5h) or mock infected and processed for immunofluorescence microscopy for the indicated proteins. Monochrome images of cells in Fig 4C. (D) Mean±SEM of average number of punctae per infected cell with punctae from at least 3 experiments in B and C. (E) U2OS cells were infected with RVFV (MOI 10, 12h), SINV-mKate (MOI 10, 5h), or mock infected and processed for immunofluorescence microscopy for hZCCHC8 (green) and nuclei (blue). Representative images are shown (n=2). (F) U2OS cells were transfected with siRNA to CRM1 or control and samples were processed for immunoblot 72 h post transfection. A representative blot is shown (n=3).

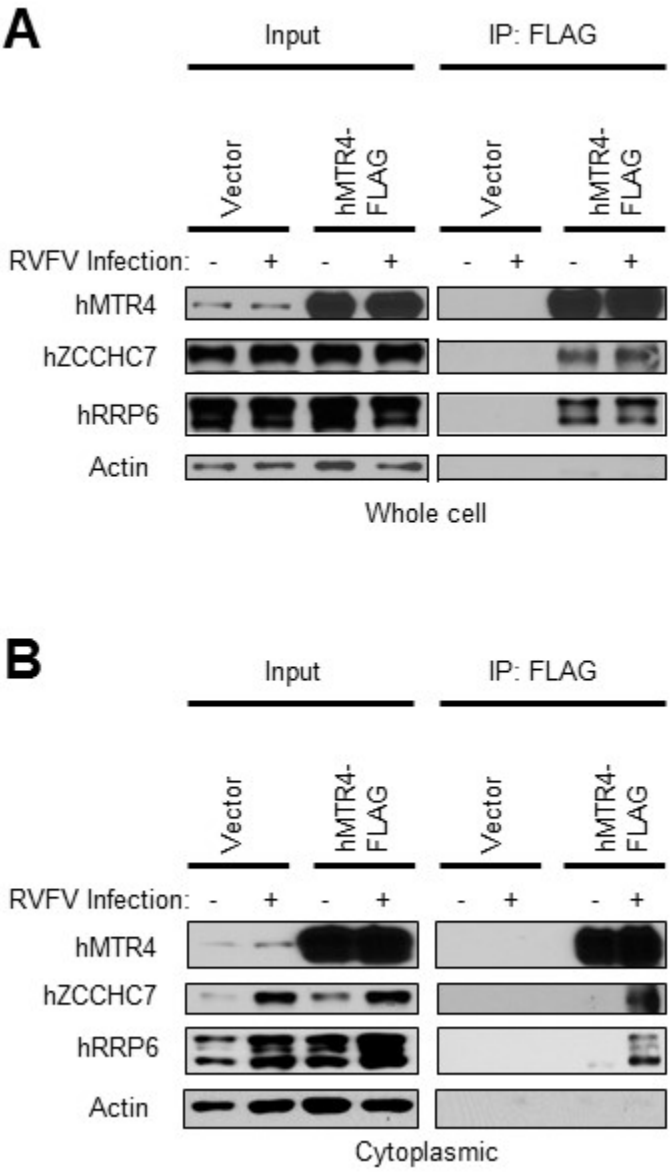

Figure 11: Human MTR4 and ZCCHC7 form a cytoplasmic complex with the exosome upon infection. U2OS cells were transfected with an hMTR4-FLAG expression vector or empty vector and infected with RVFV (MOI 10, 12h) or mock-infected, then either (A) whole cell lysates or (B) cytoplasmic fractions were processed for co-immunoprecipitation. 4% input was loaded for hMTR4 immunoblot, 8% input for other proteins. Actin was used as a loading control. Representative blots shown (n≥3).

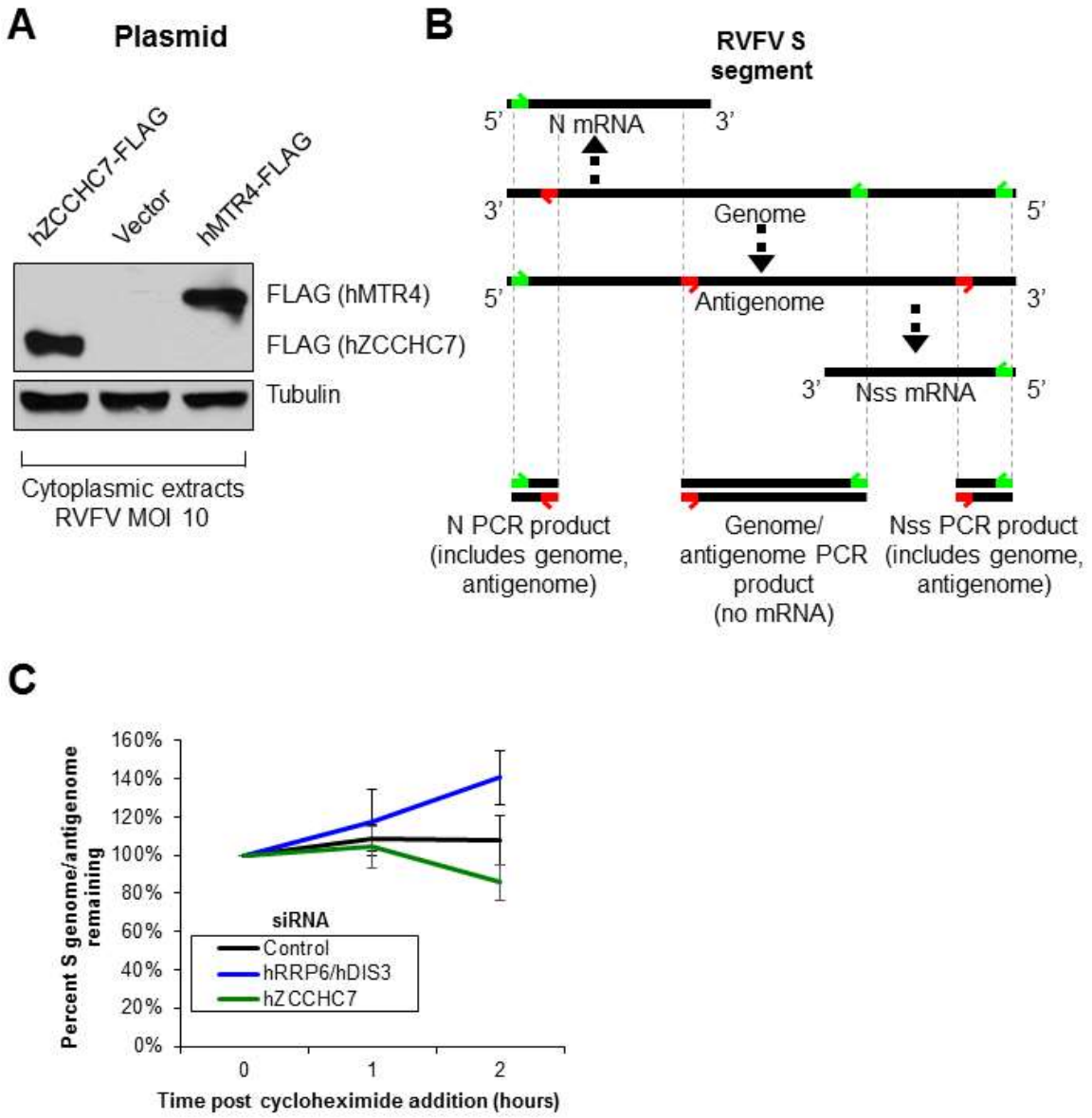

Figure 12: Human MTR4 and ZCCHC7 can be ectopically expressed. (A) U2OS cells were transfected with the indicated vectors, induced with doxycycline at 24 h, and infected with RVFV (MOI 10, 12h) at 48 h post-transfection. Nuclear/cytoplasmic fractionation was performed, and cytoplasmic fractions were subject to anti-FLAG immunoblot. A representative blot is shown (n=2). (B) Schematic of the RVFV S segment RNAs and PCR products produced during RNA immunoprecipitation. Forward primers are shown in green, reverse primers in red. N and Nss mRNA products also amplify genome and antigenome, but the genome/antigenome product does not amplify mRNAs. (C) U2OS cells were transfected with the indicated siRNAs and infected with RVFV (MOI 1, 12h). Infected cells were treated with cycloheximide (50 ug/ml) and processed for RT-qPCR at the indicated timepoints. Mean±SEM shown normalized to hDCP2 (n≥3).

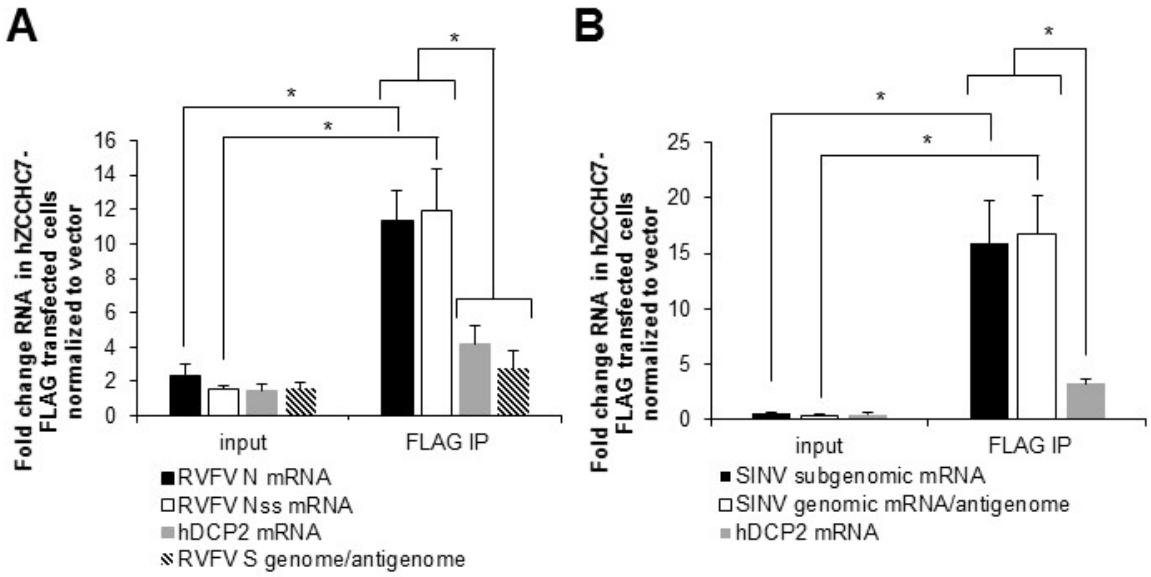

Figure 13: Viral mRNA is bound by hZCCHC7. (A-B) U2OS cells were transfected with an hZCCHC7-FLAG expression vector or empty vector and infected with (A) RVFV (MOI 10, 12h) or (B) SINV-GFP (MOI 10, 8h), then fractionated. Cytoplasmic extracts were collected (input) and a fraction was subject to FLAG immunoprecipitation and processed for RT-qPCR. RNA quantification was normalized to vector control input or FLAG IP. Fold change in hZCCHC7-bound RNA normalized to vector-bound RNA is presented. hDCP2 is used as an endogenous mRNA control as it is not known to be regulated during RVFV or SINV infection. Mean±SEM shown. *$p<0.05$ by Student's t-test.

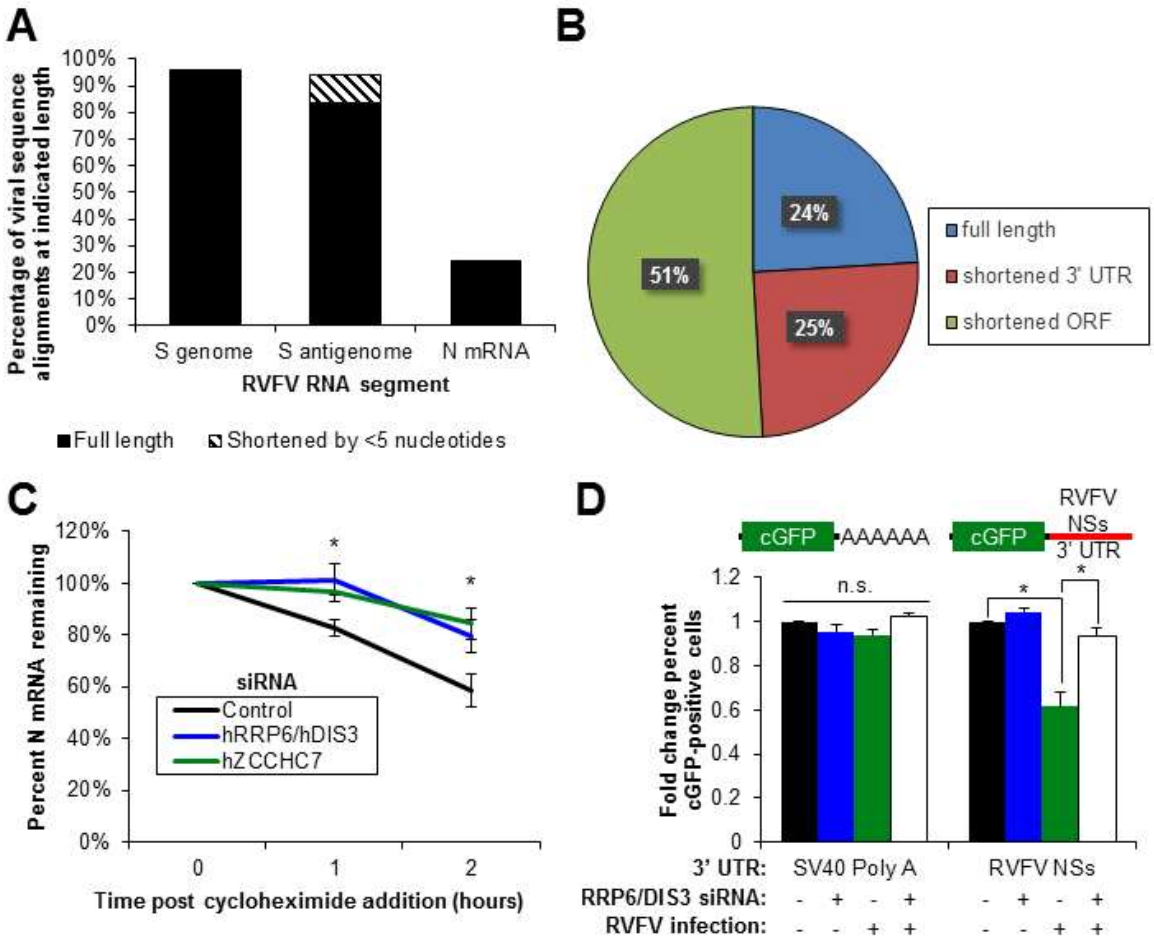

Figure 14: The RNA exosome and hZCCHC7 target viral mRNAs for decay. (A) U2OS cells were infected with RVFV (MOI 0.3, 18h) and 3' RACE was performed using primers that detect the RVFV small segment RNAs indicated. Sequenced reads were aligned to RVFV and classified as full-length or shortened, and the percentage of sequencing reads to be classified as full length or slightly shortened (less than 5 nucleotides) was plotted. Pooled data from three biological replicates is shown. (B) Pie chart of N mRNA reads from A that are full length (blue), encode a full length ORF but truncated 3' UTR (red), or that encode a truncated ORF are shown (green). (C) U2OS cells were transfected with the indicated siRNAs and infected with RVFV (MOI 1, 12h). Infected cells were treated with cycloheximide (50 µg/ml) and processed for RT-qPCR at the indicated timepoints. Mean±SEM shown normalized to hDCP2 (n≥3). *p<0.05 compared to control by Student's t-test. (D) U2OS cells stably expressing cGFP reporters with the indicated 3' UTRs were transfected with siRNAs targeting hRRP6 and hDIS3 or control and either uninfected or infected with RVFV (MOI 10, 18h). Cells were subsequently processed for automated immunofluorescence microscopy. Mean±SEM shown normalized to mock-infected control (n≥3). *p<0.05 compared to control by Student's t-test. A-B in collaboration with Sanjay Menghani. D in collaboration with Jeremy Wilusz.

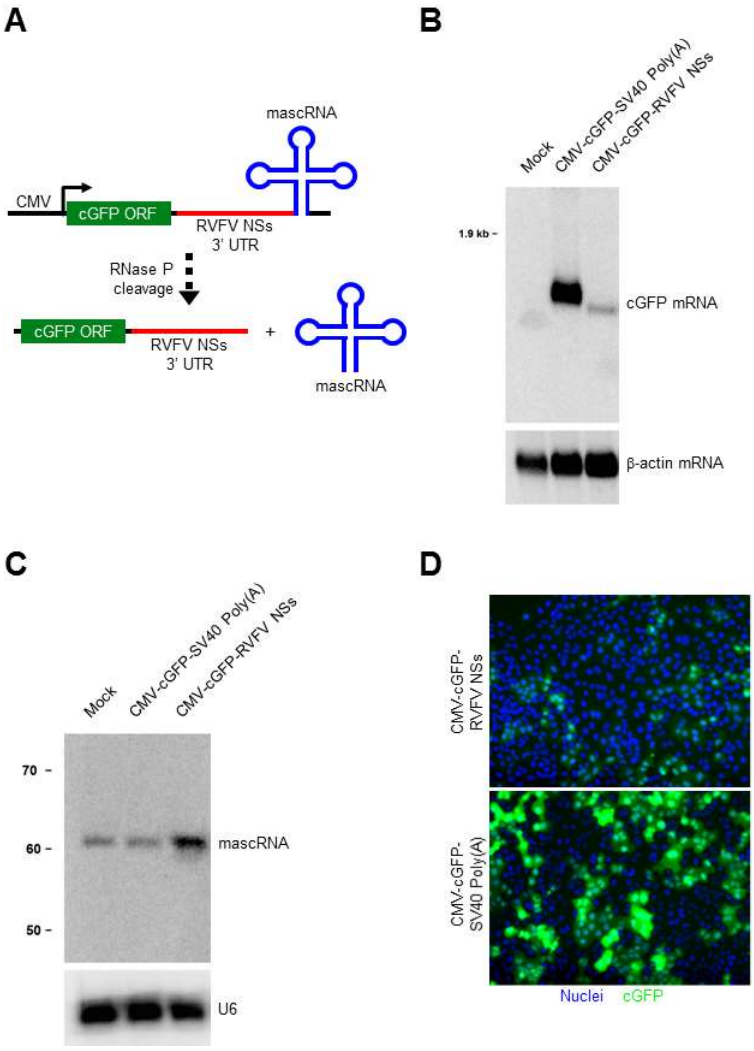

Figure 15: A cGFP reporter with the RVFV NSs 3' UTR can be expressed. (A) Schematic of the cGFP RVFV NSs-3' UTR reporter. A cGFP ORF is expressed with a downstream RVFV NSs 3' UTR and mascRNA sequence. RNase P cleavage generates a mature mRNA with the appropriate 3' UTR as well as a mascRNA. (B) U2OS cells were transfected with the indicated vectors and processed for cGFP northern blot 24 h later. Actin is used as a loading control (C) U2OS cells were transfected as in A and processed for mascRNA small RNA northern blot 24 h later. U6 is used as a loading control. (D) U2OS cells were transfected as in A and processed for automated immunofluorescence microscopy for cGFP (green) and nuclei (blue). A-D in collaboration with Jeremy Wilusz.

III. PKR SENSING OF VIRAL RNA DURING SINV INFECTION RECRUITS ZCCHC7 TO STRESS GRANULES AND EXOSOME GRANULES

Introduction

Infection with RNA viruses disturbs the normal intracellular milieu, changing the molecular landscape through the production of viral nucleic acids and proteins. These pathogen-associated molecular patterns (PAMPs) are detected by a series of dedicated sensors which signal transcription and activation of antiviral effecotrs and further sensors (Mogensen 2009).These sensors include the Toll-like receptors (TLRs), which detect viral glycoproteins or viral RNA on the cell surface or in endosomes as an early system for viral detection (Jensen and Thomsen 2012). Once viruses enter the cytoplasm and begin replication, they produce virus-specific RNAs such as dsRNAs or uncapped RNAs with 5' triphosphates (Moon and Wilusz 2013). These abnormal RNA motifs are detected by a variety of cytoplasmic sensors such as the helicases RIG-I and MDA5, as well as the dsRNA-activated kinase PKR (Clemens et al. 1993; Williams 1995; Balachandran et al. 2000; Kato et al. 2006; Kato et al. 2008). Detection of viral molecules through these sensors leads to diverse effects such as induction of the interferon response, translational shutdown to combat production of viral proteins, and apoptosis to prevent the spread of viral infection (Roberts et al. 1976; Castelli et al. 1997; Sadler and Williams 2008; Brennan-Laun et al. 2014).

In addition to the dedicated sensors, many members of the RNA metabolic machinery have acquired additional antiviral roles, identifying foreign viral RNA motifs and potentially targeting them for degradation (Moon et al. 2012b; Moy et al. 2014a). In particular, we recently found that components of the RNA exosome complex and its cofactor complex TRAMP, which degrade RNA 3' to 5', are antiviral against the diverse RNA viruses vesicular stomatitis virus (VSV), Rift Valley fever virus (RVFV), and Sindbis virus (SINV) (Molleston et al. 2016). Furthermore, the antiviral components of the TRAMP complex, hMTR4 and hZCCHC7, are exported from their

normal localization in the nucleolus to the cytoplasm in response to viral infection. There, hZCCHC7 specifically identifies viral mRNAs and targets them for exosomal degradation. Though we do not yet understand the signals which lead to TRAMP component export, we found that hZCCHC7 localizes to cytoplasmic punctae during viral infection, suggesting that it may be coregulated with ribonucleoprotein (RNP) granules.

RNP granules are localized collections of RNA-processing proteins and their bound RNA targets which form in the cytoplasm in a coregulated fashion (Thomas et al. 2011). The most extensively characterized of these RNP granules are stress granules, which form in response to a variety of stressors such as temperature shock or oxidative stress (Protter and Parker 2016). They are largely comprised of stalled initiation complexes on their bound mRNAs, as well as RNA-binding chaperones thought to remove regulated RNAs from translation and protect RNAs from damage during periods of stress. In addition to sequestering RNAs, stress granules are capable of passing stalled RNAs to other RNP structures such as processing bodies (P-bodies), which are composed of RNAs targeted for degradation as well as decapping and 5’ to 3’ decay enzymes (Kedersha et al. 2005).

Stress granules are also increasingly recognized as a component of the intrinsic immune response to viral infection. During infection, activation of PKR by viral RNA leads to the phosphorylation of the initiation factor eIF2α which stalls translation, blocking synthesis of new viral and host proteins and triggering the rapid accumulation of stress granules (Kedersha et al. 1999; Lindquist et al. 2011; Okonski and Samuel 2013). Stress granule formation has been shown for a variety of viruses, including Newcastle disease virus, encephalomyocarditis virus, influenza A virus, poliovirus, and SINV (Ng et al. 2013). In infection with several of these viruses, including SINV, these stress granules have also been shown to recruit RNA sensors and effectors such as RIG-I and RNASEL, which is believed to concentrate these proteins and their viral RNA targets together to better antagonize viral infection (Onomoto et al. 2012).

A third type of RNP granule, exosome granules, are much less well-characterized than P-bodies or stress granules. These granules are composed of structural components of the 3' to 5' RNA exosome complex as well as RNAs targeted for exosomal decay such as those containing AU-rich elements (Lin et al. 2007; Zurla et al. 2011). An emerging literature has linked a variety of antiviral RNA-binding proteins to the exosome, which potentially serves as a convergent effector of many sensors (Guo et al. 2007; Miyashita et al. 2011; Liang et al. 2015). As we demonstrated that hMTR4 and hZCCHC7 bind to the exosome in the cytoplasm during viral infection, it is likely that they colocalize with exosome granules (Molleston et al. 2016). However, the sensing pathways necessary for this protein movement are unknown, and whether these punctae represent exosome granules, stress granules, P-bodies, or unique structures has also yet to be determined.

In this study, we tested the hypothesis that the movement of hZCCHC7 is coregulated with the formation of known RNP granules in response to SINV infection. We determined that dsRNA, a known trigger for stress granule formation, is both necessary and sufficient to induce cytoplasmic hZCCHC7 punctae. We screened key innate immune signaling adaptors and sensors for their effects on hZCCHC7 movement and found that formation of hZCCHC7 punctae is PKR-dependent. Finally, we imaged components of the three major classes of RNP granules and found that hZCCHC7 granules colocalize with both exosome granules and stress granules, but not P-bodies, during SINV infection. Overall, we propose that PKR sensing of dsRNA during viral replication recruits the normally nucleolar hZCCHC7 to both stress granules and exosome granules, allowing it to sense translationally-stalled viral RNA and bring it to the exosome for degradation.

Results

Double-stranded RNA is sufficient to induce formation of cytoplasmic hZCCHC7 granules

We previously demonstrated that infection with SINV leads to the relocalization of components of the RNA exosome cofactor complex TRAMP, including hZCCHC7, from their normal localization in the nucleolus to the cytoplasm, where they form cytoplasmic punctae (Molleston et al. 2016). We found that this relocalization is activated by diverse viruses including VSV and RVFV. Since a major PAMP formed during replication of these diverse RNA viruses is dsRNA, we tested whether dsRNA is sufficient to induce this relocalization. To differentiate between effects mediated by the endosomal dsRNA sensor TLR3 and the cytosolic sensors such as RIG-I, MDA5, and PKR, we either added the synthetic dsRNA polyinosinic-polycytidylic acid (poly(I:C)) to the extracellular media or transfected it into the cytoplasm of cells (Kato et al. 2008; Barbalat et al. 2011; Laredj and Beard 2011). Cells were treated for 8 hours, after which immunofluorescence was performed for hZCCHC7 (Figure 16A,B). Extracellular treatment with poly(I:C) did not induce movement of hZCCHC7 to the cytoplasm, suggesting that RNA sensing by endosomal sensors is not sufficient for export. However, transfection of poly(I:C) induced formation of cytoplasmic hZCCHC7 punctae in a majority of transfected cells, suggesting that the presence of dsRNA in the cytoplasm is sufficient to induce export of hZCCHC7.

UV inactivated SINV cannot induce the formation of hZCCHC7 granules

Cytoplasmic sensors of dsRNA, such as RIG-I, MDA5, and PKR, require replication of RNA viruses in order to generate the dsRNA intermediates which they target (Triantafilou et al. ; da Conceição et al. 2013; Nikonov et al. 2013). Thus, infection with UV-inactivated viruses, which cannot replicate, does not activate these sensors, allowing differentiation between viral sensing through these pathways and replication-independent pathways. Therefore, we infected human U2OS cells with either live or UV-inactivated SINV. Cells were fixed and immunofluorescence was performed for hZCCHC7 and viral antigens (Figure 16C). We found that live SINV induced cytoplasmic hZCCHC7 punctae as previously published (Molleston et al. 2016). However, UV-

inactivated SINV did not, suggesting that viral replication is required for detection and export of hZCCHC7.

PKR is necessary for efficient hZCCHC7 export in response to SINV infection

Most TLR-mediated viral sensing requires the adaptors MyD88 or TRIF, while cytosolic RNA sensing by RIG-I and MDA5 requires the adaptor MAVS. PKR also detects cytosolic dsRNA. Therefore, we set out to determine whether any of these pathways were required for SINV-induced hZCCHC7 relocalization. To this end, we transfected U2OS cells with siRNAs targeting PKR, MAVS, or a combination of MyD88 and TRIF. Three days later we infected the cells with SINV and performed immunofluorescence to detect hZCCHC7 and viral infection (Figure 17A). We used image analysis to quantify the number of cells with cytoplasmic hZCCHC7 punctae and found that hZCCHC7 cytoplasmic accumulation in response to SINV infection is dependent on the cytosolic dsRNA sensor PKR (Figure 17B). This is consistent with our observation that hZCCHC7 export can be induced by poly(I:C) transfection and requires replication-competent SINV since PKR can be activated by poly(I:C) or SINV and requires viral replication for induction (Burke et al. 2009; Zhang et al. 2014).

ZCCHC7-containing granules can colocalize with exosome granules and stress granules

Previous work demonstrated that stress granules form during SINV infection in a PKR-dependent manner (Onomoto et al. 2012; Ng et al. 2013). Given the PKR-dependence of hZCCHC7 relocalization and its role as an antiviral sensor, we hypothesized that hZCCHC7 punctae may colocalize with stress granules during SINV infection. Therefore, we performed immunofluorescence for hZCCHC7 and the stress granule component TIAR in SINV or mock-infected U2OS cells (Figure 18A). We found that, as previously demonstrated, SINV infection induced the formation of TIAR-containing stress granules. Furthermore, these granules colocalized with hZCCHC7 (Figure 18D) suggesting that hZCCHC7 is recruited to stress granules during viral infection.

We previously found that hZCCHC7 co-immunoprecipitates with the exosome in the cytoplasm during infection (Molleston et al. 2016). Recent studies have suggested that exosome structural components such as hRRP41 accumulate in exosome granules that are distinct from stress granules (Sheth and Parker 2003; Graham et al. 2006; Lin et al. 2007). Therefore, we also tested whether SINV-induced hZCCHC7 co-localized with exosome granules. To this end, we performed immunofluorescence for hZCCHC7 and hRRP41 in U2OS cells infected with SINV or mock-infected (Figure 18B). We found that hRRP41 formed granules in SINV-infected cells, and that these granules colocalized with hZCCHC7-containing granules (Figure 18D).

A third major RNA granule are P-bodies. While P-bodies are also known to be modulated by viral infection (Reineke and Lloyd 2013; Hopkins et al. 2015) we observed that SINV infection does not lead to the formation of P-bodies during infection as measured by GW182 accumulation (Figure 18C). Altogether, these data suggest that virus-induced cytoplasmic hZCCHC7 granules localize to stress and exosome granules, but remain distinct from P-bodies.

Discussion

An emerging literature has identified a variety of antiviral RNA-binding proteins which relocalize from the nucleus to the cytoplasm during infection with cytoplasmic viruses (Moy et al. 2014a; Shapiro et al. 2014). In this study, we focused on the antiviral RNA binding protein hZCCHC7, an exosome cofactor of the TRAMP complex, which is exported to the cytoplasm during infection with several families of RNA viruses to restrict viral replication by targeting viral mRNA for decay (Molleston et al. 2016).

We first investigated the viral stimuli necessary for hZCCHC7 relocalization. Since RNA viruses are largely sensed by their nucleic acids, we hypothesized that viral RNA would likely be the pathogen-associated molecular pattern (PAMP) detected by infected cells. Indeed, we found that transfection of the synthetic immunostimulatory dsRNA poly(I:C) induced the formation of

cytoplasmic hZCCHC7 punctae. As SINV is a positive-sense signle-stranded RNA virus, the incoming viral RNA is not thought to be double stranded (Strauss and Strauss 1994). Rather, viral replication by the RNA dependent RNA polymerase produces viral dsRNA intermediates. Therefore, we tested whether UV-inactivated virus could induce the formation of punctae and found that UV-inactivated SINV could not induce the formation of hZCCHC7 punctae, demonstrating that viral replication is required.

Viral dsRNA is a known PAMP detected by a wide variety of sensors including TLR3, RIG-I, MDA5, and PKR (Barbalat et al. 2011). We tested the requirements for these sensors and their adaptors and found that SINV-induced hZCCHC7 relocalization was PKR-dependent. This is consistent with prior studies, which have shown that SINV can be detected by PKR (Burke et al. 2009). Furthermore, PKR signaling is known to depend on the presence of dsRNA during viral infection; UV-inactivated viruses cannot activate PKR, while poly(I:C) can (Zhang et al. 2014).Our findings suggest the presence of a two-sensor system for detection of viral infection in which sensing by PKR triggers export of hZCCHC7 which in turn targets viral RNA for exosomal degradation. This functionally parallels the two-sensor system of oligoadenylate synthase, which is also activated by viral dsRNA, triggering the activation of RNASEL, which degrades viral and cellular RNAs (Silverman 2007; Barbalat et al. 2011). The addition of hZCCHC7 to the list of antiviral effectors regulated in response to dsRNA further underlines the importance of this PAMP in recruiting RNA-specific antiviral effectors.

Since SINV is known to be detected by PKR and induce the formation of stress granules, we hypothesized that PKR-induced cytoplasmic hZCCHC7 would be recruited to stress granules. Therefore, we tested hZCCHC7 colocalization with markers of multiple types of RNP granules and found that SINV-induced hZCCHC7 granules colocalize with both exosome granules and stress granules. PKR-induced stress granules, known as “antiviral stress granules”, have previously been characterized as induced by a wide range of viruses including SINV (Onomoto et

al. 2012; Ng et al. 2013). These findings suggest that during SINV infection, hZCCHC7 is recruited to antiviral stress granules, which are known to recruit other antiviral RNA-binding proteins such as RIG-I and RNASEL. We hypothesize that focusing multiple antiviral sensors and effectors in one compartment is beneficial to the infected host and potentiates antiviral defense (Onomoto et al. 2014).

Our finding that virus-induced exosome granules and stress granules coalesce with ZCCHC7 demonstrates the flexibility of these RNP granules and furthermore suggests the possibility that stress and exosome granules may interact with each other. Stress granules have been previously observed to interact with p-bodies to pass RNAs to the 5' degradation machinery, and it has been suggested that mRNAs targeted to stress granules are also targeted to exosome granules, implying some overlap between stress granules and 3' degradation (Kedersha et al. 2005; Zurla et al. 2011). However, this work represents the first example of exosome cofactor proteins colocalizing with stress granule components. We hypothesize that infection-induced relocalization of hZCCHC7 causes retargeting of the RNA exosome to viral RNA in many locations, including stress granules, but it remains to be seen whether viral infection induces direct interaction between exosome and stress granules.

Overall, we have identified a new pathway by which detection of replicating SINV RNA by PKR leads to recruitment of nucleolar hZCCHC7 to RNP granules which have characteristics of both exosome granules and stress granules. These findings suggest that innate immunity is intimately associated with the RNA decay machinery and future studies will seek to further develop this important connection.

Materials and Methods

Cells, viruses, antibodies, and reagents

Human U2OS cells were grown and maintained as previously described (Moser et al. 2012). SINV-mKate (gift from M. Heise) was grown in C636 cells as described (Burnham et al. 2007).

Viral titers were calculated by plaque assay on BHK cells. Antibodies to hZCCHC7 were obtained from Sigma. Antibodies to hRRP41 were acquired from Santa Cruz. Antibodies to GW182 were acquired from Abcam. Antibodies to TIAR were acquired from BD. Fluorescent secondary antibodies were obtained from Invitrogen, and HRP-conjugated antibodies were from Amersham. Other chemicals were purchased from Sigma.

Mammalian RNAi

Ambion Silencer Select siRNAs were used for PKR, GE Dharmacon On-Target siRNAs were used for MAVS, MyD88, and TRIF. Transfection into U2OS cells was performed using HiPerFect (Qiagen) as per the manufacturer's protocol. Cells were incubated for 3 days. Silencer Select Negative Control #2 (Ambion) was used as a non-targeting control.

Viral infections

Three days post-RNAi, cells were infected with the indicated viruses. U2OS cells were infected with SINV-mKate (MOI = 10) for 5 hours.

Immunofluorescence

U2OS cells grown on coverslips were imaged with a Leica DMI 4000 B fluorescent microscope. MetaXpress software was used to quantify cytoplasmic hZCCHC7 punctae between .8 and 2 μm in size in mock infected and infected or transfected cells (infection was verified by immunofluorescence for each cell to be quantified) with at least 25 cells quantified per condition. All experiments were performed at least three times.

Transfection of polyinosinic-polycytidylic acid

Polyinosinic-polycytidylic acid (poly(I:C)) was transfected using Lipofectamine 2000 reagent (Thermo Fisher) according to the manufacturer's protocol. Cells were plated on coverslips in 24-well cell culture plates (40,000 cells/well). Five μg of poly(I:C) was transfected 24 hours after cell

plating, and media was changed 3 hours after transfection. Eight hours after transfection, cells were fixed and processed for immunofluorescence.

UV-inactivation of viruses

SINV-mKate and RVFV viral stocks were inactivated by treatment with 2 million microjoules of UV radiation in a UV Stratalinker 2400 hybridization oven. Viral infection was performed at a theoretical MOI of 25 for 5 hours (SINV) or 12 hours (RVFV) with parallel infection of live virus. Inactivation of viral replication was confirmed by loss of immunofluorescence signal compared to live virus.

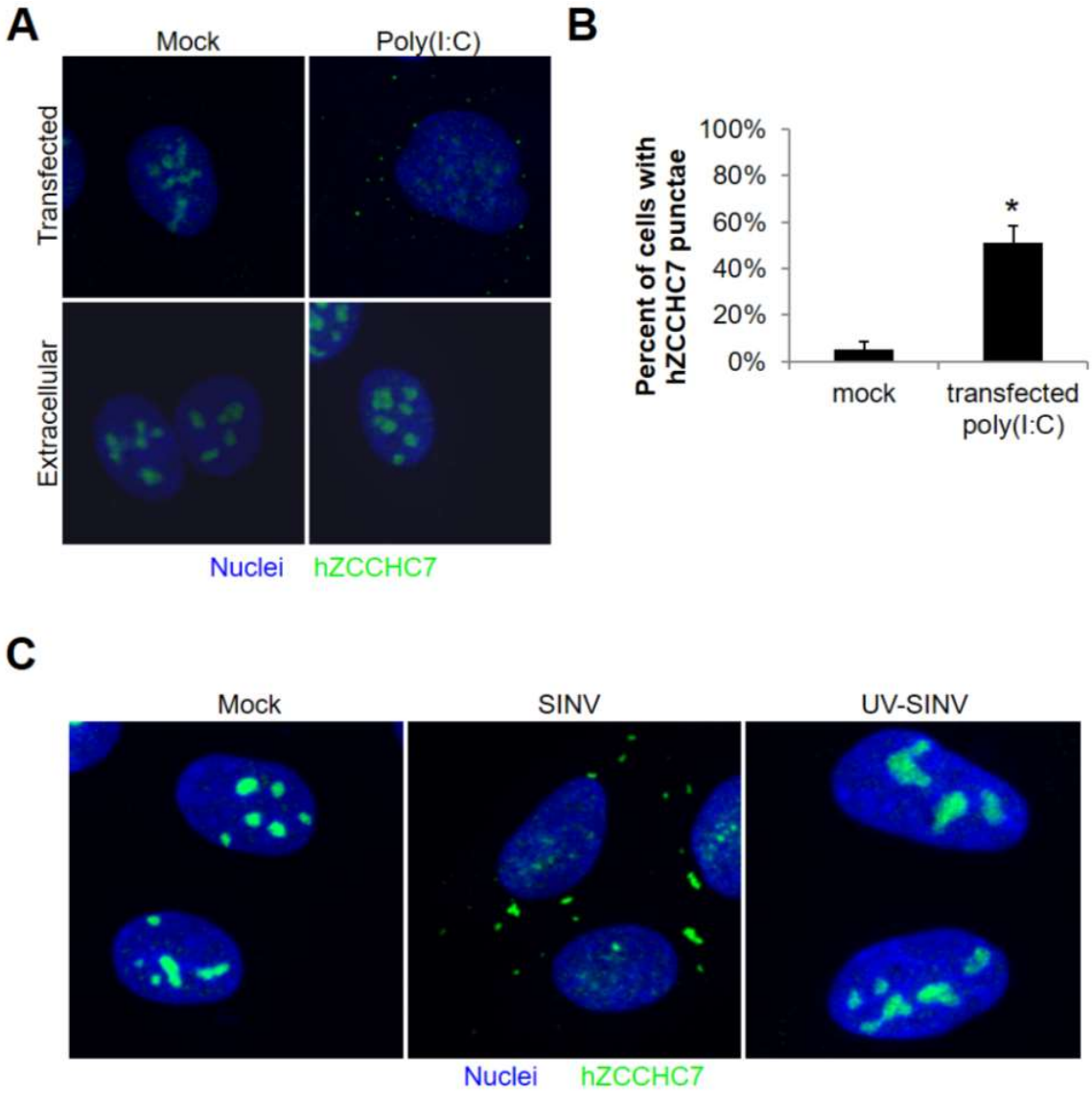

Figure 16: Export of hZCCHC7 to the cytoplasm requires replication of viral RNA. (A) U2OS cells were treated with poly(I:C) by transfection or extracellular addition to media for 8h and processed for immunofluorescence microscopy for hZCCHC7 (green) and nuclei (blue). (B) Quantification of the percentage of cells with cytoplasmic hZCCHC7 punctae in at least 3 experiments as in A. Mean±SEM shown. *$p<0.05$ compared to mock by Student's t-test. (C) U2OS cells were infected with live or UV-inactivated SINV-mKate (MOI 25, 5h) or mock infected and processed for immunofluorescence for hZCCHC7 (green) and nuclei (blue). Representative images of at least 3 experiments are shown.

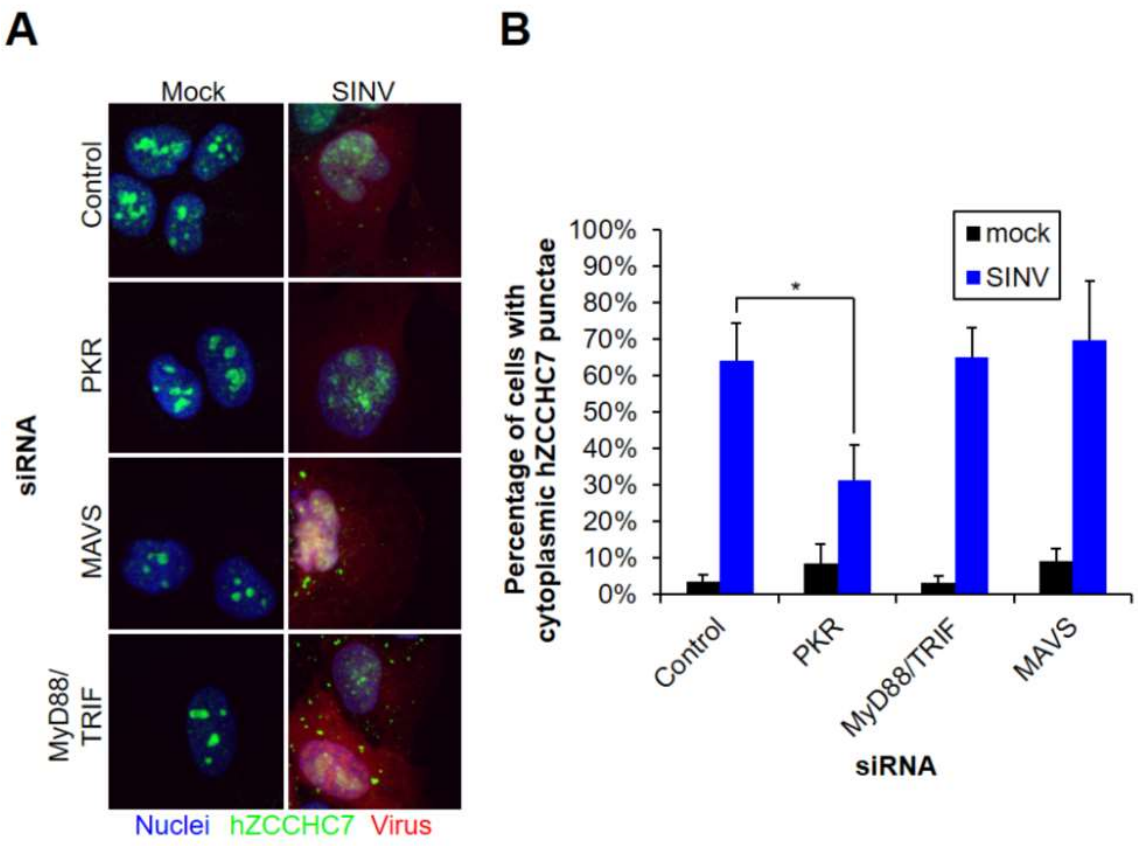

Figure 17: SINV-induced export of hZCCHC7 is PKR-dependent. (A) U2OS cells were transfected with the indicated siRNAs and infected with SINV-mKate (MOI 10, 5h) or mock infected and processed for immunofluorescence microscopy for hZCCHC7 (green), mKate (red), and nuclei (blue). (B) Quantification of the percentage of cells with cytoplasmic hZCCHC7 punctae in mock- or SINV-infected cells in at least 3 experiments as in A. Mean±SEM shown. *$p<0.05$ compared to mock by Student's t-test.

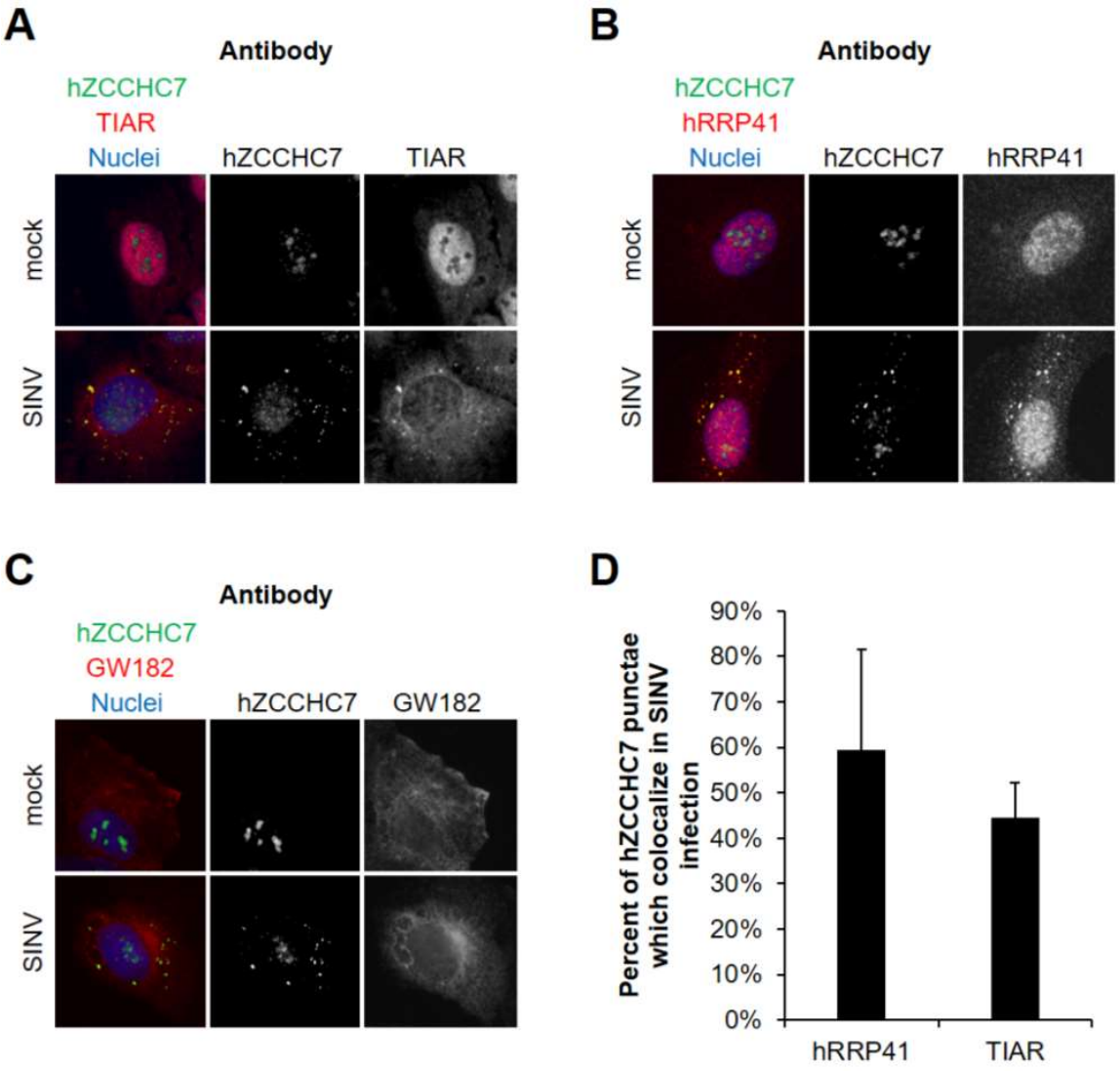

Figure 18: SINV-induced hZCCHC7 granules colocalize with exosome and stress granules. U2OS cells were infected with SINV-mKate (MOI 10, 5h) and processed for immunofluorescence for hZCCHC7 (green), nuclei (blue) or (A) TIAR, (B) hRRP41, or (C) GW182 (red). Representative images of at least 3 experiments are shown. (D) Quantification of the percentage of hZCCHC7 punctae which colocalize with hRRP41 or TIAR in SINV-infected cells in at least 3 experiments as in A and B. Mean±SEM shown.

IV. CONCLUDING REMARKS

Summary

The RNA processing machinery interacts with nearly every facet of cellular biology. In addition to its canonical cellular roles, it is increasingly recognized as one of the most ancient responses to RNA virus infection. RNA silencing, the 5' cap binding complex, the 5' decay machinery, and myriad RNA helicases have all been shown to double as antiviral effectors. However, the full cohort of antiviral proteins among the RNA processing machinery is not fully characterized. It is likely that additional roles exist in restriction of viral infection across virus families for previously identified RNA-binding proteins. To discover new roles for genes involved in RNA biology, we performed an RNAi screen to identify those with antiviral effects against the disparate arboviruses, vesicular stomatitis virus (VSV) and Sindbis virus (SINV).

The exosome as a conserved antiviral effector

Our screen identified 26 genes with antiviral effects against both VSV and SINV, including Ars2 and two components of the nuclear cap-binding complex (CBC20 and CBC80) which we had previously characterized as broadly antiviral (Sabin et al. 2009). In addition, several genes active at the 3' end of mRNA were identified; these include *hiiragi*, a poly(A) polymerase, as well as CG7185, the probable *Drosophila* ortholog of CPSF6, a cleavage and polyadenylation factor (Sabin et al. 2009; Sabath et al. 2013). Of particular interest to us was the identification of dRrp6, one of the key 3' to 5' exonucleases in the RNA exosome complex, and the only exosome component in the screening panel. In a previous genome-wide RNAi screen using Rift Valley fever virus (RVFV), we found the other exosomal exonuclease, dDis3, to be antiviral (Hopkins et al. 2013). The combination of multiple exosome genes identified as antiviral in screens against diverse RNA viruses suggested a broad role for the exosome complex as a whole. Thus, we tested the exonucleases dRrp6 and dDis3 as well as the exosome structural components dRrp4 and dRrp41 against VSV, SINV, and RVFV, and found that each of these genes is antiviral

against all three viruses tested. Furthermore, we found that the antiviral effects of these genes are conserved from flies into human cells.

The exosome has long been suggested to play an antiviral role in diverse organisms including humans and yeast. Several of the exosome core and cofactor genes were first identified due to the “superkiller” phenotype, in which yeast strains mutant in exosome core or cofactor genes were killed far more efficiently by dsRNA viruses (Masison et al. 1995; Anderson and Parker 1998; Benard et al. 1998). At the time this was attributed to translational rather than RNA stability effects. However, in light of the subsequent characterization of the RNA exosome complex, it is likely that degradation of viral RNA plays a role in controlling yeast viruses. In human cells, several different RNA-binding proteins with antiviral activity, such as ZAP, DDX60, and AID, were found to bind to exosome components (Guo et al. 2007; Miyashita et al. 2011; Liang et al. 2015). However, the studies characterizing these interactions did not independently identify effects of exosome depletion on viral replication. I hypothesize that an antiviral role for the exosome was not previously observed due to the incomplete depletion of these genes by RNAi in human cells, resulting in only modest effects on viral replication. In *Drosophila*, dsRNA more efficiently depletes targets, resulting in substantially more pronounced effects of exosome depletion on viral RNA. Furthermore, the strongest antiviral effects on viral RNA in *Drosophila* were from the exosome exonucleases, the original antiviral hits from our screens. These exonucleases have not been studied in the context of viral infection previously. Rather, all prior studies instead focused on the structural components of the exosome which have a less pronounced antiviral phenotype.

By screening components of the known exosome cofactor complexes Ski, TRAMP, and NEXT, I was able to determine that two components of the TRAMP complex, dMtr4 and dZcchc7, were antiviral against all viruses tested. However, neither the TRAMP-associated poly(A) polymerase dTrf4-1, nor the Ski and NEXT complexes had this activity. Furthermore, I found that the antiviral roles of Mtr4 and Zcchc7 are conserved in their human orthologs, hMTR4 and hZCCHC7. In the

case of Mtr4, the conserved antiviral role between humans and *Drosophila* is not surprising given the high level of amino acid conservation; the protein has approximately 67% identity between these two species, and 51% identity between humans and yeast (Houseley and Tollervey 2008). However, Zcchc7 is not nearly as conserved; the yeast Zcchc7 ortholog, Air2, is only 34% identical to hZCCHC7 in the zinc finger region, with no homology elsewhere in the protein. Similarly, hZCCHC7 is only 33% identical to dZcchc7 in the zinc finger region and completely dissimilar elsewhere, suggesting that Zcchc7/Air is divergent across species. While Mtr4 has been found to have a role in processing of the 5.8s rRNA in both yeast and humans, the only identified RNA to be targeted by the other TRAMP components in humans is the 5' ETS spacer remaining during rRNA processing (de la Cruz et al. 1998; Shcherbik et al. 2010; Lubas et al. 2011). Most other yeast TRAMP roles have been taken over by the human NEXT complex, which shares hMTR4 with TRAMP. In light of my new findings, it seems that the loss of other important roles for Zcchc7 in animals has permitted it to develop new targeting specificities which include viral RNA. It is clear that despite continued sequence divergence between *Drosophila* and humans, Zcchc7 has retained enough functional conservation to have broad antiviral roles in both species.

It is surprising that no components of the Ski complex were antiviral against any of the viruses tested, given that the first discovered role for the yeast Ski genes was in restriction of dsRNA yeast viruses (Toh-E et al. 1978). Furthermore, the use of a cytoplasmic cofactor complex in restriction of cytoplasmic RNA viruses is much simpler than movement of a nucleolar complex into the cytoplasm. There are several potential reasons why the Ski complex is not antiviral. Firstly, it may not be involved in degradation of viral RNA even in yeast; despite later being found to be exosome cofactors, the yeast Ski genes were not found to affect degradation rates of viral RNA, rather antagonizing viral replication at the level of translation (Masison et al. 1995). Secondly, it is possible that viruses have developed evasion or antagonism strategies to the Ski complex due to its presence in the cytoplasmic compartment across kingdoms. Both RVFV and

SINV are known to make accessory proteins which induce degradation or inhibit transcription of antiviral factors, so they may have found a way to antagonize Ski, necessitating the repurposing of TRAMP to the cytoplasm as a new antiviral weapon (Bouloy et al. 2001; Frolova et al. 2002; Billecocq et al. 2004; Gorchakov et al. 2004; Garmashova et al. 2006; Ikegami et al. 2009). Finally, it is possible that Ski has an antiviral role which is obscured by its additional regulatory roles; the human Ski helicase SKI2L was recently found to downregulate interferon production to prevent autoimmunity, and though *Drosophila* lacks interferon, it is possible that dSki2 has regulatory roles in flies as well (Eckard et al. 2014). If depletion of Ski genes results in overproduction of antiviral factors such as interferon, the effect on viral replication may not be predictable, obfuscating the many potential roles of the Ski complex.

The regulation of TRAMP component export

Due to the broad antiviral role of the RNA exosome and TRAMP cofactor components in human cells, I hypothesized that the RNA-binding TRAMP components target viral RNA for exosomal degradation. However, VSV, SINV, and RVFV all replicate in the cytoplasm, while the TRAMP components are restricted to the nucleus. Thus, a direct antiviral role would require relocalization of these components to the cytoplasm. Interestingly, precedent exists for this type of intracellular movement in response to infection; an increasing number of nuclear RNA-processing proteins have been identified which move to the cytoplasm to target viral RNA. The pri-miRNA-processing nuclease Drosha is exported to the cytoplasm in response to infection with diverse arboviruses or treatment with the synthetic dsRNA poly(I:C) and mediates an antiviral response (Shapiro et al. 2014). In addition, the splicing and transcriptional regulator DDX17 moves to the cytoplasm during bunyavirus infection and binds bunyavirus RNA to restrict viral replication (Moy et al. 2014a). Consistent with the behavior of these other nuclear antiviral RNA-binding proteins, I found that the canonically nucleolar hMTR4 and hZCCHC7 are exported to the cytoplasm during infection with VSV, SINV, or RVFV. Furthermore, hZCCHC7 forms cytoplasmic granules during viral infection that can colocalize with stress granules and exosome granules.

I investigated the sensing mechanisms responsible for the relocalization of these proteins and found that transfection with poly(I:C) was sufficient to trigger protein export from the nucleus. Consistent with this, the dsRNA-sensitive kinase PKR, which is known to respond to both SINV and poly(I:C), was necessary for hZCCHC7 movement during SINV infection. As with Drosha, the antiviral TRAMP components move in response to a variety of viral signals in addition to poly(I:C), suggesting the possibility that the export of these proteins is regulated in the same way. Though RVFV also induces hZCCHC7 movement to cytoplasmic punctae, it is likely not regulated in the same way; RVFV induces PKR degradation during viral infection and prevents the formation of PKR-dependent granules such as stress granules, making it likely that it is sensed in another way to induce hZCCHC7 granules (Ikegami et al. 2009; Hopkins et al. 2015; Kainulainen et al. 2016). In order to determine whether viral replication is necessary for cellular sensing and subsequent export of TRAMP components, I infected cells with UV-inactivated or live virus and found that UV-inactivated virus could not induce hZCCHC7 relocalization to the cytoplasm. This finding is consistent with PKR as the sensor; PKR is activated by dsRNA intermediates which form during viral infection thus requires viral replication (Burke et al. 2009; Zhang et al. 2014).

A cytoplasmic TRAMP-like complex

In order to function as cofactors for the exosome, RNA-binding proteins must interact with exosome proteins to deliver targeted RNA for degradation. In their canonical nucleolar roles, the TRAMP components hMTR4 and hZCCHC7 interact with the exosome exonuclease hRRP6, which is itself both nuclear and cytoplasmic (Tomecki et al. 2010; Lubas et al. 2011). In order to target viral RNA for degradation, I hypothesized that hMTR4 and hZCCCH7 would interact with hRRP6 as well as viral RNA in the cytoplasm. Indeed, I was able to find that hMTR4 immunoprecipitates with hRRP6 and hZCCHC7 in cytoplasmic fractions only during virus infection, suggesting the formation of an infection-dependent cytoplasmic complex in addition to the canonical nucleolar TRAMP complex. Furthermore, cytoplasmic hZCCHC7 specifically binds viral mRNA, suggesting that this cytoplasmic complex of TRAMP components targets viral RNA

for degradation. This interaction between RNA-binding antiviral proteins and components of the exosome is an emerging theme in the literature. For example, ZAP, DDX60, and AID have all been shown to bind exosome components, though none of them demonstrated an infection-dependent complex (Guo et al. 2007; Miyashita et al. 2011; Liang et al. 2015). Furthermore, all of these proteins have been found to bind viral RNA, as hZCCHC7 does. I hypothesize that these RNA-binding proteins serve as sensors for different classes of viruses which all converge on the RNA exosome for their effector function. It is likely that these antiviral sensors have some synergistic roles as well; DDX17 binds bunyaviral RNA and immunoprecipitates with both ZAP and hMTR4, suggesting the possibility that sensors of different viral RNA motifs may physically group together to recruit the exosome (Chen et al. 2008; Lubas et al. 2011; Moy et al. 2014a).

This cytoplasmic complex of TRAMP components and the exosome likely operates independently of the canonical TRAMP complex. In the nuclear and nucleolar roles of TRAMP, the poly(A) polymerase Trf4 adds 5-6 adenines to RNAs targeted for exosomal degradation (Egecioglu et al. 2006). My 3' RACE analysis revealed no evidence of untemplated oligoadenlyation on any RVFV RNAs. Combined with our verification that the TRAMP poly(A) polymerase dTrf4-1 is not antiviral, these data suggest that the role for the TRAMP components in RVFV infection is distinct from that of canonical TRAMP. Oligoadenylation of RNA targets is believed to have evolved to create a "launching pad" of unstructured RNA to permit degradation of heavily structured targets such as tRNAs, and is dispensable for many other targets (Paolo et al. 2009). Viral RNAs, which are less structured than tRNAs, likely do not require adenylation for exosomal degradation.

Recent evidence has demonstrated roles for Mtr4 in a variety of "TRAMP-like" complexes independent of the Trf4 polymerase. In yeast, Mtr4 has been shown to interact with different RNA-binding adaptor proteins to process distinct rRNA targets (Thoms et al. 2015). Human MTR4 forms both the nucleolar TRAMP and nucleoplasmic NEXT complexes (Lubas et al. 2011). Given that Mtr4 exists as part of several distinct and co-occuring complexes, it has been

suggested that these complexes, such as NEXT, should be named to reflect their protein composition and localization as compared to canonical TRAMP. Therefore, I propose that the cytoplasmic complex I describe be called the VICE (Virus-Induced Cytoplasmic Exosome) complex.

Viral RNAs as RNA regulons

Classes of mRNAs such as immune mediators are tightly regulated together in groups called RNA regulons. These regulons contain sequences in the 3' UTR, such as AU-rich elements or C-rich motifs, that are recognized by RNA-binding proteins, leading to up- or down-regulation of these RNAs by altering their susceptibility to degradation machinery including the exosome (Chen et al. 2001; Mukherjee et al. 2002; Keene 2007; Singer et al. 2012; Blackinton and Keene 2014). As the exosome degrades several classes of mRNAs based on signals in their 3' UTR's, I hypothesized that the 3' UTR of RVFV is the RNA sequence which recruits the exosome for degradation, and used a cGFP-3'UTR reporter system to test this hypothesis. I found that expression of the RVFV NSs 3' UTR downstream of the cGFP ORF was sufficient to induce exosome-dependent reduction of cGFP expression during RVFV infection. A similar construct with an SV40 polyadenylation signal was not affected by RVFV infection nor exosome depletion, suggesting that the effect of the exosome on the NSs 3' UTR is specific and not merely a byproduct of normal exosome-mediated mRNA turnover. The requirement of viral infection for exosome-dependent restriction of a viral 3' UTR suggests that this recognition is regulated. We previously found that RVFV infection induced 5' degradation of mRNAs containing 5' terminal oligopyrimidine tracts (Hopkins et al. 2015). Just as these endogenous mRNAs are subject to degradation during RVFV infection, it is possible that changes such as the movement of hZCCHC7 and hMTR4 induce restriction of exogenous viral mRNAs by recognition of their 3' UTRs. This apparent viral RNA regulon could in fact be just one example of a larger group of mRNAs regulated during viral infection by the VICE complex.

Though I have demonstrated binding of RVFV and SINV mRNA by hZCCHC7, the specific viral RNA sequence within the 3' UTR necessary for binding remains unknown. RNA viruses frequently have higher order structures such as stem loops. Our lab and others have previously identified several of these structures in the 3' UTRs of RVFV (Ikegami et al. 2007; Moy et al. 2014a). Alternatively, RVFV mRNAs, which are not polyadenylated, may be recognized by cytoplasmic TRAMP components in the VICE complex due to their missing poly-A tails. This mirrors one of the nuclear roles of yeast TRAMP, wherein it degrades mRNA precursors which fail to polyadenylate (Milligan et al. 2005). It is likely that structural motifs rather than specific sequence motifs drive recognition of RVFV mRNAs, as the different mRNAs have 3' UTRs which vary both in length and sequence composition, making one common sequence motif unlikely (Ikegami et al. 2007).

Future directions

While I have successfully characterized a virus-induced cytoplasmic exosome complex, much remains unclear about the induction, composition, and RNA target identification of this complex. Thus, I propose a range of future studies in these three broad areas to better understand both the regulation of exosomal targeting and the determinants of antiviral activity of this novel complex.

Though I have found that manipulating PKR levels by siRNA affects hZCCHC7 export in response to SINV infection, a better understanding of the signaling is needed. First, my studies of sensors and adaptors only involved siRNA depletion. The creation of genetic mutant cells, perhaps using CRISPR, would allow me to assess whether hZCCHC7 movement can be completely abolished in the absence PKR, thus establishing it as necessary for viral sensing in this context. Furthermore, though it is unlikely that PKR senses RVFV infection, the sensor that drives hZCCHC7 export during RVFV is still unknown. Future studies should involve an siRNA screen of TLRs and RLRs assessing hZCCHC7 export by immunofluorescence or nuclear/cytoplasmic fractionation to determine which cellular sensors of viral infection are

responsible for this movement in RVFV infection. Identification of the sensor pathway involved will lead to a better understanding of the viral pathogen associated molecular pattern as well as its detection method.

In addition to better characterization of events upstream of the sensors of virus infection, future studies should also explore the signal transduction downstream of the sensor. In addition to its canonical role in phosphorylation of eIF2α, PKR has been suggested to converge on the innate immune signaling cascade at the level of binding TRAF proteins and the IKK complex (Zamanian-Daryoush et al. 2000; García et al. 2004; Mogensen 2009). Measuring the activation of each step in the pathway of PKR activation, both the canonical steps of autophosphorylation and phosphorylation of eIF2α as well as the putative PKR-involved innate immune pathways of phosphorylation of IKKβ and translocation of NF-κB to the nucleus, would demonstrate which signals downstream of PKR are activated by SINV infection, as well as providing a clue to the point of convergence between responses to SINV and RVFV infection. Furthermore, manipulation of these intermediaries through siRNA or genetic knockouts would allow me to demonstrate which signaling pathways are important for the export of TRAMP components.

After signal transduction, a likely candidate for a direct molecular signal affecting TRAMP component localization is the small ubiquitin-like modifier (SUMO). SUMO is, like ubiquitin, a small protein which is covalently linked to lysines (Seeler and Dejean 2003; Gareau and Lima 2010). Changes in SUMOylation of proteins affect protein function, stability, and localization, which is of particular relevance to hMTR4 and hZCCHC7. CRM1-mediated export of proteins such as TEL and p53 require that the proteins are SUMOylated as they are exported in order to be released from CRM1 into the cytoplasm (Wood et al. 2003; Santiago et al. 2013). Furthermore, patterns of SUMOylation are altered by the interferon response during viral infection, and increased SUMOylation of antiviral effectors is integral to deactivating inflammatory signals as viruses are cleared (Liu et al. 2013; Sahin et al. 2014; Decque et al. 2016). In light of these interactions, it is unsurprising that viruses such as IAV cause widespread changes in the

SUMOylation of transcription factors and other proteins (Domingues et al. 2015). ZCCHC7 has several putative SUMOylation sites identified by mass spectrometry, some of which are adjacent to computationally-predicted nuclear export and nucleolar localization signals (Hendriks et al. 2014; Lamoliatte et al. 2014; Hendriks et al. 2015a; Hendriks et al. 2015b; Xiao et al. 2015). Identification of differential SUMOylation of hZCCHC7 by immunoprecipitation in nuclear and cytoplasmic fractions, as well as mutation of putative SUMOylation sites in the protein, would help identify whether these changes are necessary for virus-induced export. Additionally, mutation of the SUMO ligases and deSUMOylating enzymes may perturb hZCCHC7 localization and reveal how this protein is exported.

The second major area of potential future study is in the composition of the VICE complex. My studies focused on the proteins which were identified in antiviral roles in *Drosophila*, namely Mtr4 and Zcchc7, and confirmed that these proteins are antiviral in humans and form a virus-induced cytoplasmic complex. I was also able to demonstrate that hZCCHC8, which also interacts with hMTR4 in the nucleus as part of the NEXT complex, is not exported during viral infection, suggesting some specificity to TRAMP component export. However, I did not study the third TRAMP component, the poly(A) polymerase Trf4 (hTRF4-1 and hTRF4-2 in humans), as dTrf4-1 was not antiviral and I found no evidence of adenylation of RVFV RNAs by 3' RACE. However, whether this protein is exported during viral infection or not remains an open question, and would help to determine whether VICE shares the composition of TRAMP or is in fact a compositionally-distinct TRAMP-like complex. Though target RNAs of TRAMP are generally known to be adenylated by Trf4, this adenylation is not essential for degradation of every target. Furthermore, despite the dispensability of dTrf4-1 in *Drosophila*, it is possible that hTRF4-1 or hTRF4-2 does restrict virus infection in human cells.

The TRAMP-like complex NEXT, which shares hMTR4 with TRAMP but has otherwise different composition, was discovered by performing mass spectrometry on immunoprecipitated hMTR4 to identify binding partners (Lubas et al. 2011). By performing a similar experiment on cytoplasmic

hMTR4 during virus infection, I could identify additional binding partners of hMTR4 and hZCCHC7 that might be involved in restriction of viral infection. If the VICE complex has different composition than TRAMP, it could involve other proteins not seen in the canonical TRAMP complex. Lysates from nuclear and cytoplasmic fractions, as well as from infected and uninfected cells, would help determine binding partners which are specific to the cytoplasmic compartment and to viral infection.

The final area in which there are major unanswered questions is in the RNA motifs which are bound by TRAMP components and recruit the exosome for degradation. One way to identify these specific motifs would be with CLIP-seq analysis of hMTR4 or hZCCHC7. Though immunoprecipitation analysis of these proteins has been performed in many organisms and CLIP-seq approaches have been performed in yeast, no study has yet explored the full complement of RNAs bound by the human TRAMP components (Schneider et al. 2012; Tuck and Tollervey 2013). Performing such a study in both infected and uninfected cells could elucidate the full range of RNAs targeted by TRAMP as well as the cytoplasmic counterpart, VICE. This analysis would provide a key piece of information about human TRAMP, which does not target most of the RNAs targeted by yeast TRAMP, leaving its function in cellular homeostasis largely unknown (Lubas et al. 2011). Additionally, performing CLIP-seq in viral infection could identify the specific viral sequences bound by VICE, broadening our understanding of how viral RNAs are targeted.

More specific methods could also be used to address this question. The genome of SINV is amenable to insertion of various RNA sequences, which we have previously used to test sequences for DDX17 binding (Moy et al. 2014a). Similarly, candidate RNA sequences could be inserted into or removed from the SINV genome and RNA immunoprecipitation performed to assess the effects on hZCCHC7 binding levels. The GFP 3' UTR reporter which I used is another key tool; we can remove areas of the RVFV 3' UTR from the GFP reporter, or clone in other bunyaviral and other 3' UTRs, in order to identify the minimal sequence necessary for control by the exosome during viral infection.

In conclusion, I have used RNAi screening in a *Drosophila* model system to discover a broad and conserved antiviral role for both the RNA exosome and its cofactors. I have mechanistically explored how components of the TRAMP complex move to the cytoplasm in response to viral RNA, colocalize with other RNP granules, bind to the exosome and viral mRNA, and target this RNA for degradation based on sequences in the viral 3' UTR. Furthermore, I have demonstrated the first cytoplasmic role for components of the TRAMP complex and characterized a new way in which exosomal targeting is regulated by cofactor relocalization. These studies have highlighted the role of RNA decay and targeting in antiviral defense, and provided a better understanding of the convergent pathways that respond to a variety of viral threats with a common downstream response. A more complete understanding of both RNA regulation and antiviral defense will enable new treatments for viral infections and a more thorough understanding of the interaction between disease and immunity at the level of RNA.

V. BIBLIOGRAPHY

Albarino CG, Bird BH, Nichol ST. 2007. A Shared Transcription Termination Signal on Negative and Ambisense RNA Genome Segments of Rift Valley Fever, Sandfly Fever Sicilian, and Toscana Viruses. *Journal of Virology* **81**: 5246-5256.

Allmang C, Kufel J, Chanfreau G, Mitchell P, Petfalski E, Tollervey D. 1999a. Functions of the exosome in rRNA, snoRNA and snRNA synthesis. *The EMBO journal* **18**: 5399-5410.

Allmang C, Petfalski E, Podtelejnikov A, Mann M, Tollervey D, Mitchell P. 1999b. The yeast exosome and human PM-Scl are related complexes of 3' --> 5' exonucleases. *Genes & Development* **13**: 2148-2158.

Andersen PR, Domanski M, Kristiansen MS, Storvall H, Ntini E, Verheggen C, Schein A, Bunkenborg J, Poser I, Hallais M et al. 2013. The human cap-binding complex is functionally connected to the nuclear RNA exosome. *Nature structural & molecular biology* **20**: 1367-1376.

Anderson JS, Parker RP. 1998. The 3' to 5' degradation of yeast mRNAs is a general mechanism for mRNA turnover that requires the SKI2 DEVH box protein and 3' to 5' exonucleases of the exosome complex. *The EMBO journal* **17**: 1497-1506.

Araki Y, Takahashi S, Kobayashi T, Kajiho H, Hoshino S, Katada T. 2001. Ski7p G protein interacts with the exosome and the Ski complex for 3'-to-5' mRNA decay in yeast. *The EMBO journal* **20**: 4684-4693.

Ayache J, Bénard M, Ernoult-Lange M, Minshall N, Standart N, Kress M, Weil D. 2015. P-body assembly requires DDX6 repression complexes rather than decay or Ataxin2/2L complexes. *Molecular biology of the cell* **26**: 2579-2595.

Balachandran S, Roberts PC, Brown LE, Truong H, Pattnaik AK, Archer DR, Barber GN. 2000. Essential Role for the dsRNA-Dependent Protein Kinase PKR in Innate Immunity to Viral Infection. *Immunity* **13**: 129-141.

Barbalat R, Ewald SE, Mouchess ML, Barton GM. 2011. Nucleic acid recognition by the innate immune system. *Annual Review of Immunology* **29**: 185-214.

Barr JN. 2007. Bunyavirus mRNA synthesis is coupled to translation to prevent premature transcription termination. *RNA (New York, NY)* **13**: 731-736.

Benard L, Carroll K, Valle RCP, Wickner RB. 1998. Ski6p Is a Homolog of RNA-Processing Enzymes That Affects Translation of Non-Poly(A) mRNAs and 60S Ribosomal Subunit Biogenesis. *Molecular and Cellular Biology* **18**: 2688-2696.

Billecocq A, Spiegel M, Vialat P, Kohl A, Weber F, Bouloy M, Haller O. 2004. NSs protein of Rift Valley fever virus blocks interferon production by inhibiting host gene transcription. *Journal of virology* **78**: 9798-9806.

Bird BH, Ksiazek TG, Nichol ST, Maclachlan NJ. 2009. Rift Valley fever virus. *Journal of the American Veterinary Medical Association* **234**: 883-893.

Blackinton JG, Keene JD. 2014. Post-transcriptional RNA regulons affecting cell cycle and proliferation. *Seminars in cell & developmental biology* **34**: 44-54.

Bouloy M, Janzen C, Vialat P, Khun H, Pavlovic J, Huerre M, Haller O. 2001. Genetic evidence for an interferon-antagonistic function of rift valley fever virus nonstructural protein NSs. *Journal of virology* **75**: 1371-1377.

Bouloy M, Weber F. 2010. Molecular biology of rift valley Fever virus. *The open virology journal* **4**: 8-14.

Boutros M, Kiger AA, Armknecht S, Kerr K, Hild M, Koch B, Haas SA, Paro R, Perrimon N. 2004. Genome-wide RNAi analysis of growth and viability in Drosophila cells. *Science (New York, NY)* **303**: 832-835.

Brengues M, Teixeira D, Parker R. 2005. Movement of Eukaryotic mRNAs Between Polysomes and Cytoplasmic Processing Bodies. *Science* **310**.

Brennan-Laun SE, Ezelle HJ, Li X-L, Hassel BA. 2014. RNase-L control of cellular mRNAs: roles in biologic functions and mechanisms of substrate targeting. *Journal of interferon & cytokine research : the official journal of the International Society for Interferon and Cytokine Research* **34**: 275-288.

Brown JT, Bai X, Johnson AW. 2000. The yeast antiviral proteins Ski2p, Ski3p, and Ski8p exist as a complex in vivo. *RNA* **6**: 449-457.

Burke CW, Gardner CL, Steffan JJ, Ryman KD, Klimstra WB. 2009. Characteristics of alpha/beta interferon induction after infection of murine fibroblasts with wild-type and mutant alphaviruses. *Virology* **395**: 121-132.

Burnham AJ, Gong L, Hardy RW. 2007. Heterogeneous nuclear ribonuclear protein K interacts with Sindbis virus nonstructural proteins and viral subgenomic mRNA. *Virology* **367**: 212-221.

Cai X, Chiu Y-H, Chen Zhijian J. 2014. The cGAS-cGAMP-STING Pathway of Cytosolic DNA Sensing and Signaling. *Molecular Cell* **54**: 289-296.

Callahan KP, Butler JS. 2008. Evidence for core exosome independent function of the nuclear exoribonuclease Rrp6p. *Nucleic Acids Research* **36**: 6645-6655.

Castelli JC, Hassel BA, Wood KA, Li XL, Amemiya K, Dalakas MC, Torrence PF, Youle RJ. 1997. A study of the interferon antiviral mechanism: apoptosis activation by the 2-5A system. *The Journal of experimental medicine* **186**: 967-972.

Chacko MS, Adamo ML. 2011. Double-Stranded RNA Decreases IGF-I Gene Expression in a Protein Kinase R-Dependent, but Type I Interferon-Independent, Mechanism in C6 Rat Glioma Cells. in *Endocrinology*. Endocrine Society.

Chahar HS, Chen S, Manjunath N. 2013. P-body components LSM1, GW182, DDX3, DDX6 and XRN1 are recruited to WNV replication sites and positively regulate viral replication. *Virology* **436**: 1-7.

Chang H-M, Triboulet R, Thornton JE, Gregory RI. 2013. A role for the Perlman syndrome exonuclease Dis3l2 in the Lin28-let-7 pathway. *Nature* **497**: 244-248.

Chen CY, Gherzi R, Ong SE, Chan EL, Raijmakers R, Pruijn GJ, Stoecklin G, Moroni C, Mann M, Karin M. 2001. AU binding proteins recruit the exosome to degrade ARE-containing mRNAs. *Cell* **107**: 451-464.

Chen G, Guo X, Lv F, Xu Y, Gao G. 2008. p72 DEAD box RNA helicase is required for optimal function of the zinc-finger antiviral protein. *Proceedings of the National Academy of Sciences of the United States of America* **105**: 4352-4357.

Cherry S. 2005. Genome-wide RNAi screen reveals a specific sensitivity of IRES-containing RNA viruses to host translation inhibition. *Genes & Development* **19**: 445-452.

Cherry S, Perrimon N. 2004. Entry is a rate-limiting step for viral infection in a Drosophila melanogaster model of pathogenesis. *Nature Immunology* **5**: 81-87.

Clemens MJ, Hershey JW, Hovanessian AC, Jacobs BC, Katze MG, Kaufman RJ, Lengyel P, Samuel CE, Sen GC, Williams BR. 1993. PKR: proposed nomenclature for the RNA-dependent protein kinase induced by interferon. *Journal of interferon research* **13**: 241.

Coombs K, Brown B, Brown DT. 1984. Evidence for a change in capsid morphology during Sindbis virus envelopment. *Virus Research* **1**: 297-302.

Crow YJ, Rehwinkel J. 2009. Aicardi-Goutieres syndrome and related phenotypes: linking nucleic acid metabolism with autoimmunity. *Human molecular genetics* **18**: R130-136.

da Conceição TM, Rust NM, Berbel ACER, Martins NB, do Nascimento Santos CA, Da Poian AT, de Arruda LB. 2013. Essential role of RIG-I in the activation of endothelial cells by dengue virus. *Virology* **435**: 281-292.

de la Cruz J, Kressler D, Tollervey D, Linder P. 1998. Dob1p (Mtr4p) is a putative ATP-dependent RNA helicase required for the 3' end formation of 5.8S rRNA in Saccharomyces cerevisiae. *The EMBO journal* **17**: 1128-1140.

Decque A, Joffre O, Magalhaes JG, Cossec J-C, Blecher-Gonen R, Lapaquette P, Silvin A, Manel N, Joubert P-E, Seeler J-S et al. 2016. Sumoylation coordinates the repression of

inflammatory and anti-viral gene-expression programs during innate sensing. *Nature immunology* **17**: 140-149.
Decroly E, Ferron F, Lescar J, Canard B. 2012. Conventional and unconventional mechanisms for capping viral mRNA. *Nature reviews Microbiology* **10**: 51-65.
Deddouche S, Matt N, Budd A, Mueller S, Kemp C, Galiana-Arnoux D, Dostert C, Antoniewski C, Hoffmann JA, Imler J-L. 2008. The DExD/H-box helicase Dicer-2 mediates the induction of antiviral activity in drosophila. *Nature Immunology* **9**: 1425-1432.
Deutscher MP. 2006. Degradation of RNA in bacteria: comparison of mRNA and stable RNA. *Nucleic acids research* **34**: 659-666.
Domingues P, Golebiowski F, Tatham MH, Lopes AM, Taggart A, Hay RT, Hale BG. 2015. Global Reprogramming of Host SUMOylation during Influenza Virus Infection. *Cell Reports*.
Dong Y, Ye W, Yang J, Han P, Wang Y, Ye C, Weng D, Zhang F, Xu Z, Lei Y. 2016. DDX21 translocates from nucleus to cytoplasm and stimulates the innate immune response due to dengue virus infection. *Biochemical and biophysical research communications* **473**: 648-653.
Dorweiler JE, Ni T, Zhu J, Munroe SH, Anderson JT. 2014. Certain Adenylated Non-Coding RNAs, Including 5′ Leader Sequences of Primary MicroRNA Transcripts, Accumulate in Mouse Cells following Depletion of the RNA Helicase MTR4. *PloS one* **9**: e99430.
Dougherty JD, White JP, Lloyd RE. 2011. Poliovirus-mediated disruption of cytoplasmic processing bodies. *Journal of virology* **85**: 64-75.
Dziembowski A, Lorentzen E, Conti E, Séraphin B. 2007. A single subunit, Dis3, is essentially responsible for yeast exosome core activity. *Nature structural & molecular biology* **14**: 15-22.
Eckard SC, Rice GI, Fabre A, Badens C, Gray EE, Hartley JL, Crow YJ, Stetson DB. 2014. The SKIV2L RNA exosome limits activation of the RIG-I-like receptors. *Nature Immunology* **advance on**.
Eckwahl MJ, Sim S, Smith D, Telesnitsky A, Wolin SL. 2015. A retrovirus packages nascent host noncoding RNAs from a novel surveillance pathway. *Genes & development* **29**: 646-657.
Egecioglu DE, Henras AK, Chanfreau GF. 2006. Contributions of Trf4p- and Trf5p-dependent polyadenylation to the processing and degradative functions of the yeast nuclear exosome. *RNA* **12**: 26-32.
Emara MM, Brinton MA. 2007. Interaction of TIA-1/TIAR with West Nile and dengue virus products in infected cells interferes with stress granule formation and processing body assembly. *Proceedings of the National Academy of Sciences of the United States of America* **104**: 9041-9046.
Eulalio A, Behm-Ansmant I, Schweizer D, Izaurralde E. 2007. P-body formation is a consequence, not the cause, of RNA-mediated gene silencing. *Molecular and cellular biology* **27**: 3970-3981.
Fasken MB, Leung SW, Banerjee A, Kodani MO, Chavez R, Bowman EA, Purohit MK, Rubinson ME, Rubinson EH, Corbett AH. 2011. Air1 zinc knuckles 4 and 5 and a conserved IWRXY motif are critical for the function and integrity of the Trf4/5-Air1/2-Mtr4 polyadenylation (TRAMP) RNA quality control complex. *The Journal of biological chemistry* **286**: 37429-37445.
Filone CM, Hanna SL, Caino MC, Bambina S, Doms RW, Cherry S. 2010. Rift valley fever virus infection of human cells and insect hosts is promoted by protein kinase C epsilon. *PloS one* **5**: e15483.
Ford LP, Wilusz J. 1999. 3'-Terminal RNA structures and poly(U) tracts inhibit initiation by a 3'-5' exonuclease in vitro. *Nucleic acids research* **27**: 1159-1167.
Frolova EI, Fayzulin RZ, Cook SH, Griffin DE, Rice CM, Frolov I. 2002. Roles of Nonstructural Protein nsP2 and Alpha/Beta Interferons in Determining the Outcome of Sindbis Virus Infection. *Journal of Virology* **76**: 11254-11264.

Gale M, Katze MG. 1998. Molecular Mechanisms of Interferon Resistance Mediated by Viral-Directed Inhibition of PKR, the Interferon-Induced Protein Kinase. *Pharmacology & Therapeutics* **78**: 29-46.
Galiana-Arnoux D, Dostert C, Schneemann A, Hoffmann JA, Imler J-L. 2006. Essential function in vivo for Dicer-2 in host defense against RNA viruses in drosophila. *Nature Immunology* **7**: 590-597.
García MA, Gomez-puertas P, Guerra S, Rullas J, Nakano H, Esteban M. 2004. TRAF Family Proteins Link PKR with NF-kB Activation. *Society* **24**: 4502-4512.
Gareau JR, Lima CD. 2010. The SUMO pathway: emerging mechanisms that shape specificity, conjugation and recognition. *Nature reviews Molecular cell biology* **11**: 861-871.
Garmashova N, Gorchakov R, Frolova E, Frolov I. 2006. Sindbis virus nonstructural protein nsP2 is cytotoxic and inhibits cellular transcription. *Journal of virology* **80**: 5686-5696.
Garneau NL, Sokoloski KJ, Opyrchal M, Neff CP, Wilusz CJ, Wilusz J. 2008. The 3' untranslated region of sindbis virus represses deadenylation of viral transcripts in mosquito and Mammalian cells. *Journal of virology* **82**: 880-892.
Garneau NL, Wilusz J, Wilusz CJ. 2007. The highways and byways of mRNA decay. *Nature reviews Molecular cell biology* **8**: 113-126.
Gitlin L, Barchet W, Gilfillan S, Cella M, Beutler B, Flavell RA, Diamond MS, Colonna M. 2006. Essential role of mda-5 in type I IFN responses to polyriboinosinic:polyribocytidylic acid and encephalomyocarditis picornavirus. *Proceedings of the National Academy of Sciences of the United States of America* **103**: 8459-8464.
Gorchakov R, Frolova E, Williams BRG, Rice CM, Frolov I. 2004. PKR-dependent and -independent mechanisms are involved in translational shutoff during Sindbis virus infection. *Journal of virology* **78**: 8455-8467.
Graham AC, Kiss DL, Andrulis ED. 2006. Differential distribution of exosome subunits at the nuclear lamina and in cytoplasmic foci. *Molecular biology of the cell* **17**: 1399-1409.
Guo J, Cheng P, Yuan H, Liu Y. 2009. The exosome regulates circadian gene expression in a posttranscriptional negative feedback loop. *Cell* **138**: 1236-1246.
Guo TB, Boros LG, Chan KC, Hikim APS, Hudson AP, Swerdloff RS, Mitchell AP, Salameh WA. 2003. Spermatogenetic Expression of RNA-Binding Motif Protein 7, a Protein That Interacts With Splicing Factors. *Journal of Andrology* **24**: 204-214.
Guo X, Carroll J-WN, Macdonald MR, Goff SP, Gao G. 2004. The zinc finger antiviral protein directly binds to specific viral mRNAs through the CCCH zinc finger motifs. *Journal of virology* **78**: 12781-12787.
Guo X, Ma J, Sun J, Gao G. 2007. The zinc-finger antiviral protein recruits the RNA processing exosome to degrade the target mRNA. *Proc Natl Acad Sci USA* **104**: 151-156.
Gustafson MP, Welcker M, Hwang HC, Clurman BE. 2005. Zcchc8 is a glycogen synthase kinase-3 substrate that interacts with RNA-binding proteins. *Biochemical and biophysical research communications* **338**: 1359-1367.
Hassel BA, Zhou A, Sotomayor C, Maran A, Silverman RH. 1993. A dominant negative mutant of 2-5A-dependent RNase suppresses antiproliferative and antiviral effects of interferon. *The EMBO journal* **12**: 3297-3304.
Hendriks IA, D'Souza RC, Chang J-G, Mann M, Vertegaal ACO. 2015a. System-wide identification of wild-type SUMO-2 conjugation sites. *Nature communications* **6**: 7289.
Hendriks IA, D'Souza RCJ, Yang B, Verlaan-de Vries M, Mann M, Vertegaal ACO. 2014. Uncovering global SUMOylation signaling networks in a site-specific manner. *Nature structural & molecular biology* **21**: 927-936.
Hendriks IA, Treffers LW, Verlaan-deVries M, Olsen JV, Vertegaal ACO. 2015b. SUMO-2 Orchestrates Chromatin Modifiers in Response to DNA Damage. *Cell Reports* **10**: 1778-1791.
Hessle V, Björk P, Sokolowski M, González de Valdivia E, Silverstein R, Artemenko K, Tyagi A, Maddalo G, Ilag L, Helbig R et al. 2009. The exosome associates cotranscriptionally with

the nascent pre-mRNP through interactions with heterogeneous nuclear ribonucleoproteins. *Molecular biology of the cell* **20**: 3459-3470.
Hinnebusch AG. 1994. The eIF-2α kinases: regulators of protein synthesis in starvation and stress. *Seminars in Cell Biology* **5**: 417-426.
Hopkins KC, McLane LM, Maqbool T, Panda D, Gordesky-Gold B, Cherry S. 2013. A genome-wide RNAi screen reveals that mRNA decapping restricts bunyaviral replication by limiting the pools of Dcp2-accessible targets for cap-snatching. *Genes & Development* **27**: 1511-1525.
Hopkins KC, Tartell MA, Herrmann C, Hackett BA, Taschuk F, Panda D, Menghani SV, Sabin LR, Cherry S. 2015. Virus-induced translational arrest through 4EBP1/2-dependent decay of 5′-TOP mRNAs restricts viral infection. *Proceedings of the National Academy of Sciences* **112**: 201418805.
Horikawa W, Endo K, Wada M, Ito K. 2016. Mutations in the G-domain of Ski7 cause specific dysfunction in non-stop decay. *Scientific reports* **6**: 29295.
Hornung V, Ellegast J, Kim S, Brzózka K, Jung A, Kato H, Poeck H, Akira S, Conzelmann K-K, Schlee M et al. 2006. 5'-Triphosphate RNA is the ligand for RIG-I. *Science (New York, NY)* **314**: 994-997.
Houseley J, LaCava J, Tollervey D. 2006. RNA-quality control by the exosome. *Nature reviews Molecular cell biology* **7**: 529-539.
Houseley J, Tollervey D. 2008. The nuclear RNA surveillance machinery: The link between ncRNAs and genome structure in budding yeast? *Biochimica et Biophysica Acta (BBA) - Gene Regulatory Mechanisms* **1779**: 239-246.
-. 2009. The many pathways of RNA degradation. *Cell* **136**: 763-776.
Hovanessian AG, Laurent AG, Chebath J, Galabru J, Robert N, Svab J. 1987. Identification of 69-kd and 100-kd forms of 2-5A synthetase in interferon-treated human cells by specific monoclonal antibodies. *The EMBO journal* **6**: 1273-1280.
Hsu CL, Stevens A. 1993. Yeast cells lacking 5'-->3' exoribonuclease 1 contain mRNA species that are poly(A) deficient and partially lack the 5' cap structure. *Mol Cell Biol* **13**: 4826-4835.
Huarte J, Stutz A, O'Connell ML, Gubler P, Belin D, Darrow AL, Strickland S, Vassalli J-D. 1992. Transient translational silencing by reversible mRNA deadenylation. *Cell* **69**: 1021-1030.
Ikegami T, Narayanan K, Won S, Kamitani W, Peters CJ, Makino S. 2009. Rift Valley fever virus NSs protein promotes post-transcriptional downregulation of protein kinase PKR and inhibits eIF2alpha phosphorylation. *PLoS pathogens* **5**: e1000287.
Ikegami T, Won S, Peters CJ, Makino S. 2007. Characterization of Rift Valley fever virus transcriptional terminations. *Journal of virology* **81**: 8421-8438.
Isken O, Maquat LE. 2007. Quality control of eukaryotic mRNA: safeguarding cells from abnormal mRNA function. *Genes & development* **21**: 1833-1856.
Iwakawa H-O, Tajima Y, Taniguchi T, Kaido M, Mise K, Tomari Y, Taniguchi H, Okuno T. 2012. Poly(A)-binding protein facilitates translation of an uncapped/nonpolyadenylated viral RNA by binding to the 3' untranslated region. *Journal of virology* **86**: 7836-7849.
Jackson RN, Klauer AA, Hintze BJ, Robinson H, van Hoof A, Johnson SJ. 2010. The crystal structure of Mtr4 reveals a novel arch domain required for rRNA processing. *The EMBO journal* **29**: 2205-2216.
Jacobs Anderson JS, Parker R. 1998. The 3' to 5' degradation of yeast mRNAs is a general mechanism for mRNA turnover that requires the SKI2 DEVH box protein and 3' to 5' exonucleases of the exosome complex. *The EMBO journal* **17**: 1497-1506.
Jensen S, Thomsen AR. 2012. Sensing of RNA viruses: a review of innate immune receptors involved in recognizing RNA virus invasion. *Journal of virology* **86**: 2900-2910.
Jones DM, Domingues P, Targett-Adams P, McLauchlan J. 2010. Comparison of U2OS and Huh-7 cells for identifying host factors that affect hepatitis C virus RNA replication. *The Journal of general virology* **91**: 2238-2248.

Kadaba S. 2004. Nuclear surveillance and degradation of hypomodified initiator tRNAMet in S. cerevisiae. *Genes & Development* **18**: 1227-1240.
Kainulainen M, Lau S, Samuel CE, Hornung V, Weber F. 2016. NSs Virulence Factor of Rift Valley Fever Virus Engages the F-Box Proteins FBXW11 and β-TRCP1 To Degrade the Antiviral Protein Kinase PKR. *Journal of virology* **90**: 6140-6147.
Kato H, Takeuchi O, Mikamo-Satoh E, Hirai R, Kawai T, Matsushita K, Hiiragi A, Dermody TS, Fujita T, Akira S. 2008. Length-dependent recognition of double-stranded ribonucleic acids by retinoic acid-inducible gene-I and melanoma differentiation-associated gene 5. *The Journal of experimental medicine* **205**: 1601-1610.
Kato H, Takeuchi O, Sato S, Yoneyama M, Yamamoto M, Matsui K, Uematsu S, Jung A, Kawai T, Ishii KJ et al. 2006. Differential roles of MDA5 and RIG-I helicases in the recognition of RNA viruses. *Nature* **441**: 101-105.
Kawai T, Takahashi K, Sato S, Coban C, Kumar H, Kato H, Ishii KJ, Takeuchi O, Akira S. 2005. IPS-1, an adaptor triggering RIG-I- and Mda5-mediated type I interferon induction. *Nature immunology* **6**: 981-988.
Kedersha N, Stoecklin G, Ayodele M, Yacono P, Lykke-Andersen J, Fritzler MJ, Scheuner D, Kaufman RJ, Golan DE, Anderson P. 2005. Stress granules and processing bodies are dynamically linked sites of mRNP remodeling. *The Journal of cell biology* **169**: 871-884.
Kedersha NL, Gupta M, Li W, Miller I, Anderson P. 1999. RNA-Binding Proteins Tia-1 and Tiar Link the Phosphorylation of Eif-2α to the Assembly of Mammalian Stress Granules. *The Journal of Cell Biology* **147**: 1431-1442.
Keene JD. 2007. RNA regulons: coordination of post-transcriptional events. *Nature reviews Genetics* **8**: 533-543.
Kiss DL, Andrulis ED. 2011. The exozyme model: a continuum of functionally distinct complexes. *RNA* **17**: 1-13.
Kolakofsky D, Hacker D. 1991. Bunyavirus RNA synthesis: genome transcription and replication. *Current topics in microbiology and immunology* **169**: 143-159.
Koonin EV, Moss B. 2010. Viruses know more than one way to don a cap. *Proceedings of the National Academy of Sciences of the United States of America* **107**: 3283-3284.
Kurkela S, Manni T, Myllynen J, Vaheri A, Vapalahti O. 2005. Clinical and laboratory manifestations of Sindbis virus infection: prospective study, Finland, 2002-2003. *The Journal of infectious diseases* **191**: 1820-1829.
LaCava J, Houseley J, Saveanu C, Petfalski E, Thompson E, Jacquier A, Tollervey D. 2005. RNA Degradation by the Exosome Is Promoted by a Nuclear Polyadenylation Complex. *Cell* **121**: 713-724.
Lamoliatte F, Caron D, Durette C, Mahrouche L, Maroui MA, Caron-Lizotte O, Bonneil E, Chelbi-Alix MK, Thibault P. 2014. Large-scale analysis of lysine SUMOylation by SUMO remnant immunoaffinity profiling. *Nature communications* **5**: 5409.
Lara E, Billecocq A, Leger P, Bouloy M. 2011. Characterization of wild-type and alternate transcription termination signals in the Rift Valley fever virus genome. *Journal of virology* **85**: 12134-12145.
Laredj LN, Beard P. 2011. Adeno-associated virus activates an innate immune response in normal human cells but not in osteosarcoma cells. *Journal of virology* **85**: 13133-13143.
Lee YS Nakahara K Pham JW Kim K He Z Sontheimer EJ Carthew RW Abrahante JE Daul AL Li M et al. 2004. Distinct Roles for Drosophila Dicer-1 and Dicer-2 in the siRNA/miRNA Silencing Pathways. *Cell* **117**: 69-81.
Lejeune F, Li X, Maquat LE. 2003. Nonsense-Mediated mRNA Decay in Mammalian Cells Involves Decapping, Deadenylating, and Exonucleolytic Activities. *Molecular Cell* **12**: 675-687.
Letchworth GJ, Rodriguez LL, Del cbarrera J. 1999. Vesicular stomatitis. *Veterinary journal (London, England : 1997)* **157**: 239-260.

Li Y, Song M, Kiledjian M. 2011. Differential utilization of decapping enzymes in mammalian mRNA decay pathways. *RNA (New York, NY)* **17**: 419-428.
Li Z, Reimers S, Pandit S, Deutscher MP, Bradford M, Carpousis A, Vanzo N, Raynal L, Coburn G, Mackie G et al. 2002. RNA quality control: degradation of defective transfer RNA. *The EMBO journal* **21**: 1132-1138.
Liang G, Liu G, Kitamura K, Wang Z, Chowdhury S, Monjurul AM, Wakae K, Koura M, Shimadu M, Kinoshita K et al. 2015. TGF-β Suppression of HBV RNA through AID-Dependent Recruitment of an RNA Exosome Complex. *PLOS Pathogens* **11**: e1004780.
Lin W-J, Duffy A, Chen C-Y. 2007. Localization of AU-rich element-containing mRNA in cytoplasmic granules containing exosome subunits. *The Journal of biological chemistry* **282**: 19958-19968.
Lindquist ME, Mainou BA, Dermody TS, Crowe JE. 2011. Activation of protein kinase R is required for induction of stress granules by respiratory syncytial virus but dispensable for viral replication. *Virology* **413**: 103-110.
Liu L, Chen G, Ji X, Gao G. 2004. ZAP is a CRM1-dependent nucleocytoplasmic shuttling protein. *Biochemical and Biophysical Research Communications* **321**: 517-523.
Liu Q, Greimann JC, Lima CD. 2006. Reconstitution, Activities, and Structure of the Eukaryotic RNA Exosome. *Cell* **127**: 1223-1237.
Liu X, Chen W, Wang Q, Li L, Wang C. 2013. Negative regulation of TLR inflammatory signaling by the SUMO-deconjugating enzyme SENP6. *PLoS pathogens* **9**: e1003480.
Lubas M, Andersen PR, Schein A, Dziembowski A, Kudla G, Jensen TH. 2015. The human nuclear exosome targeting complex is loaded onto newly synthesized RNA to direct early ribonucleolysis. *Cell reports* **10**: 178-192.
Lubas M, Christensen MS, Kristiansen MS, Domanski M, Falkenby LG, Lykke-Andersen S, Andersen JS, Dziembowski A, Jensen TH. 2011. Interaction Profiling Identifies the Human Nuclear Exosome Targeting Complex. *Molecular Cell* **43**: 624-637.
Maillard PV, Ciaudo C, Marchais A, Li Y, Jay F, Ding SW, Voinnet O. 2013. Antiviral RNA Interference in Mammalian Cells. *Science* **342**.
Makino DL, Baumgärtner M, Conti E. 2013. Crystal structure of an RNA-bound 11-subunit eukaryotic exosome complex. *Nature* **495**: 70-75.
Masison DC, Blanc A, Ribas JC, Carroll K, Sonenberg N, Wickner RB. 1995. Decoying the cap-mRNA degradation system by a double-stranded RNA virus and poly(A)- mRNA surveillance by a yeast antiviral system. *Molecular and cellular biology* **15**: 2763-2771.
Meurs E, Chong K, Galabru J, Thomas NSB, Kerr IM, Williams BRG, Hovanessian AG. 1990. Molecular cloning and characterization of the human double-stranded RNA-activated protein kinase induced by interferon. *Cell* **62**: 379-390.
Meylan E, Curran J, Hofmann K, Moradpour D, Binder M, Bartenschlager R, Tschopp J. 2005. Cardif is an adaptor protein in the RIG-I antiviral pathway and is targeted by hepatitis C virus. *Nature* **437**: 1167-1172.
Milligan L, Torchet C, Allmang C, Shipman T, Tollervey D. 2005. A Nuclear Surveillance Pathway for mRNAs with Defective Polyadenylation. *Molecular and Cellular Biology* **25**: 9996-10004.
Mitchell P, Petfalski E, Shevchenko A, Mann M, Tollervey D. 1997. The exosome: a conserved eukaryotic RNA processing complex containing multiple 3'-->5' exoribonucleases. *Cell* **91**: 457-466.
Miyashita M, Oshiumi H, Matsumoto M, Seya T. 2011. DDX60, a DEXD/H Box Helicase, Is a Novel Antiviral Factor Promoting RIG-I-Like Receptor-Mediated Signaling. *Molecular and Cellular Biology* **31**: 3802-3819.
Mogensen TH. 2009. Pathogen recognition and inflammatory signaling in innate immune defenses. *Clinical microbiology reviews* **22**: 240-273, Table of Contents.
Molleston JM, Sabin LR, Moy RH, Menghani SV, Rausch K, Gordesky-Gold B, Hopkins KC, Zhou R, Jensen TH, Wilusz JE et al. 2016. A conserved virus-induced cytoplasmic TRAMP-like

complex recruits the exosome to target viral RNA for degradation. *Genes & development* **30**: 1658-1670.
Moon SL, Anderson JR, Kumagai Y, Wilusz CJ, Akira S, Khromykh AA, Wilusz J. 2012a. A noncoding RNA produced by arthropod-borne flaviviruses inhibits the cellular exoribonuclease XRN1 and alters host mRNA stability. *RNA (New York, NY)* **18**: 2029-2040.
Moon SL, Barnhart MD, Wilusz J. 2012b. Inhibition and avoidance of mRNA degradation by RNA viruses. *Current Opinion in Microbiology* **15**: 500-505.
Moon SL, Wilusz J. 2013. Cytoplasmic viruses: rage against the (cellular RNA decay) machine. *PLoS pathogens* **9**: e1003762.
Moser TS, Schieffer D, Cherry S. 2012. AMP-Activated Kinase Restricts Rift Valley Fever Virus Infection by Inhibiting Fatty Acid Synthesis. *PLoS Pathogens* **8**: e1002661.
Moy RH, Cole BS, Yasunaga A, Gold B, Shankarling G, Varble A, Molleston JM, tenOever BR, Lynch KW, Cherry S. 2014a. Stem-Loop Recognition by DDX17 Facilitates miRNA Processing and Antiviral Defense. *Cell* **158**: 764-777.
Moy RH, Gold B, Molleston JM, Schad V, Yanger K, Salzano MV, Yagi Y, Fitzgerald KA, Stanger BZ, Soldan SS et al. 2014b. Antiviral autophagy restricts rift valley fever virus infection and is conserved from flies to mammals. *Immunity* **40**: 51-65.
Muhlrad D, Decker CJ, Parker R. 1994. Deadenylation of the unstable mRNA encoded by the yeast MFA2 gene leads to decapping followed by 5'-->3' digestion of the transcript. *Genes & Development* **8**: 855-866.
Mukherjee D, Gao M, O'Connor JP, Raijmakers R, Pruijn G, Lutz CS, Wilusz J. 2002. The mammalian exosome mediates the efficient degradation of mRNAs that contain AU-rich elements. *The EMBO journal* **21**: 165-174.
Nakamura R, Takeuchi R, Takata K-i, Shimanouchi K, Abe Y, Kanai Y, Ruike T, Ihara A, Sakaguchi K. 2008. TRF4 is involved in polyadenylation of snRNAs in Drosophila melanogaster. *Molecular and cellular biology* **28**: 6620-6631.
Ng CS, Jogi M, Yoo J-S, Onomoto K, Koike S, Iwasaki T, Yoneyama M, Kato H, Fujita T. 2013. Encephalomyocarditis virus disrupts stress granules, the critical platform for triggering antiviral innate immune responses. *Journal of virology* **87**: 9511-9522.
Nikonov A, Mölder T, Sikut R, Kiiver K, Männik A, Toots U, Lulla A, Lulla V, Utt A, Merits A et al. 2013. RIG-I and MDA-5 detection of viral RNA-dependent RNA polymerase activity restricts positive-strand RNA virus replication. *PLoS pathogens* **9**: e1003610.
Okonski KM, Samuel CE. 2013. Stress granule formation induced by measles virus is protein kinase PKR dependent and impaired by RNA adenosine deaminase ADAR1. *Journal of virology* **87**: 756-766.
Onomoto K, Jogi M, Yoo J-S, Narita R, Morimoto S, Takemura A, Sambhara S, Kawaguchi A, Osari S, Nagata K et al. 2012. Critical role of an antiviral stress granule containing RIG-I and PKR in viral detection and innate immunity. *PloS one* **7**: e43031.
Onomoto K, Yoneyama M, Fung G, Kato H, Fujita T. 2014. Antiviral innate immunity and stress granule responses. *Trends in immunology* **35**: 420-428.
Orban TI, Izaurralde E. 2005. Decay of mRNAs targeted by RISC requires XRN1, the Ski complex, and the exosome. *RNA (New York, NY)* **11**: 459-469.
Paolo SS, Vanacova S, Schenk L, Scherrer T, Blank D, Keller W, Gerber AP. 2009. Distinct Roles of Non-Canonical Poly(A) Polymerases in RNA Metabolism. *PLoS Genetics* **5**: e1000555.
Parker R, Sheth U. 2007. P Bodies and the Control of mRNA Translation and Degradation. *Molecular Cell* **25**: 635-646.
Patterson JL, Holloway B, Kolakofsky D. 1984. La Crosse virions contain a primer-stimulated RNA polymerase and a methylated cap-dependent endonuclease. *Journal of virology* **52**: 215-222.

Pichlmair A, Schulz O, Tan C-P, Rehwinkel J, Kato H, Takeuchi O, Akira S, Way M, Schiavo G, Reis e Sousa C. 2009. Activation of MDA5 requires higher-order RNA structures generated during virus infection. *Journal of virology* **83**: 10761-10769.

Pichlmair A, Schulz O, Tan CP, Naslund TI, Liljestrom P, Weber F, Reis e Sousa C. 2006. RIG-I-Mediated Antiviral Responses to Single-Stranded RNA Bearing 5'-Phosphates. *Science* **314**: 997-1001.

Protter DSW, Parker R. 2016. Principles and Properties of Stress Granules. *Trends in cell biology* **26**: 668-679.

Raijmakers R, Egberts WV, van Venrooij WJ, Pruijn GJM. 2002. Protein–Protein Interactions between Human Exosome Components Support the Assembly of RNase PH-type Subunits into a Six-membered PNPase-like Ring. *Journal of Molecular Biology* **323**: 653-663.

Ramsburg E, Publicover J, Buonocore L, Poholek A, Robek M, Palin A, Rose JK. 2005. A vesicular stomatitis virus recombinant expressing granulocyte-macrophage colony-stimulating factor induces enhanced T-cell responses and is highly attenuated for replication in animals. *Journal of virology* **79**: 15043-15053.

Reguera J, Weber F, Cusack S. 2010. Bunyaviridae RNA polymerases (L-protein) have an N-terminal, influenza-like endonuclease domain, essential for viral cap-dependent transcription. *PLoS pathogens* **6**: e1001101.

Reineke LC, Lloyd RE. 2013. Diversion of stress granules and P-bodies during viral infection. *Virology* **436**: 255-267.

Roberts WK, Hovanessian A, Brown RE, Clemens MJ, Kerr IM. 1976. Interferon-mediated protein kinase and low-molecular-weight inhibitor of protein synthesis. *Nature* **264**: 477-480.

Sabath I, Skrajna A, Yang X-C, Dadlez M, Marzluff WF, Dominski Z. 2013. 3'-End processing of histone pre-mRNAs in Drosophila: U7 snRNP is associated with FLASH and polyadenylation factors. *RNA (New York, NY)* **19**: 1726-1744.

Sabin LR, Zhou R, Gruber JJ, Lukinova N, Bambina S, Berman A, Lau C-K, Thompson CB, Cherry S. 2009. Ars2 Regulates Both miRNA- and siRNA- Dependent Silencing and Suppresses RNA Virus Infection in Drosophila. *Cell* **138**: 340-351.

Sadler AJ, Williams BRG. 2008. Interferon-inducible antiviral effectors. *Nature reviews Immunology* **8**: 559-568.

Sahin U, Ferhi O, Carnec X, Zamborlini A, Peres L, Jollivet F, Vitaliano-Prunier A, de Thé H, Lallemand-Breitenbach V. 2014. Interferon controls SUMO availability via the Lin28 and let-7 axis to impede virus replication. *Nature communications* **5**: 4187.

Santiago A, Li D, Zhao LY, Godsey A, Liao D. 2013. p53 SUMOylation promotes its nuclear export by facilitating its release from the nuclear export receptor CRM1. *Molecular biology of the cell* **24**: 2739-2752.

Schmidt K, Xu Z, Mathews DH, Butler JS. 2012. Air proteins control differential TRAMP substrate specificity for nuclear RNA surveillance. *RNA* **18**: 1934-1945.

Schneider C, Anderson JT, Tollervey D. 2007. The exosome subunit Rrp44 plays a direct role in RNA substrate recognition. *Molecular Cell* **27**: 324-331.

Schneider C, Kudla G, Wlotzka W, Tuck A, Tollervey D. 2012. Transcriptome-wide Analysis of Exosome Targets. *Molecular Cell* **48**: 422-433.

Schneider C, Tollervey D. 2013. Threading the barrel of the RNA exosome. *Trends in biochemical sciences*.

Schnell MJ, Buonocore L, Whitt MA, Rose JK. 1996. The minimal conserved transcription stop-start signal promotes stable expression of a foreign gene in vesicular stomatitis virus. *Journal of virology* **70**: 2318-2323.

Schubert M, Keene JD, Herman RC, Lazzarini RA. 1980. Site on the vesicular stomatitis virus genome specifying polyadenylation and the end of the L gene mRNA. *J Virol* **34**: 550-559.

Seeler J-S, Dejean A. 2003. Nuclear and unclear functions of SUMO. *Nature reviews Molecular cell biology* **4**: 690-699.
Sen A, Pruijssers AJ, Dermody TS, García-Sastre A, Greenberg HB. 2011. The early interferon response to rotavirus is regulated by PKR and depends on MAVS/IPS-1, RIG-I, MDA-5, and IRF3. *Journal of virology* **85**: 3717-3732.
Seth RB, Sun L, Ea C-K, Chen ZJ. 2005. Identification and characterization of MAVS, a mitochondrial antiviral signaling protein that activates NF-kappaB and IRF 3. *Cell* **122**: 669-682.
Shapiro JS, Schmid S, Aguado LC, Sabin LR, Yasunaga A, Shim JV, Sachs D, Cherry S, tenOever BR. 2014. Drosha as an interferon-independent antiviral factor. *Proceedings of the National Academy of Sciences of the United States of America* **111**: 7108-7113.
Shapiro JS, Varble A, Pham AM, Tenoever BR. 2010. Noncanonical cytoplasmic processing of viral microRNAs. *RNA* **16**: 2068-2074.
Shcherbik N, Wang M, Lapik YR, Srivastava L, Pestov DG. 2010. Polyadenylation and degradation of incomplete RNA polymerase I transcripts in mammalian cells. *EMBO reports* **11**: 106-111.
Shelly S, Lukinova N, Bambina S, Berman A, Cherry S. 2009. Autophagy Is an Essential Component of Drosophila Immunity against Vesicular Stomatitis Virus. *Immunity* **30**: 588-598.
Sheth U, Parker R. 2003. Decapping and decay of messenger RNA occur in cytoplasmic processing bodies. *Science (New York, NY)* **300**: 805-808.
Silva PAGC, Pereira CF, Dalebout TJ, Spaan WJM, Bredenbeek PJ. 2010. An RNA pseudoknot is required for production of yellow fever virus subgenomic RNA by the host nuclease XRN1. *Journal of virology* **84**: 11395-11406.
Silverman RH. 2007. Viral encounters with 2',5'-oligoadenylate synthetase and RNase L during the interferon antiviral response. *Journal of virology* **81**: 12720-12729.
Singer S, Zhao R, Barsotti AM, Ouwehand A, Fazollahi M, Coutavas E, Breuhahn K, Neumann O, Longerich T, Pusterla T et al. 2012. Nuclear pore component Nup98 is a potential tumor suppressor and regulates posttranscriptional expression of select p53 target genes. *Molecular cell* **48**: 799-810.
Stetson DB, Ko JS, Heidmann T, Medzhitov R. 2008. Trex1 prevents cell-intrinsic initiation of autoimmunity. *Cell* **134**: 587-598.
Strauss JH, Strauss EG. 1994. The alphaviruses: gene expression, replication, and evolution. *Microbiological reviews* **58**: 491-562.
Takeuchi O, Akira S. 2008. RIG-I-like antiviral protein in flies. *Nature immunology* **9**: 1327-1328.
Tao YJ, Ye Q. 2010. RNA virus replication complexes. *PLoS pathogens* **6**: e1000943.
Teixeira D, Sheth U, Valencia-Sanchez MA, Brengues M, Parker R. 2005. Processing bodies require RNA for assembly and contain nontranslating mRNAs. *RNA (New York, NY)* **11**: 371-382.
Thomas MG, Loschi M, Desbats MA, Boccaccio GL. 2011. RNA granules: the good, the bad and the ugly. *Cellular signalling* **23**: 324-334.
Thomas MP, Liu X, Whangbo J, McCrossan G, Sanborn KB, Basar E, Walch M, Lieberman J. 2015. Apoptosis Triggers Specific, Rapid, and Global mRNA Decay with 3' Uridylated Intermediates Degraded by DIS3L2. *Cell reports* **11**: 1079-1089.
Thoms M, Thomson E, Baßler J, Gnädig M, Griesel S, Hurt E. 2015. The Exosome Is Recruited to RNA Substrates through Specific Adaptor Proteins. *Cell* **162**: 1029-1038.
Toh-E A, Guerry P, Wickner RB. 1978. Chromosomal superkiller mutants of Saccharomyces cerevisiae. *Journal of bacteriology* **136**: 1002-1007.
Tomecki R, Kristiansen MS, Lykke-Andersen S, Chlebowski A, Larsen KM, Szczesny RJ, Drazkowska K, Pastula A, Andersen JS, Stepien PP et al. 2010. The human core exosome interacts with differentially localized processive RNases: hDIS3 and hDIS3L. *The EMBO journal* **29**: 2342-2357.

Triantafilou K, Vakakis E, Richer EAJ, Evans GL, Villiers JP, Triantafilou M. Human rhinovirus recognition in non-immune cells is mediated by Toll-like receptors and MDA-5, which trigger a synergetic pro-inflammatory immune response. *Virulence* **2**: 22-29.

Tuck AC, Tollervey D. 2013. A transcriptome-wide atlas of RNP composition reveals diverse classes of mRNAs and lncRNAs. *Cell* **154**: 996-1009.

Ustianenko D, Hrossova D, Potesil D, Chalupnikova K, Hrazdilova K, Pachernik J, Cetkovska K, Uldrijan S, Zdrahal Z, Vanacova S. 2013. Mammalian DIS3L2 exoribonuclease targets the uridylated precursors of let-7 miRNAs. *RNA (New York, NY)* **19**: 1632-1638.

van Hoof A, Frischmeyer PA, Dietz HC, Parker R. 2002. Exosome-mediated recognition and degradation of mRNAs lacking a termination codon. *Science (New York, NY)* **295**: 2262-2264.

van Rij RP, Saleh M-C, Berry B, Foo C, Houk A, Antoniewski C, Andino R. 2006. The RNA silencing endonuclease Argonaute 2 mediates specific antiviral immunity in Drosophila melanogaster. *Genes & development* **20**: 2985-2995.

Vanácová S, Wolf J, Martin G, Blank D, Dettwiler S, Friedlein A, Langen H, Keith G, Keller W. 2005. A new yeast poly(A) polymerase complex involved in RNA quality control. *PLoS biology* **3**: e189.

Vidal S, Khush RS, Leulier F, Tzou P, Nakamura M, Lemaitre B. 2001. Mutations in the Drosophila dTAK1 gene reveal a conserved function for MAPKKKs in the control of rel/NF-kappaB-dependent innate immune responses. *Genes & development* **15**: 1900-1912.

Wang X-H, Aliyari R, Li W-X, Li H-W, Kim K, Carthew R, Atkinson P, Ding S-W. 2006. RNA interference directs innate immunity against viruses in adult Drosophila. *Science (New York, NY)* **312**: 452-454.

Ward AM, Bidet K, Yinglin A, Ler SG, Hogue K, Blackstock W, Gunaratne J, Garcia-Blanco MA. 2011. Quantitative mass spectrometry of DENV-2 RNA-interacting proteins reveals that the DEAD-box RNA helicase DDX6 binds the DB1 and DB2 3' UTR structures. *RNA biology* **8**: 1173-1186.

Weaver SC, Barrett ADT. 2004. Transmission cycles, host range, evolution and emergence of arboviral disease. *Nature Reviews Microbiology* **2**: 789-801.

Weaver SC, Reisen WK. 2010. Present and future arboviral threats. *Antiviral Research* **85**: 328-345.

Wilczynska A, Aigueperse C, Kress M, Dautry F, Weil D. 2005. The translational regulator CPEB1 provides a link between dcp1 bodies and stress granules. *Journal of Cell Science* **118**.

Williams BRG. 1995. The role of the dsRNA-activated kinase, PKR, in signal transduction. *Seminars in Virology* **6**: 191-202.

Wilusz JE, Freier SM, Spector DL. 2008. 3' end processing of a long nuclear-retained noncoding RNA yields a tRNA-like cytoplasmic RNA. *Cell* **135**: 919-932.

Wilusz JE, JnBaptiste CK, Lu LY, Kuhn C-D, Joshua-Tor L, Sharp PA. 2012. A triple helix stabilizes the 3' ends of long noncoding RNAs that lack poly(A) tails. *Genes & development* **26**: 2392-2407.

Wood LD, Irvin BJ, Nucifora G, Luce KS, Hiebert SW. 2003. Small ubiquitin-like modifier conjugation regulates nuclear export of TEL, a putative tumor suppressor. *Proceedings of the National Academy of Sciences of the United States of America* **100**: 3257-3262.

Wyers F, Rougemaille M, Badis G, Rousselle J-C, Dufour M-E, Boulay J, Régnault B, Devaux F, Namane A, Séraphin B. 2005. Cryptic Pol II Transcripts Are Degraded by a Nuclear Quality Control Pathway Involving a New Poly(A) Polymerase. *Cell* **121**: 725-737.

Xiao Z, Chang J-G, Hendriks IA, Sigurðsson JO, Olsen JV, Vertegaal ACO. 2015. System-wide Analysis of SUMOylation Dynamics in Response to Replication Stress Reveals Novel Small Ubiquitin-like Modified Target Proteins and Acceptor Lysines Relevant for Genome Stability. *Molecular & cellular proteomics : MCP* **14**: 1419-1434.

Xu J, Grant G, Sabin LR, Gordesky-Gold B, Yasunaga A, Tudor M, Cherry S. 2012. Transcriptional pausing controls a rapid antiviral innate immune response in Drosophila. *Cell host & microbe* **12**: 531-543.
Xu L-G, Wang Y-Y, Han K-J, Li L-Y, Zhai Z, Shu H-B. 2005. VISA is an adapter protein required for virus-triggered IFN-beta signaling. *Molecular cell* **19**: 727-740.
Xue Z, Yuan H, Guo J, Liu Y. 2012. Reconstitution of an Argonaute-dependent small RNA biogenesis pathway reveals a handover mechanism involving the RNA exosome and the exonuclease QIP. *Molecular cell* **46**: 299-310.
Yasunaga A, Hanna SL, Li J, Cho H, Rose PP, Spiridigliozzi A, Gold B, Diamond MS, Cherry S. 2014. Genome-wide RNAi screen identifies broadly-acting host factors that inhibit arbovirus infection. *PLoS pathogens* **10**: e1003914.
Zamanian-Daryoush M, Mogensen TH, DiDonato JA, Williams BRG. 2000. NF-kappa B Activation by Double-Stranded-RNA-Activated Protein Kinase (PKR) Is Mediated through NF-kappa B-Inducing Kinase and Ikappa B Kinase. *Molecular and Cellular Biology* **20**: 1278-1290.
Zhang P, Langland JO, Jacobs BL, Samuel CE. 2009. Protein kinase PKR-dependent activation of mitogen-activated protein kinases occurs through mitochondrial adapter IPS-1 and is antagonized by vaccinia virus E3L. *Journal of virology* **83**: 5718-5725.
Zhang S, Sun Y, Chen H, Dai Y, Zhan Y, Yu S, Qiu X, Tan L, Song C, Ding C. 2014. Activation of the PKR/eIF2α signaling cascade inhibits replication of Newcastle disease virus. *Virology journal* **11**: 62.
Zhou R, Hotta I, Denli AM, Hong P, Perrimon N, Hannon GJ. 2008. Comparative Analysis of Argonaute-Dependent Small RNA Pathways in Drosophila. *Molecular Cell* **32**: 592-599.
Zhu B, Mandal SS, Pham A-D, Zheng Y, Erdjument-Bromage H, Batra SK, Tempst P, Reinberg D. 2005. The human PAF complex coordinates transcription with events downstream of RNA synthesis. *Genes & Development* **19**: 1668-1673.
Zhu Y, Chen G, Lv F, Wang X, Ji X, Xu Y, Sun J, Wu L, Zheng Y-T, Gao G. 2011. Zinc-finger antiviral protein inhibits HIV-1 infection by selectively targeting multiply spliced viral mRNAs for degradation. *Proceedings of the National Academy of Sciences of the United States of America* **108**: 15834-15839.
Zurla C, Lifland AW, Santangelo PJ. 2011. Characterizing mRNA interactions with RNA granules during translation initiation inhibition. *PloS one* **6**: e19727.